



Evaluation of Barriers for Very High Speed Roadways



Research/Test Report 0-6071-2

Cooperative Research Program

**TEXAS TRANSPORTATION INSTITUTE
THE TEXAS A&M UNIVERSITY SYSTEM
COLLEGE STATION, TEXAS**

in cooperation with the
Federal Highway Administration and the
Texas Department of Transportation
<http://tti.tamu.edu/documents/0-6071-2.pdf>

1. Report No. FHWA/TX-10/0-6071-2		2. Government Accession No.		3. Recipient's Catalog No.	
4. Title and Subtitle Evaluation of Barriers for Very High Speed Roadways				5. Report Date January 2010 Published: March 2010	
				6. Performing Organization Code	
7. Author(s) Roger P. Bligh, Nauman M. Sheikh, Akram Y. Abu-Odeh, and Wanda L. Menges				8. Performing Organization Report No. Report 0-6071-2	
9. Performing Organization Name and Address Texas Transportation Institute Proving Ground The Texas A&M University System College Station, Texas 77843-3135				10. Work Unit No. (TRAIS)	
				11. Contract or Grant No. Project 0-6071	
12. Sponsoring Agency Name and Address Texas Department of Transportation Research and Technology Implementation Office P.O. Box 5080 Austin, Texas 78763-5080				13. Type of Report and Period Covered Technical/Test Report: September 2007 – August 2009	
				14. Sponsoring Agency Code	
15. Supplementary Notes Project performed in cooperation with the Texas Department of Transportation and the Federal Highway Administration. Project Title: Development of Roadside Safety Devices for Very High Speed Roadways URL: http://tti.tamu.edu/documents/0-6071-2.pdf					
16. Abstract <p>As TxDOT plans for future expansion of the state’s highway network, interest in higher design speeds has been expressed as a means of promoting faster and more efficient travel and movement of goods within the state. TxDOT funded project 0-6071 as part of a proactive consideration of safety on these high-speed facilities. This project began the process of developing roadside safety hardware suitable for use on high-speed highways. The impact conditions selected for the design, testing, and evaluation of this high-speed hardware include a speed of 85 mi/h and an angle of 25 degrees for barrier impacts. The design vehicles are those specified by the pending AASHTO <i>Manual for Assessing Safety Hardware (MASH)</i> and include a 5000-lb, ½-ton, 4-door pickup truck and a 2425-lb passenger car.</p> <p>After consideration of several barrier systems, two designs were selected for further evaluation through full-scale crash testing. These included an energy absorbing bridge rail concept and a modified wood post thrie beam guardrail. The results of the full-scale crash testing are presented and recommendations for future research are discussed.</p>					
17. Key Words High-Speed Roadways, Bridge Rail, Longitudinal Barriers, Crash Testing, Roadside Safety			18. Distribution Statement No restrictions. This document is available to the public through NTIS: National Technical Information Service Springfield, Virginia 22161 http://www.ntis.gov		
19. Security Classif.(of this report) Unclassified		20. Security Classif.(of this page) Unclassified		21. No. of Pages 150	22. Price

EVALUATION OF BARRIERS FOR VERY HIGH SPEED ROADWAYS

by

Roger P. Bligh, P.E.
Research Engineer
Texas Transportation Institute

Nauman M. Sheikh
Associate Transportation Researcher
Texas Transportation Institute

Akram Y. Obu-Odeh
Associate Research Scientist
Texas Transportation Institute

and

Wanda L. Menges
Research Specialist
Texas Transportation Institute

Report 0-6071-2
Project 0-6071
Project Title: Development of Roadside Safety Devices
for Very High Speed Roadways

Performed in cooperation with the
Texas Department of Transportation
and the
Federal Highway Administration

January 2010
Published: March 2010

TEXAS TRANSPORTATION INSTITUTE
The Texas A&M University System
College Station, Texas 77843-3135

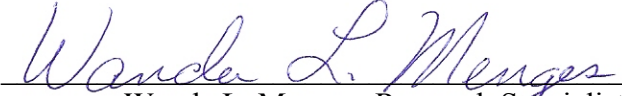
DISCLAIMER

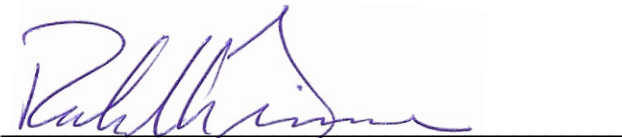
This research was performed in cooperation with the Texas Department of Transportation (TxDOT) and the Federal Highway Administration (FHWA). The contents of this report reflect the views of the authors, who are responsible for the facts and the accuracy of the data presented herein. The contents do not necessarily reflect the official view or policies of the FHWA or TxDOT. This report does not constitute a standard, specification, or regulation, and its contents are not intended for construction, bidding, or permit purposes. In addition, the above listed agencies assume no liability for its contents or use thereof. The United States Government and the State of Texas do not endorse products or manufacturers. Trade or manufacturers' names appear herein solely because they are considered essential to the object of this report. The engineer in charge of the project was Roger P. Bligh, P.E. (Texas, #78550).

TTI PROVING GROUND DISCLAIMER

The results of the crash testing reported herein apply only to the article being tested.




Wanda L. Menges, Research Specialist
Deputy Quality Manager


Richard A. Zimmer, Senior Research Specialist
Test Facility Manager
Quality Manager
Technical Manager

ACKNOWLEDGMENTS

This research project was conducted under a cooperative program between the Texas Transportation Institute, the Texas Department of Transportation, and the Federal Highway Administration. The TxDOT project director for this research was Bobby Dye (DES). Rory Meza (DES), John Holt (BRG), Michael McKissick (AUS), Jon Ries (BRG), and Edward Sewell (WFS) served as project advisors, and Wade Odell (RTI) was the TxDOT research engineer. The authors acknowledge and appreciate their guidance and assistance.

This work was partially supported by the U.S. Department of Transportation, the Illinois Department of Transportation, and the Transportation Research and Analysis Computing Center. Their support in providing computational resources for simulation analyses is greatly appreciated.

TABLE OF CONTENTS

	Page
LIST OF FIGURES	x
LIST OF TABLES	xiii
CHAPTER 1. INTRODUCTION	1
INTRODUCTION	1
DESIGN IMPACT CONDITIONS	1
OBJECTIVES/SCOPE OF RESEARCH	2
CHAPTER 2. DESIGN AND ANALYSES OF AN ENERGY ABSORBING BRIDGE RAIL..	3
INTRODUCTION	3
DESIGN AND ANALYSIS	3
Rail Size	5
Rail Height	5
Pipe Thickness	7
Pipe Spacing	7
CONCLUSIONS	10
CHAPTER 3. ANALYSIS OF A MODIFIED WOOD POST THRIE BEAM GUARDRAIL SYSTEM.....	11
MODELING AND SIMULATION	11
CONCLUSIONS	16
CHAPTER 4. FULL-SCALE CRASH TEST PROCEDURES	17
TEST FACILITY	17
CRASH TEST CONDITIONS	17
EVALUATION CRITERIA	18
CHAPTER 5. FULL-SCALE CRASH TESTING OF THE ENERGY ABSORBING BRIDGE RAIL	19
TEST ARTICLE	19
Design and Construction	19
Material Specifications	19
TEST NO. 460719-1 (<i>MASH</i> TEST 3-10)	22
Test Designation and Actual Impact Conditions	22
Test Vehicle	22
Weather Conditions	22
Test Description	22
Damage to Test Installation	25
Vehicle Damage	25
Occupant Risk Factors	29
Assessment of Test Results	29

TABLE OF CONTENTS

	Page
TEST NO. 460719-2 (<i>MASH</i> TEST DESIGNATION 3-11).....	32
Test Designation and Actual Impact Conditions	32
Test Vehicle	32
Weather Conditions	32
Test Description	32
Damage to Test Installation	35
Vehicle Damage.....	35
Occupant Risk Factors	35
Assessment of Test Results.....	41
CHAPTER 6. FULL-SCALE CRASH TESTING OF THE MODIFIED WOOD POST THRIE BEAM GUARDRAIL	43
TEST ARTICLE.....	43
Design and Construction.....	43
Material Specifications	43
Soil Conditions.....	43
TEST NO. 460719-3 (<i>MASH</i> TEST DESIGNATION 3-11).....	46
Test Vehicle	46
Weather Conditions	46
Test Description	46
Damage to Test Installation	49
Vehicle Damage.....	49
Occupant Risk Factors	49
Assessment of Test Results.....	55
CHAPTER 7. SUMMARY AND CONCLUSIONS	57
ENERGY ABSORBING BRIDGE RAIL	57
MODIFIED WOOD POST THRIE BEAM GUARDRAIL.....	58
CHAPTER 8. IMPLEMENTATION STATEMENT.....	63
BRIDGE RAIL	63
GUARDRAIL.....	64
REFERENCES	67
APPENDIX A. CRASH TEST AND DATA ANALYSIS PROCEDURES	69
ELECTRONIC INSTRUMENTATION AND DATA PROCESSING	69
ANTHROPOMORPHIC DUMMY INSTRUMENTATION.....	70
PHOTOGRAPHIC INSTRUMENTATION AND DATA PROCESSING	70
TEST VEHICLE PROPULSION AND GUIDANCE.....	70
APPENDIX B. DETAILS OF THE HIGH-SPEED ENERGY-ABSORBING BRIDGE RAIL .	73

TABLE OF CONTENTS

	Page
APPENDIX C. TEST VEHICLE PROPERTIES AND INFORMATION	83
APPENDIX D. SEQUENTIAL PHOTOGRAPHS	93
APPENDIX E. VEHICLE ANGULAR DISPLACEMENTS AND ACCELERATIONS	103
APPENDIX F. DETAILS OF THE HIGH-SPEED THRIE BEAM GUARDRAIL.....	125
APPENDIX G. SOIL STRENGTH DOCUMENTATION	135

LIST OF FIGURES

Figure	Page
Figure 2.1. Conceptual Drawing of the Energy Absorbing Bridge Rail.....	3
Figure 2.2. Finite Element Model of the Energy Absorbing Bridge Rail.....	4
Figure 2.3. Finite Element Models Used in the Simulation Analysis.....	5
Figure 2.4. Pickup Truck Redirects but has a High Roll after Impact with the Rail at 31-Inch Rail Height.	6
Figure 2.5. Deformation of the Small Car after Impact with the Rail at 36-Inch Rail Height. ..	6
Figure 2.6. Performance of Schedule 40 (Top) and Schedule 80 (Bottom) Pipe Spacers.....	8
Figure 2.7. Affect of Pipe Spacing	9
Figure 3.1. Cross Section of the Modified Wood Post Thrie-Beam System from Drawings and Model.	12
Figure 3.2. System Layout with Vehicle Impact Location.	12
Figure 3.3. Iso-Parametric View of the 2270 kg Vehicle Set Up with the Modified Thrie-Beam Rail.	13
Figure 3.4. Sequential Images of 2270P Impact with Modified Wood Post Thrie Beam Guardrail.....	14
Figure 3.5. Impact at Time of Maximum Rail Deflection.	14
Figure 3.6. Longitudinal Acceleration History for CG of the 2270 kg Vehicle.	15
Figure 3.7. Damage to the Vehicle in the 85 mi/h Simulation.	15
Figure 5.1. Details of the High-Speed Energy-Absorbing Bridge Rail.	20
Figure 5.2. Energy-Absorbing Bridge Rail Installation before Test Nos. 470619-1 and 2.	21
Figure 5.3. Vehicle/Installation Geometrics for Test No. 460719-1.	23
Figure 5.4. Vehicle before Test No. 460719-1.	24
Figure 5.5. Installation after Test No. 460719-1.....	26
Figure 5.6. Vehicle after Test No. 460719-1.	27
Figure 5.7. Interior of Vehicle for Test No. 460719-1.	28
Figure 5.8. Summary of Results for <i>MASH</i> Test 3-10 on the Energy-Absorbing Bridge Rail.	30
Figure 5.9. Vehicle/Installation Geometrics for Test No. 460719-2.	33
Figure 5.10. Vehicle before Test No. 460719-2.	34
Figure 5.11. After Impact Trajectory Path for Test No. 460719-2.	36
Figure 5.12. Installation after Test No. 460719-2.....	37
Figure 5.13. Vehicle after Test No. 460719-2.	38
Figure 5.14. Interior of Vehicle for Test No. 460719-2.	39
Figure 5.15. Summary of Results for <i>MASH</i> Test 3-11 on the Energy-Absorbing Bridge Rail.	40
Figure 6.1. Details of the High-Speed Thrie Beam Guardrail.	44
Figure 6.2. Test Article/Installation before Test No. 470619-3.....	45
Figure 6.3. Vehicle/Installation Geometrics for Test No. 460719-3.	47
Figure 6.4. Vehicle before Test No. 460719-3.	48
Figure 6.5. After Impact Trajectory Path for Test No. 460719-3.	50
Figure 6.6. Installation after Test No. 460719-3.....	51
Figure 6.7. Vehicle after Test No. 460719-3.	52

LIST OF FIGURES

Figure		Page
Figure 6.8.	Interior of Vehicle for Test No. 460719-3.	53
Figure 6.9.	Summary of Results for <i>MASH</i> Test 3-11 on the Thrie Beam Guardrail.....	54
Figure C1.	Vehicle Properties for Test No. 406719-1.....	83
Figure C2.	Vehicle Properties for Test No. 460719-2.....	86
Figure C3.	Vehicle Properties for Test No. 460719-3.....	89
Figure D1.	Sequential Photographs for Test No. 460719-1 (Overhead and Frontal Views)....	93
Figure D2.	Sequential Photographs for Test No. 460719-1 (Rear View).	95
Figure D3.	Sequential Photographs for Test 460719-2 (Overhead and Frontal Views).	96
Figure D4.	Sequential Photographs for Test 460719-2 (Rear View).	98
Figure D5.	Sequential Photographs for Test No. 460719-3 (Overhead and Frontal Views)....	99
Figure D6.	Sequential Photographs for Test No. 460719-3 (Rear View).	101
Figure E1.	Vehicle Angular Displacements for Test No. 460719-1.	103
Figure E2.	Vehicle Longitudinal Accelerometer Trace for Test No. 460719-1 (Accelerometer Located at Center of Gravity).....	104
Figure E3.	Vehicle Lateral Accelerometer Trace for Test No. 460719-1 (Accelerometer Located at Center of Gravity).....	105
Figure E4.	Vehicle Vertical Accelerometer Trace for Test No. 460719-1 (Accelerometer Located at Center of Gravity).....	106
Figure E5.	Vehicle Longitudinal Accelerometer Trace for Test No. 460719-1 (Accelerometer Located over Rear Axle).	107
Figure E6.	Vehicle Lateral Accelerometer Trace for Test No. 460719-1 (Accelerometer Located over Rear Axle).	108
Figure E7.	Vehicle Vertical Accelerometer Trace for Test No. 460719-1 (Accelerometer Located over Rear Axle).	109
Figure E8.	Vehicle Angular Displacements for Test No. 460719-2.	110
Figure E9.	Vehicle Longitudinal Accelerometer Trace for Test No. 460719-2 (Accelerometer Located at Center of Gravity).....	111
Figure E10.	Vehicle Lateral Accelerometer Trace for Test No. 460719-2 (Accelerometer Located at Center of Gravity).....	112
Figure E11.	Vehicle Vertical Accelerometer Trace for Test No. 460719-2 (Accelerometer Located at Center of Gravity).....	113
Figure E12.	Vehicle Longitudinal Accelerometer Trace for Test No. 460719-2 (Accelerometer Located over Rear Axle).	114
Figure E13.	Vehicle Lateral Accelerometer Trace for Test No. 460719-2 (Accelerometer Located over Rear Axle).	115
Figure E14.	Vehicle Vertical Accelerometer Trace for Test No. 460719-2 (Accelerometer Located over Rear Axle).	116
Figure E15.	Vehicle Angular Displacements for Test No. 460719-3.	117
Figure E16.	Vehicle Longitudinal Accelerometer Trace for Test No. 460719-3 (Accelerometer Located at Center of Gravity).....	118
Figure E17.	Vehicle Lateral Accelerometer Trace for Test No. 460719-3 (Accelerometer Located at Center of Gravity).....	119

LIST OF FIGURES

Figure		Page
Figure E18.	Vehicle Vertical Accelerometer Trace for Test No. 460719-3 (Accelerometer Located at Center of Gravity).....	120
Figure E19.	Vehicle Longitudinal Accelerometer Trace for Test No. 460719-3 (Accelerometer Located over Rear Axle).	121
Figure E20.	Vehicle Lateral Accelerometer Trace for Test No. 460719-3 (Accelerometer Located over Rear Axle).	122
Figure E21.	Vehicle Vertical Accelerometer Trace for Test No. 460719-3 (Accelerometer Located over Rear Axle).	123
Figure G1.	Test Day Static Soil Strength Documentation.....	135
Figure G2.	Summary of Strong Soil Test Results for Establishing Installation Procedure....	136

LIST OF TABLES

Table		Page
Table 7.1.	Performance Evaluation Summary for <i>MASH</i> Test 3-10 on the Energy-Absorbing Bridge Rail.....	59
Table 7.2.	Performance Evaluation Summary for <i>MASH</i> Test 3-11 on the Energy-Absorbing Bridge Rail.....	60
Table 7.3.	Performance Evaluation Summary for <i>MASH</i> Test 3-11 on the Thrie Beam Guardrail.....	61
Table C1.	Exterior Crush Measurements for Test No. 406719-1.....	84
Table C2.	Occupant Compartment Measurements for Test No. 460719-1.....	85
Table C3.	Exterior Crush Measurements for Test No. 460719-2.....	87
Table C4.	Occupant Compartment Measurements for Test No. 460719-2.....	88
Table C5.	Exterior Crush Measurements for Test No. 460719-3.....	90
Table C6.	Occupant Compartment Measurements for Test No. 460719-3.....	91

CHAPTER 1. INTRODUCTION

INTRODUCTION

The Texas Department of Transportation (TxDOT) is embarking on a multi-decade effort to expand the state's transportation system. TxDOT has expressed an interest in using higher design speeds (above 80 mi/h) for some of these facilities to promote faster and more efficient travel within the state.

Under National Cooperative Highway Research Program (NCHRP) *Report 350*, roadside hardware was tested at a speed of 62 mi/h for passenger vehicles (1). The update to *NCHRP Report 350*, known as the American Association of State Highway and Transportation Officials (AASHTO) *Manual for Assessing Safety Hardware (MASH)*, retains this design impact speed (2). This impact speed was derived from analyses of reconstructed crash data collected on roads with design speeds up to 70 mi/h. It is reasonable to expect that both posted speeds and operating speeds will exceed these values on some of the high-speed roadways being considered by TxDOT.

The increased speeds will place more demand on roadside safety features. The ability of existing roadside safety features to accommodate more severe, higher energy impacts is not known. For economic reasons, many existing roadside safety features are optimized for the current design impact conditions. Consequently, they have little or no factor of safety for accommodating more severe impacts. Thus, existing safety devices may not be appropriate for use on facilities with higher design or operating speeds and new designs may be required.

DESIGN IMPACT CONDITIONS

At the beginning of the project, the researchers met with the project monitoring committee to establish design impact conditions for the development of roadside safety features for use on roadways with high design speeds. Impact conditions are generally defined by vehicle type, vehicle mass, impact speed, and impact angle. Under TxDOT research project 0-5544, "*Development of High Speed Roadway Design Criteria and Evaluation of Roadside Safety Features*," recommended design impact speeds for roadways with high design speeds were derived (3).

The roadway design speed selected for the project was 100 mi/h. Based on this roadway design speed and recommendations developed under research project 0-5544, a design impact speed of 85 mi/h was selected for the impact performance evaluation of high-speed roadside safety hardware under this project. Under project 0-5544, researchers found little justification for decreasing the impact angle as the impact speed increases. It was recommended that an impact angle of 25 degrees be maintained for crash testing roadside safety devices for very high speed roadways until better data become available. It was agreed to follow this recommendation, and a design impact angle of 25 degrees was chosen for this project.

Although it was not yet published during the performance of this project, it was decided that the testing and evaluation of safety features under this project follow the *MASH* guidelines. *MASH* has superseded *NCHRP Report 350* as the recommended procedures for the impact performance evaluation of roadside safety features. The design test vehicles in *MASH* include a 2425-lb passenger car and a 5000-lb, ½-ton, 4-door, pickup truck. Both of these vehicles are heavier than the design vehicles utilized under *NCHRP Report 350*.

OBJECTIVES/SCOPE OF RESEARCH

The objective of this research was to initiate the development of roadside safety hardware suitable for use on very high speed highways. Engineering analyses and finite element simulations were used to evaluate the impact performance of selected roadside safety devices subjected to very high-speed impacts. Two systems were selected for further evaluation through full-scale crash tests: an energy-absorbing bridge rail concept and a modified wood post thrie beam guardrail system.

This report presents the results of the analyses, testing, and evaluation of these two barrier systems. [Chapter 2](#) presents the design and analysis of the energy absorbing bridge rail concept. [Chapter 3](#) summarizes the simulation analyses of the modified wood post thrie beam. The full scale crash testing of the energy absorbing bridge rail and modified wood post thrie beam are presented in [Chapter 4](#) and [Chapter 5](#), respectively. A summary of the research results and conclusions is presented in [Chapter 6](#), and implementation recommendations are discussed in [Chapter 7](#).

CHAPTER 2. DESIGN AND ANALYSES OF AN ENERGY ABSORBING BRIDGE RAIL

INTRODUCTION

The researchers developed an energy absorbing bridge rail concept to try to accommodate *MASH* testing criteria at impact speeds of 85 mi/h. Several design parameters related to this concept were evaluated using finite element analyses. Details of the design and analysis process are presented in this chapter.

DESIGN AND ANALYSIS

TxDOT engineers requested that the bridge rail system incorporate a concrete parapet. Several common concrete barrier profiles were evaluated in a previous phase of this research using finite element simulation (4). While the performance issues varied depending on the profile of the concrete barrier, none were able to meet the *MASH* evaluation criteria for the high-speed impact conditions.

Therefore, the basic concept of the energy absorbing bridge rail shown in [Figure 2.1](#) was conceived. This concept involves using a vertical concrete wall to support two tubular steel rails. Pipe spacers are incorporated into the system to offset the tubular rails from the rigid concrete parapet and to function as an energy-absorbing mechanism. The spacers are intended to deform upon vehicle impact and, thereby, absorb some of the vehicle's kinetic energy to lessen the impact severity below that of impacting a rigid concrete wall.

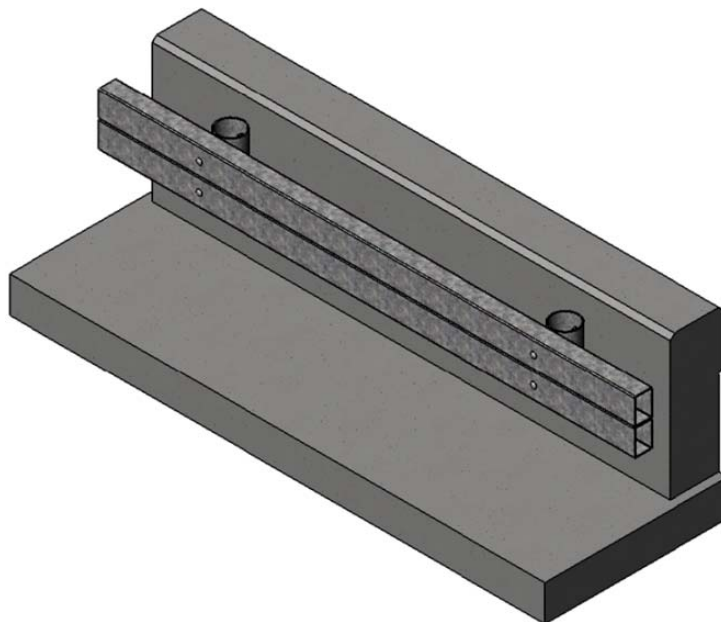


Figure 2.1. Conceptual Drawing of the Energy Absorbing Bridge Rail.

Vehicle impact simulations were performed on the conceptual design using the commercially available finite element analysis code LS-DYNA (5). LS-DYNA is a general purpose finite element code capable of simulating complex nonlinear dynamic impact problems. The performance of the bridge rail was evaluated following *MASH* criteria for a test level 3 (TL-3) impact, except that the impact speed of the vehicles was 85 mi/h rather than 62 mi/h.

The finite element model of the rail is depicted in Figure 2.2. The 32-inch tall vertical concrete wall was modeled using a rigid material representation. The 12-inch tall, 8-inch diameter Schedule 40 pipe spacers were modeled using an elastic-plastic material representation with the properties of ASTM A53 steel. In the conceptual design, the pipes spacers were connected to the wall using bolts that pass through the concrete wall. A second bolt or stud is used to attach the two 6-inch \times 4-inch \times $\frac{1}{4}$ -inch tubular steel rails to the traffic side of the pipe spacer. The two tubular steel rail sections were additionally connected to each other mid-span between pipe spacers using a through-bolt that passed from the top surface of the top rail to the bottom surface of the bottom rail.

Since no significant damage of these bolts was anticipated, they were modeled using nodal-rigid-body constraints in LS-DYNA. The use of nodal rigid body constraints in lieu of an explicit bolt model reduces the complexity of the model by eliminating edge contacts between the bolt shaft and hole that are generally difficult to numerically enforce. It also reduces computational time by eliminating the need for further mesh refinement.

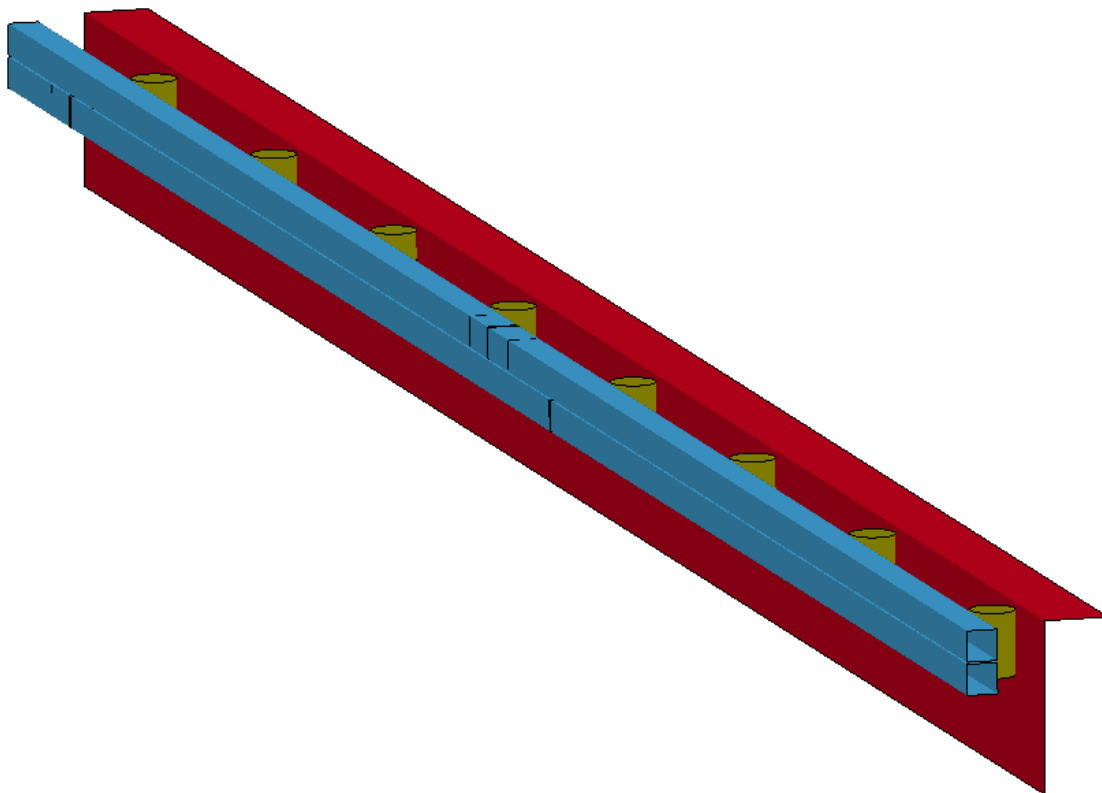


Figure 2.2. Finite Element Model of the Energy Absorbing Bridge Rail.

To evaluate the performance of the bridge rail under *MASH* criteria, impact simulations were performed with models of a pickup truck and small passenger car. The pickup truck model used was a ½-ton, 4-door Chevrolet Silverado with a weight of 5000 lb (see [Figure 2.3](#)). This model was developed by the National Crash Analysis Center under sponsorship from Federal Highway Administration and the National Highway Traffic Safety Administration.

The *MASH* test matrix for longitudinal barriers also includes a test with a 2425-lb passenger car. Since a public domain finite element model of this design vehicle was not available at the time of this research, the researchers chose to use a 2900-lb Dodge Neon model to evaluate the impact performance of the bridge rail for test designation 3-10 (see [Figure 2.3](#)). This model was considered to be a reasonable alternative for the 2425-lb design passenger car vehicle in a previous phase of this research study (4). In all of the simulations performed, the vehicle impacted the rail at a speed of 85 mi/h and an angle of 25 degrees.

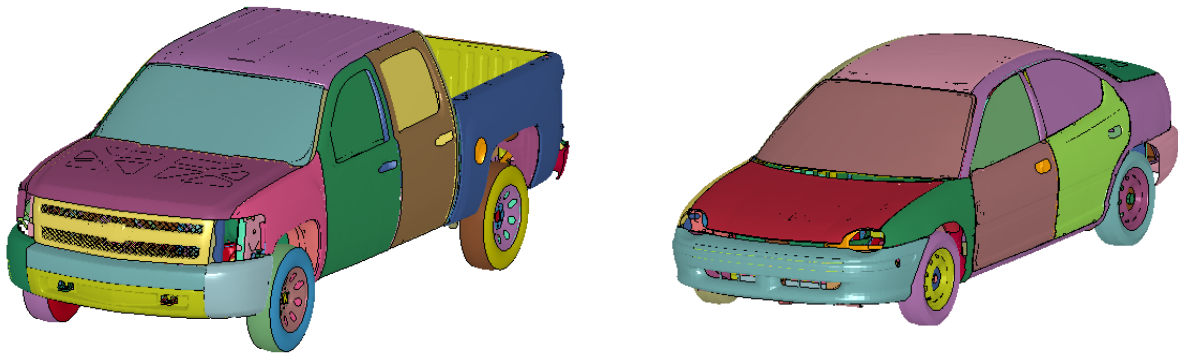


Figure 2.3. Finite Element Models Used in the Simulation Analysis.

Several key design parameters were evaluated using the finite element simulations. Findings from these simulation analyses are presented below.

Rail Size

The researchers initially performed a simulation with the pickup truck vehicle impacting two 6-inch × 4-inch × 0.25-inch tubular rail sections. The impact resulted in significant deformation of the steel tubes. A significant reduction in the rail deformation was observed in a subsequent impact simulation that incorporated two 6-inch × 6-inch × 0.25-inch tubular rail members. To reduce maintenance cost by reducing the amount of damage to the tubular rail elements, the researchers selected the 6-inch × 6-inch × 0.25-inch steel tubes for use in the bridge rail system.

Rail Height

The initial height of the tubular steel rails evaluated through simulation was 27 inches. The results of the simulation showed the pickup truck rolling over as it was redirected by the barrier. In a subsequent design iteration, the height of the rail was raised to 31 inches. Even though significant roll was observed (see [Figure 2.4](#)), the pickup truck did not rollover.

Although vehicle stability was judged to be marginal, the rail height was not further increased due to concern that it would degrade the impact performance of the small car as discussed below.

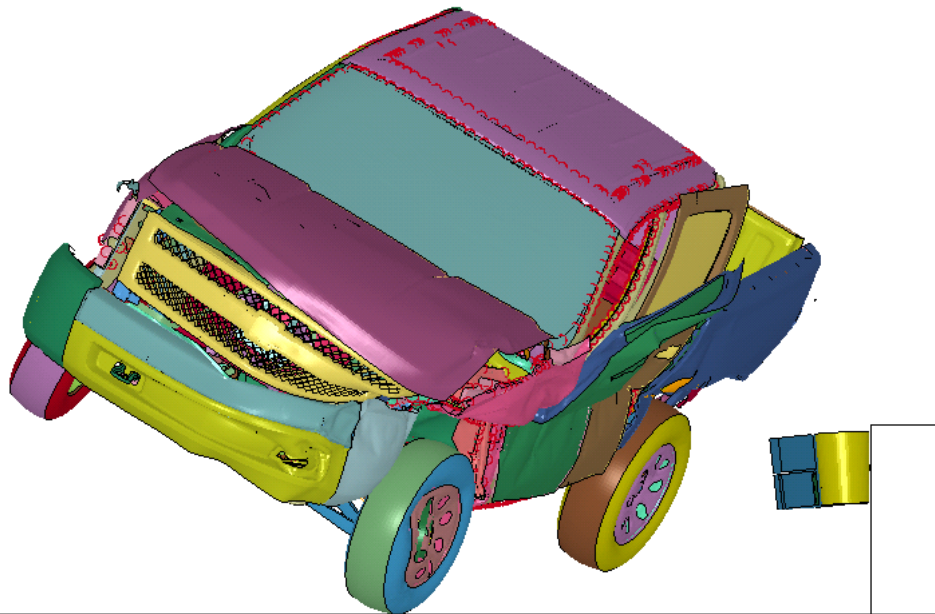


Figure 2.4. Pickup Truck Redirects but has a High Roll after Impact with the Rail at 31-Inch Rail Height.

A simulation with the 2900-lb passenger car model was performed with the tubular rails set at a height of 31 inches to the top of the stacked rails. The car was redirected in a stable manner. However, the high impact severity resulted in an occupant impact velocity (OIV) that was at the allowable threshold of 12 m/s and significant damage to the vehicle's occupant compartment as shown in Figure 2.5. The occupant compartment deformation was aggravated by the proximity of the tubular steel rails to the vehicles A-pillar. It was hypothesized that if the height of the steel rails could be reduced, or if the two rail tubes were separated such that the bottom rail could engage the small car at a lower height, it might prevent the vehicle from trying to under-ride the rails, thus lowering the occupant compartment deformation.

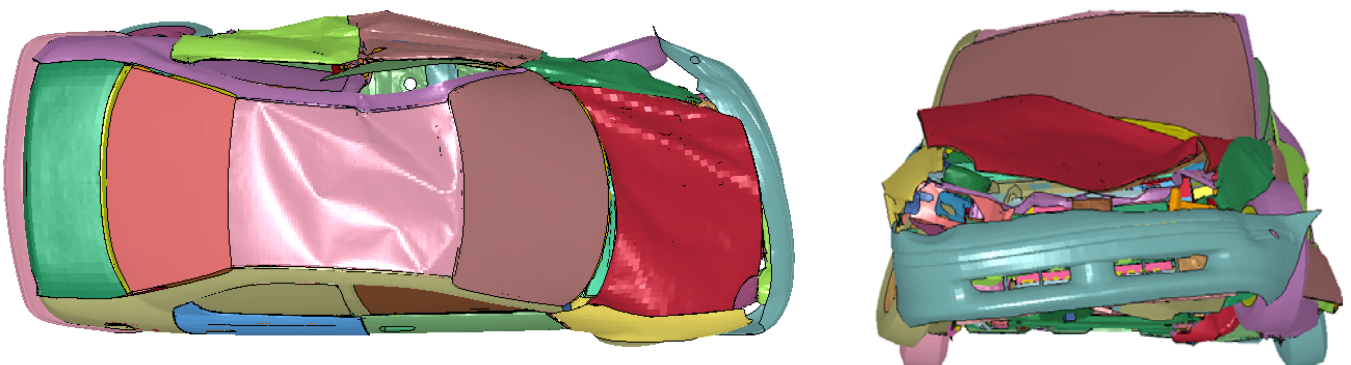


Figure 2.5. Deformation of the Small Car after Impact with the Rail at 36-Inch Rail Height.

It was already known that reducing the height of the rail by four inches results in rollover of the pickup truck. The researchers performed another small car simulation with the height of the tubular steel rails lowered two inches (i.e., 29 inch mounting height). The simulation of the small car into the bridge rail with a 2-inch reduction in rail height did not result in any significant reduction in occupant compartment deformation. The researchers then performed another simulation in which the two 6-inch × 6-inch rail sections were separated from one another. The height of the upper rail was kept at 31 inches to help maintain stability of the pickup truck. The height of the lower rail was reduced by 4 inches to determine if lower interaction on the small car could help reduce occupant compartment deformation.

The results of this simulation did not show any significant differences in the occupant compartment deformation of the small car compared to that observed in the case of the stacked rail members. The height of the rail was thus kept at 31 inches to the top of the rail in the final design. Marginal impact performance was predicted for both design vehicles. Significant vehicle roll was expected for the pickup truck impact, and high occupant compartment deformation was expected for the small passenger car.

Pipe Thickness

Results of the simulation analysis indicated that some of the Schedule 40 pipe spacers collapsed quickly during the pickup truck impact prior to any substantial redirection of the vehicle. Once the pipes collapse in the region of impact, the stiffness of the rail increases significantly and the energy management becomes less controlled. It was theorized that if the rate of collapse of the pipe spacers could be reduced through the use of stiffer pipe sections, the impulse on the pickup truck would be reduced and vehicle stability could be improved. To investigate this theory, a pickup truck impact simulation was performed with thicker Schedule 80 pipe spacers substituted for the Schedule 40 pipe spacers. The results were not significantly different from those for the system with Schedule 40 pipes (see [Figure 2.6](#)). Furthermore, none of the Schedule 80 pipes spacers were fully collapsed and this raised concern that the added stiffness could further increase the severity of the small car impact. Therefore, Schedule 40 pipes spacers were used in the final design.

Pipe Spacing

The researchers also evaluated the affect of pipe spacing on the overall performance of the rail. It was expected the by placing the pipes closer, the collapse of the pipes will occur at a slower rate, which may reduce the occupant compartment deformation in the small passenger vehicle and/or improve stability of the pickup. A small passenger car impact simulation was performed with the Schedule 40 pipes spacing on 4-ft centers along the length of the rail. The results were compared to those for the rail with 6.25-ft pipe spacing. The results are shown in [Figure 2.7](#). While the pipes collapsed at a slower rate when placed closer together, no significant differences were observed in the occupant compartment deformation. Thus the larger pipe spacing of 6.25-ft was selected for the final design.

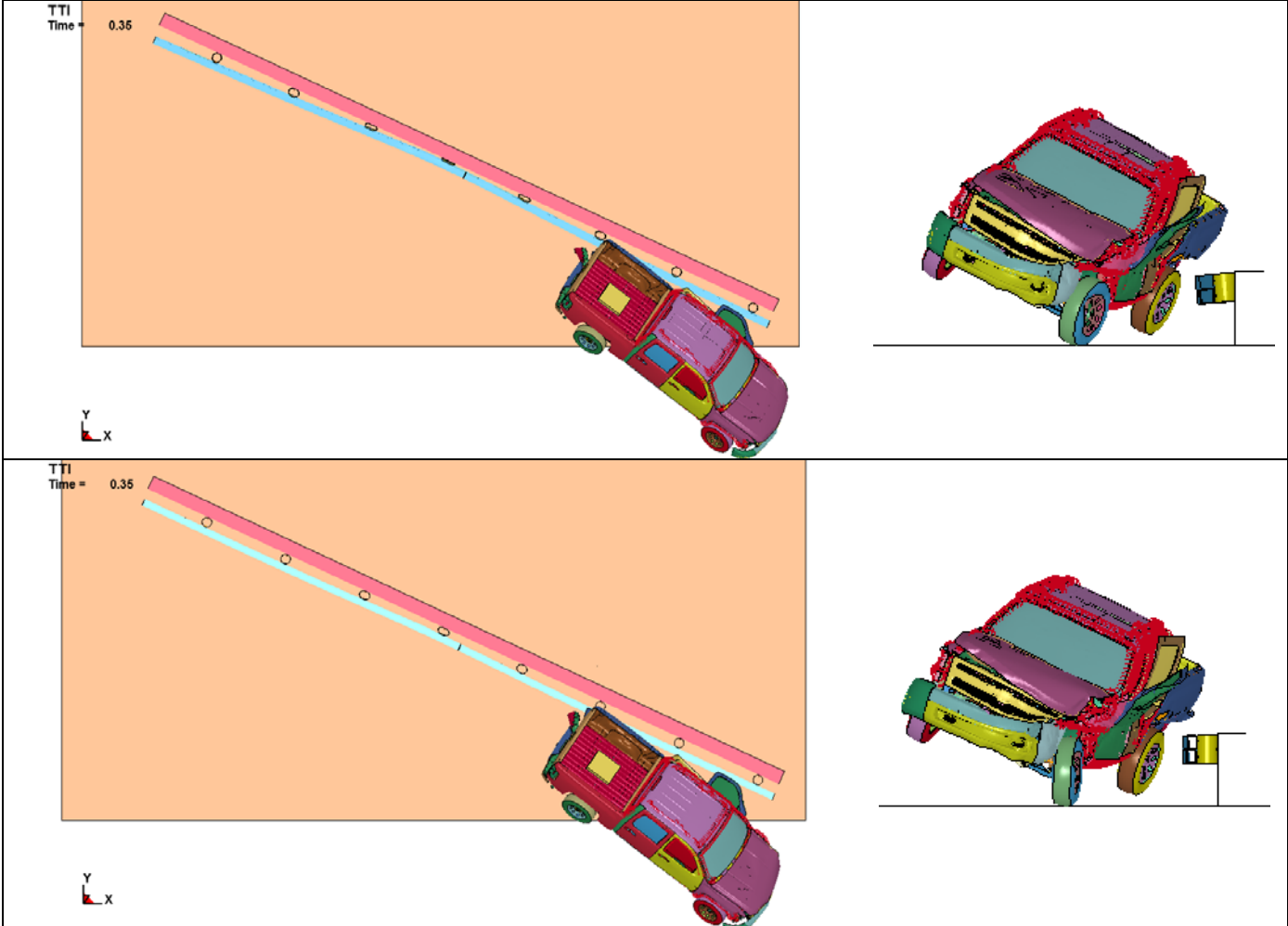
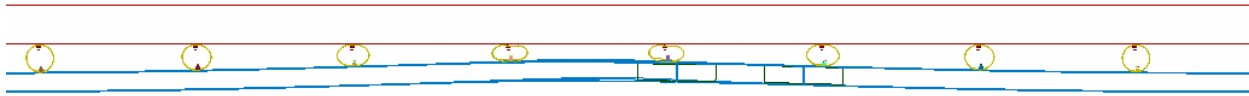


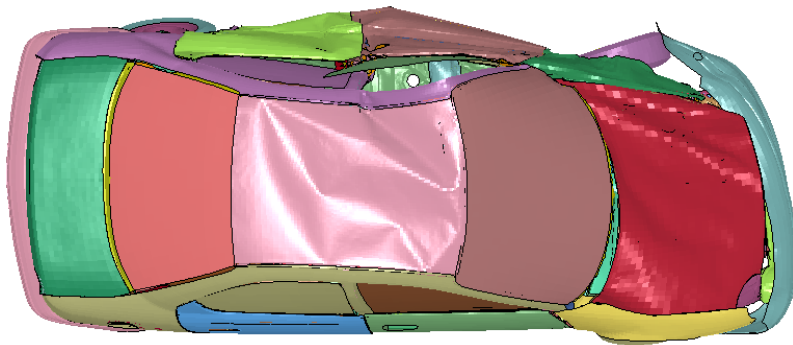
Figure 2.6. Performance of Schedule 40 (Top) and Schedule 80 (Bottom) Pipe Spacers.



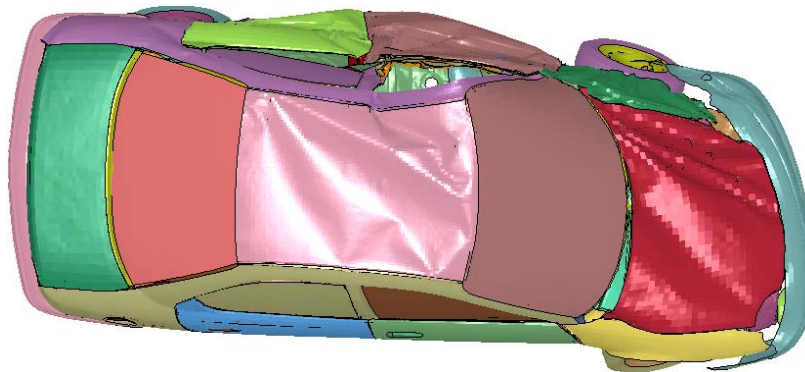
6.25-ft pipe spacing



4-ft pipe spacing



6.25-ft pipe spacing



4-ft pipe spacing

Figure 2.7. Affect of Pipe Spacing.

CONCLUSIONS

Based on the simulation analyses, the results of the 85 mi/h impacts into the energy absorbing bridge rail were expected to be marginal for both the small car and pickup truck. Even though the pickup truck did not roll over in the simulation analysis, the results predicted a high vehicle roll angle during redirection, which had the possibility of leading to a rollover in an actual crash test. The small passenger car impact simulations indicated an occupant impact velocity near the maximum acceptable value of 12 m/s and high deformation of the occupant compartment, more specifically to the A-pillar, side doors, front impact wheel area, and the windshield. However, although the results were predicted to be marginal, the analyses did not indicate any obvious failure for either vehicle. Therefore, after consultation with the project director, a decision was made to subject the bridge rail design to further evaluation through full-scale crash testing. The results of the crash testing are presented in [Chapter 4](#).

CHAPTER 3. ANALYSIS OF A MODIFIED WOOD POST THRIE BEAM GUARDRAIL SYSTEM

In the first year of this project, finite element models of the selected hardware devices were developed, validated, and used in high-speed impact simulations to assess the ability of each device to meet safety performance guidelines for very high speed applications. One of the guardrail systems evaluated was the modified thrie beam.

The modified thrie beam guardrail is the result of improvements to the standard thrie beam guardrail and was specifically designed as a high-containment system to reduce the rollover incidences for heavy vehicle impacts. The system incorporates deep offset blocks that are designed to reduce snagging interaction between the impacting vehicle and support posts, and help keep the thrie beam rail vertically aligned during impact to reduce the probability of vehicle climb, vaulting, and/or instability.

It was observed in the high-speed simulations that the steel blockouts deformed and collapsed as the vehicle progressed through the system. This reduced the offset distance between the rail and posts and led to significant interaction between the front wheel assembly and the guardrail support posts. The front wheel assembly was observed to ride over the twisted and bent steel posts, which in turn imparted a vertical acceleration to the vehicle that helped it climb over the rail.

The researchers identified some modifications designed to mitigate the climbing behavior of the pickup truck. The goal of these design modifications was to reduce the interaction between the front wheel assembly and the posts by preventing the collapse of the blockouts that offset the rail from the posts and changing the failure mode of the posts.

It was recommended that the steel posts and the blockouts used in the current modified thrie beam design be replaced with wood posts and wood blockouts. Replacing the W14×22 steel blockout with an appropriate depth wood blockout would prevent the collapse of the blockouts during impact, thus maintaining the desired spacing between the vehicle and the posts. It was further recommended that the height of the wood blockout be selected such that the lower corrugation of the thrie beam is unsupported. This permits the bottom of the thrie beam to stay more vertically aligned during impact, further reducing the probability of vehicle climb, vaulting, and/or instability.

Replacing the W6×9 steel posts with 6-inch × 8-inch wood posts would eliminate the lateral torsional bending mode of failure observed in the steel posts. It was theorized that this will permit the posts to displace further laterally through the soil and further reduce the interaction between the wheels and posts. However, it was recognized that the fracture of the wood posts could lead to pocketing of the vehicle in the rail system.

MODELING AND SIMULATION

The modified wood post thrie-beam guardrail that was modeled is shown in [Figure 3.1](#). The thrie beam rail is mounted on 6-inch × 8 inch wood posts at a height of 34 inches. The rail is offset from the post using partial depth 6-inch × 12-inch wood spacer blocks. The bottom

corrugation of the thrie beam rail is left unsupported. The rail and the blockout are attached to the post using a 5/8-inch diameter × 22-inch long bolt.

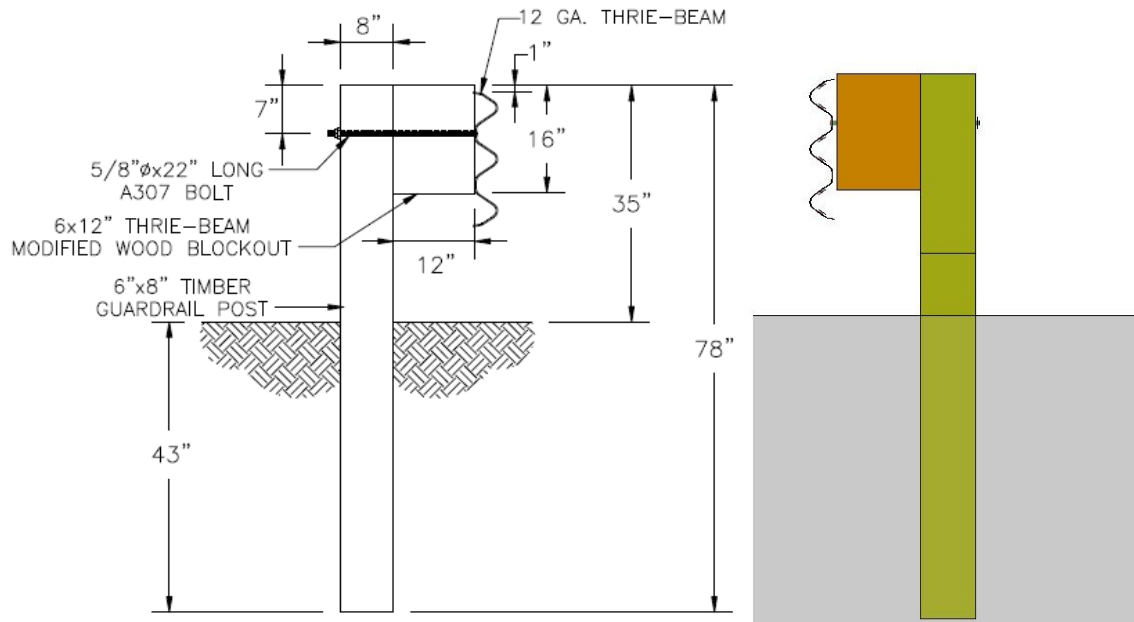


Figure 3.1. Cross Section of the Modified Wood Post Thrie-Beam System from Drawings and Model.

The length of the system modeled was 106 ft-3 inches and had 17 wood posts spaced 6 ft-3 inches center to center as shown in Figure 3.2. The ends of the thrie-beam rail were attached to springs that were assigned properties representative of the stiffness of a 37.5-ft long, *NCHRP Report 350* TL-3 compliant terminal system.

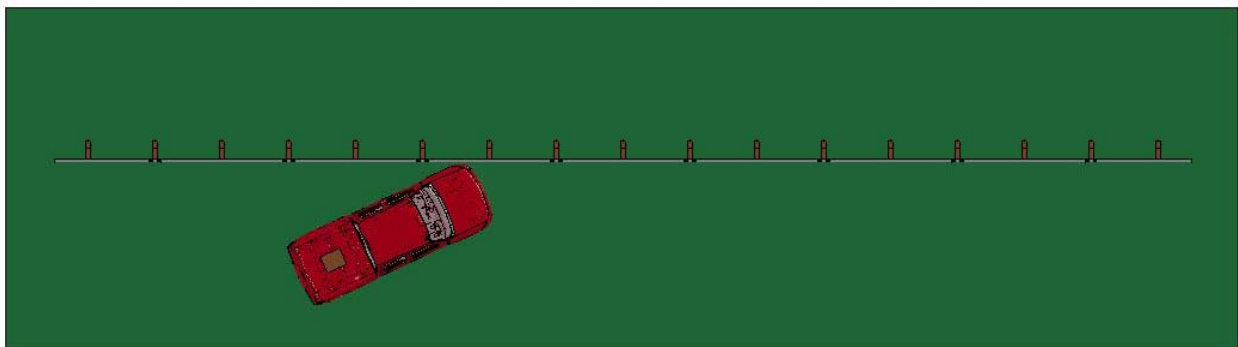


Figure 3.2. System Layout with Vehicle Impact Location.

The thrie beam rail section was assigned material properties based on published tensile tests of AASHTO M180 steel obtained from guardrail samples. This material was represented through an elastic-plastic definition in LS-DYNA. The soil surrounding the posts was assigned a pressure sensitive geological material definition with parameters that are representative of the AASHTO M147 road base material that is commonly used in test installations. The wood posts were assigned wood properties with a fracture strength derived from commonly known wood strength values. Bolts were assigned elastic-plastic material properties based on ASTM A307 material specifications.

The vehicle model used in the impact simulation was a ½-ton, 4-door, Chevrolet Silverado that is representative of the 2270P design vehicle in *MASH*. This vehicle model was developed by the National Crash Analysis Center under the sponsorship of the Federal Highway Administration. The vehicle was assigned an initial velocity of 85 mi/h and had a 25 degree impact angle with the barrier as shown in [Figures 3.2 and 3.3](#). The vehicle impact location was just before the 7th post from the upstream end of the barrier as shown in [Figure 3.2](#).

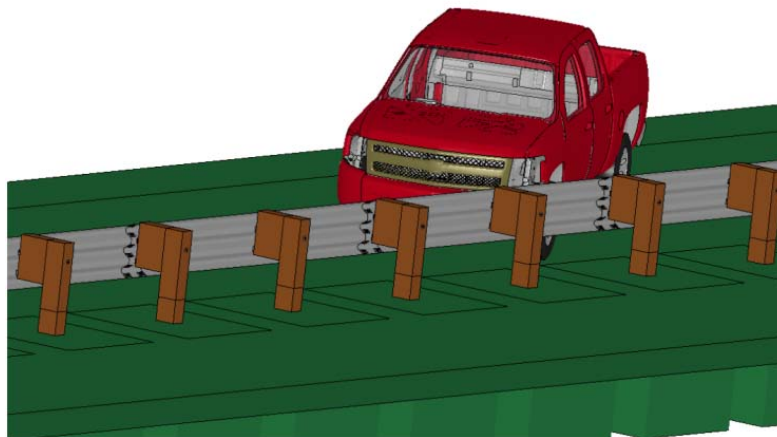


Figure 3.3. Iso-Parametric View of the 2270 kg Vehicle Set Up with the Modified Thrie-Beam Rail.

The modified wood post thrie beam guardrail system was able to contain and redirect the vehicle. Sequential images of the impact event are shown in [Figure 3.4](#). A total of 11 posts were predicted to fracture during the impact, but there were no obvious signs of pocketing or rail rupture. The maximum rail deflection was 74 inches (see [Figure 3.5](#)).

The longitudinal acceleration time history for the impact is shown in [Figure 3.6](#). All occupant risk indices were predicted to be acceptable and overall damage to the vehicle was moderate (see [Figure 3.7](#)).

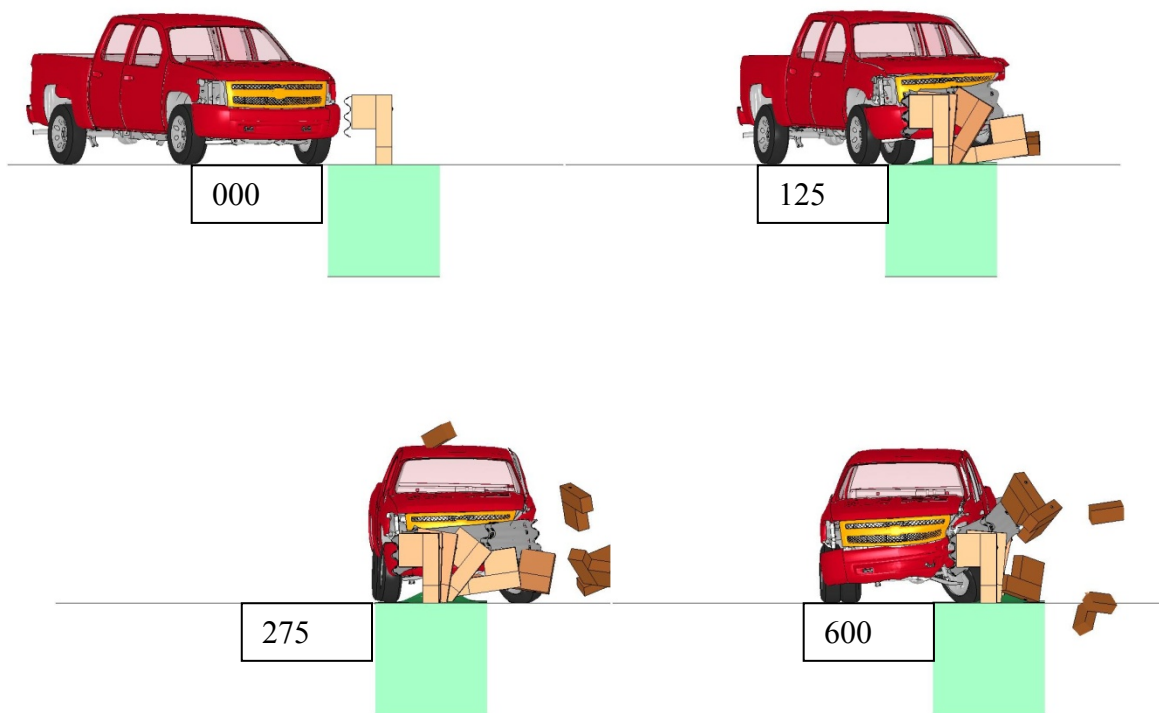


Figure 3.4. Sequential Images of 2270P Impact with Modified Wood Post Thrie Beam Guardrail.

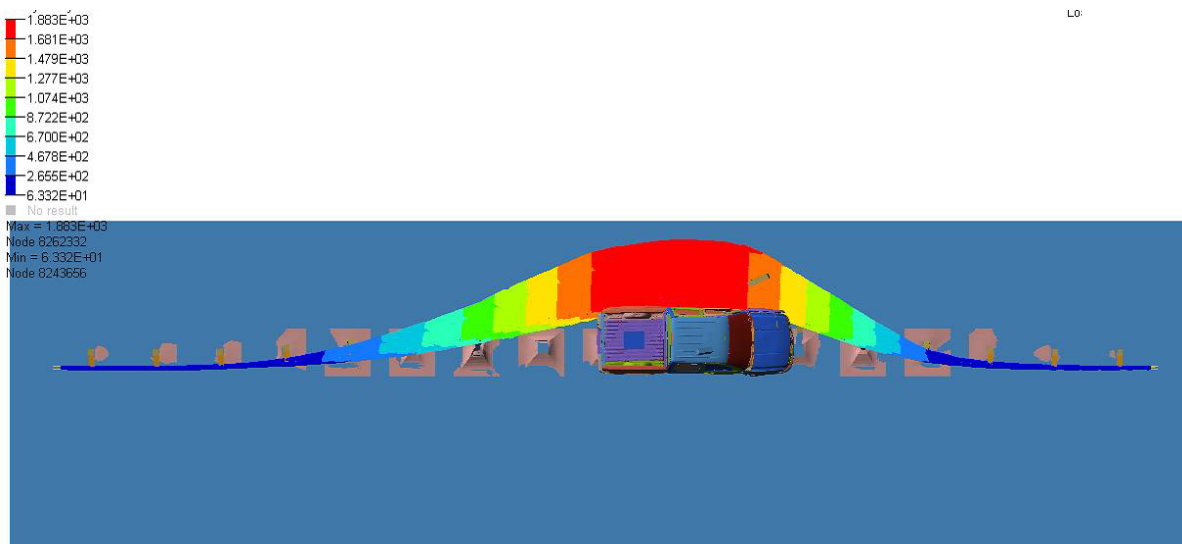


Figure 3.5. Impact at Time of Maximum Rail Deflection.

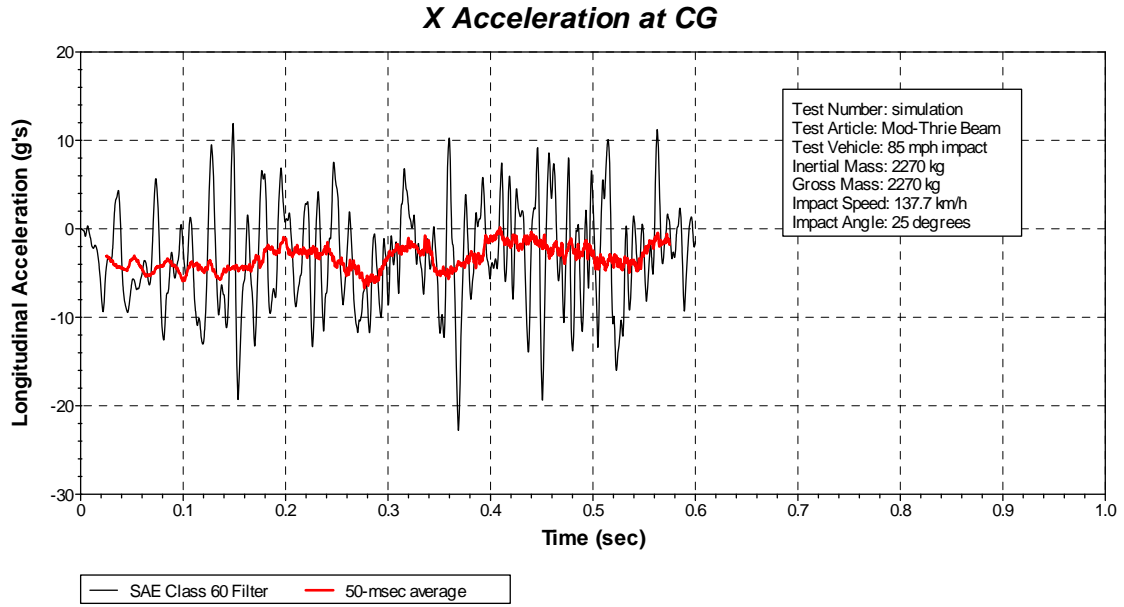


Figure 3.6. Longitudinal Acceleration History for CG of the 2270 kg Vehicle.

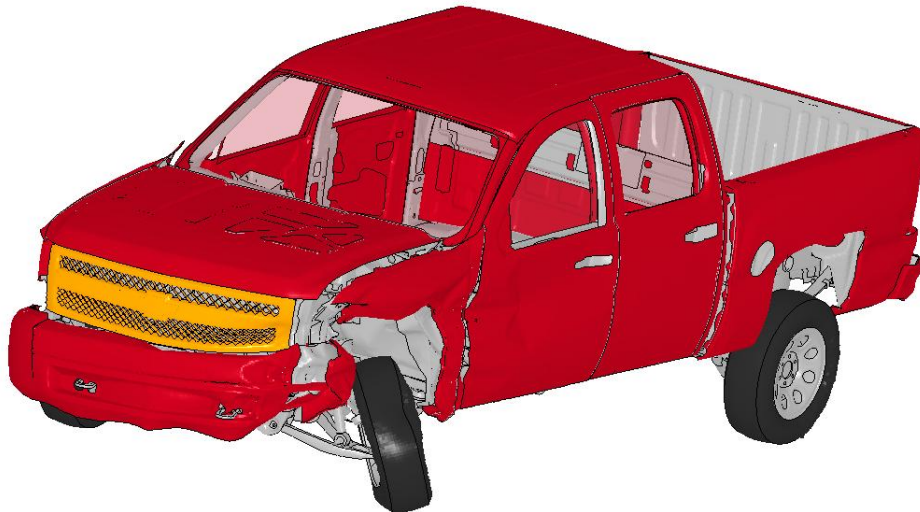


Figure 3.7. Damage to the Vehicle in the 85 mi/h Simulation.

CONCLUSIONS

The simulation results indicated that the modified wood post thrie beam guardrail had a reasonable probability of accommodating an 85 mi/h impact. The fracture of the wood posts precluded issues with wheel snagging and vehicle stability that were observed in simulations with the steel post system. The predicted number of fractured posts (11) and the relatively large dynamic deflection (74 inches) raised some concern regarding pocketing and rail rupture. However, the thrie beam rail did not approach its failure strain, and there were not obvious geometric indicators of pocketing. In some respects, the high impact severity caused this strong post guardrail system to behave in a manner similar to a weak post system. After consultation with TxDOT personnel, a decision was made to subject the modified wood post thrie beam guardrail to further evaluation through full-scale crash testing. The results of the crash testing are presented in [Chapter 5](#).

CHAPTER 4. FULL-SCALE CRASH TEST PROCEDURES

TEST FACILITY

The full-scale crash tests reported herein were performed at Texas Transportation Institute (TTI) Proving Ground. TTI Proving Ground is an International Standards Organization (ISO) 17025 accredited laboratory with American Association for Laboratory Accreditation (A2LA) Mechanical Testing certificate 2821.01. The full-scale crash test was performed according to TTI Proving Ground quality procedures and according to the *MASH* guidelines and standards.

The test facilities at the TTI Proving Ground consist of a 2000 acre complex of research and training facilities situated 10 miles northwest of the main campus of Texas A&M University. The site, formerly an Air Force Base, has large expanses of concrete runways and parking aprons well suited for experimental research and testing in the areas of vehicle performance and handling, vehicle-roadway interaction, durability and efficacy of highway pavements, and safety evaluation of roadside safety hardware. The site selected for the placement of the high-speed bridge rail was along a wide out-of-service runway. The runway consists of an unreinforced jointed concrete pavement in 12.5 ft x 15 ft blocks nominally 8–12 inches deep. The runway is over 50 years old and the joints have some displacement, but are otherwise flat and level.

CRASH TEST CONDITIONS

Per *MASH*, the recommended test matrix for longitudinal barriers consists of:

- ***MASH* test designation 3-10:** An 1100C (2425 lb/1100 kg) vehicle impacting the critical impact point (CIP) of the length of need (LON) of the barrier at a nominal impact speed and angle of 62 mi/h and 25 degrees, respectively. The primary objective of this test is to evaluate risk of occupant injury.
- ***MASH* test designation 3-11:** A 2270P (5000 lb/2270 kg) vehicle impacting the critical impact point (CIP) of the length of need (LON) of the barrier at a nominal impact speed and angle of 62 mi/h and 25 degrees, respectively. This test is primary a strength test that evaluates the ability of the barrier to contain and redirect the vehicle in a stable manner.

Both of these tests were performed on the energy-absorbing bridge rail. The CIP determined for these tests was 32 ft-8 inches downstream of the end of the bridge rail, or 47.25 inches upstream of a splice.

Only test designation 3-11 was performed on the modified three beam guardrail. The CIP determined for this test was midspan between posts 15 and 16.

All crash test, data analysis, and evaluation and reporting procedures followed under this project were in accordance with guidelines presented in *MASH* with the exception of vehicle impact speed. [Appendix A](#) presents brief descriptions of these procedures. For this project, the impact speed was increased from the nominal 62 mi/h to 85 mi/h to assess the performance of the barriers under high-speed conditions.

EVALUATION CRITERIA

The crash tests performed were evaluated in accordance with *MASH*. As stated in *MASH*, “Safety performance of a highway appurtenance cannot be measured directly but can be judged on the basis of three factors: structural adequacy, occupant risk, and vehicle trajectory after collision.” Accordingly, researchers used the safety evaluation criteria from Table 5.1 of *MASH* to evaluate the crash tests reported herein.

CHAPTER 5. FULL-SCALE CRASH TESTING OF THE ENERGY ABSORBING BRIDGE RAIL

TEST ARTICLE

Design and Construction

The concrete parapet portion of the bridge rail was similar in design to the TxDOT T221 bridge rail but with additional reinforcement to provide the strength necessary to resist the higher forces generated during the high-speed impacts. The parapet had a 10.5-inch wide wall, a 12-inch wide beam at the top, and was 32 inches tall. Vertical reinforcement in the parapet consisted of #4 “U-shaped” stirrups spaced on 6-inch centers. The longitudinal reinforcement consisted of six #5 bars spaced at 5.375 inches on both the traffic and field side of the parapet. The parapet was anchored to an unreinforced concrete runway using two #5 bars. The bars were secured into drilled holes at an embedment depth of 5 inches using an epoxy adhesive.

Two 6 inch × 6 inch × 1/4 inch tubular steel rails were attached to the traffic face of the concrete parapet at a height of 31 inches to the top of the upper rail. Adjacent rail sections were spliced to one another using a 5 inch × 5 inch × 3/8 inch tubular steel sleeve. A 5/16-inch steel plate was welded to adjoining sides of the 24-inch long sleeve to provide the desired fit inside the rail elements. The splice locations of the upper and lower rail sections were offset from one another a distance of 40 inches. The rails sections were connected to one another using a 3/4-inch diameter x 14-inch long A325 bolt that passed vertically through each of the rail members 20 inches from each splice location, which corresponded to the middle of the overlapped rail section.

Pipe spacers were used to offset the steel rail from the concrete parapet and provide a mechanism for dissipating some of the energy of the impacting vehicle. The 8-inch diameter × 12-inch long Schedule 40 pipe spacers were spaced 80 inches on center. The pipe spacers were attached to each of the tubular rail members using 5/8-inch diameter x 1-1/2-inch long A307 studs that were welded to the field side of the tubular rails. The pipe spacers were attached to the concrete parapet using a 1-inch diameter bolt inserted through a 3 inch x 1-1/2 inch 11 gauge A36 embedded sleeve. The sleeve provided horizontal tolerance to assist with assembly of the rail.

A cross section of the high-speed energy absorbing bridge rail is shown in [Figure 5.1](#). Photographs of the completed test installation are shown in [Figure 5.2](#). Detailed drawings of the bridge rail are presented in [Appendix B](#).

Material Specifications

The concrete for the parapet was specified to have a 28-day compressive strength of 3600 psi. The concrete strength on the day of the test was 4424 psi. All reinforcing steel was grade 60. The tubular rail sections and tubular splice sleeves were ASTM A500 steel. The pipe spacers were ASTM A53 steel, and the connection bolts used to attach the rails to one another and the pipe spacers to the concrete parapet were ASTM A325. The studs used to connect the pipe spacers to the tubular rail members were ASTM A307.

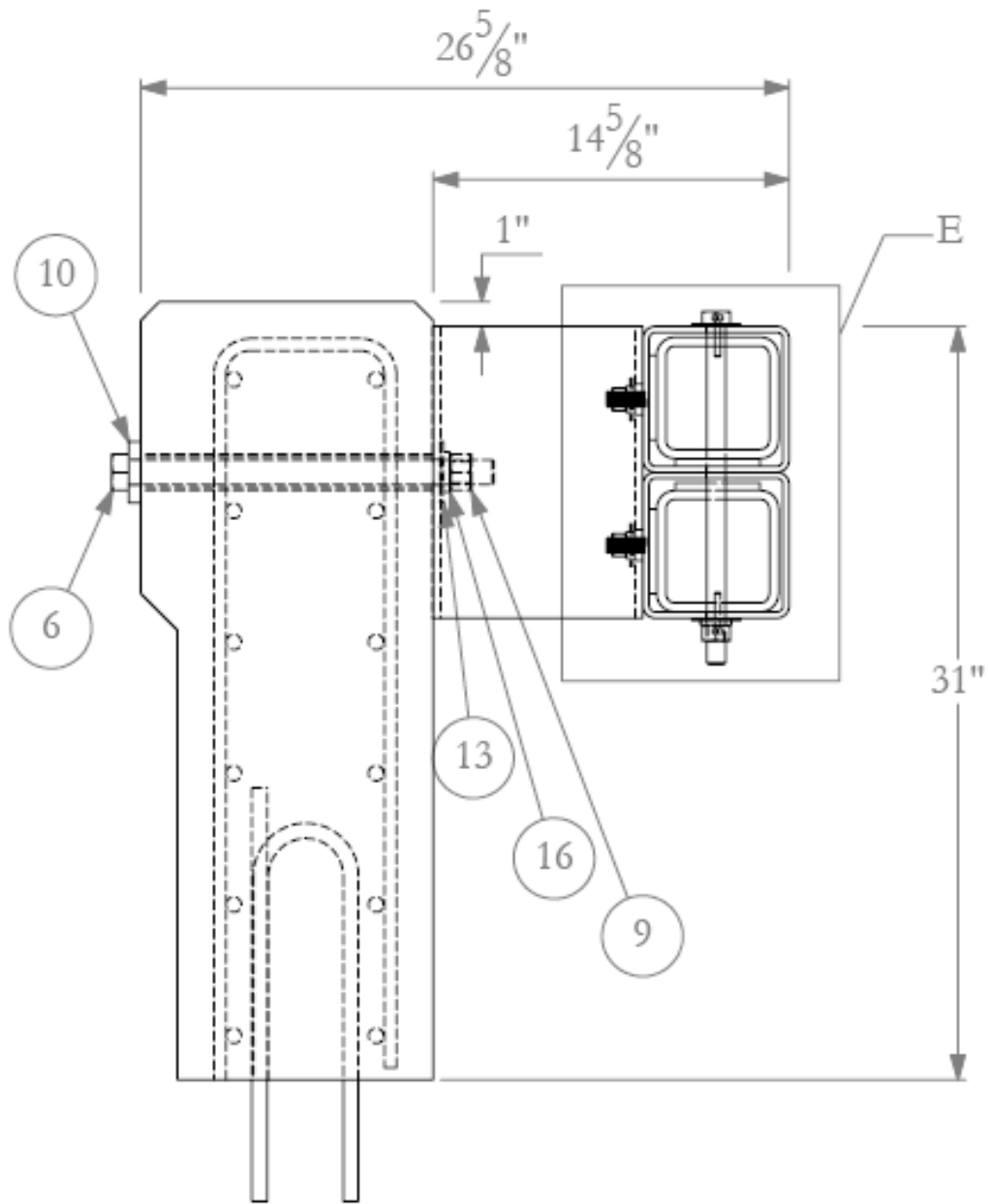


Figure 5.1. Details of the High-Speed Energy-Absorbing Bridge Rail.



Figure 5.2. Energy-Absorbing Bridge Rail Installation before Test Nos. 470619-1 and 2.

TEST NO. 460719-1 (MASH TEST 3-10)

Test Designation and Actual Impact Conditions

MASH test 3-10 involves an 1100C vehicle with test inertial mass of 2420 lb \pm 55 lb impacting the bridge rail at an impact speed of 62.2 mi/h \pm 2.5 mi/h and an angle of 25 degrees \pm 1.5 degrees. However, for this test, the target impact speed was 85 mi/h. The target impact point was 32 ft-8 inches downstream from the end of the bridge rail, which corresponded to 47.25 inches upstream of a splice. The 2002 Kia Rio used in the test had a test inertial mass of 2438 lb, and the actual impact speed and angle were 85.2 mi/h and 25.7 degrees, respectively. The actual impact point was 32 ft-5 inches downstream from the end of the bridge rail.

Test Vehicle

A 2002 Kia Rio, shown in [Figures 5.3](#) and [5.4](#), was used for the crash test. Test inertia weight of the vehicle was 2438 lb, and its gross static weight was 2606 lb. The height to the lower edge of the vehicle bumper was 8.50 inches, and the height to the upper edge of the bumper was 22.75 inches. [Figure C1](#) in [Appendix C](#) gives additional dimensions and information on the vehicle. The vehicle was directed into the installation using the cable reverse tow and guidance system and was released to be free-wheeling and unrestrained just prior to impact.

Weather Conditions

The test was performed on the morning of August 7, 2009. Weather conditions at the time of testing were as follows: Wind speed: 10 mi/h; Wind direction: 200 degrees with respect to the vehicle (vehicle was traveling in a southeasterly direction); Temperature: 93°F, Relative humidity: 42 percent.

Test Description

The 2002 Kia Rio, traveling at an impact speed of 85.2 mi/h, impacted the energy-absorbing bridge rail 32 ft-5 inches downstream from the end of the bridge rail at an impact angle of 25.7 degrees. Shortly after impact, the metal rail began to deflect as the pipe spacers began to collapse. At 0.018 s, the windshield began to shatter at the right lower corner. The frame of the passenger door began to deform at 0.019 s, and the roof over the right front passenger began to deform at 0.020 s. At 0.034 s, the glass in the right front passenger door began to shatter at the lower front corner, and at 0.039 s, the vehicle began to redirect. The glass in the right front passenger door separated from the door frame at 0.048 s, and the roof reached its maximum deformation at 0.071 s.



Figure 5.3. Vehicle/Installation Geometrics for Test No. 460719-1.



Figure 5.4. Vehicle before Test No. 460719-1.

At 0.079 s, the head of the dummy began to extend out of the right front passenger window. The rear of the vehicle contacted the rail at 0.106 s. At 0.118 s, the head of the dummy was extended its maximum distance out of the right front passenger window. Due to dust obscuring the view, it could not be ascertained if the head of the dummy actually touched the bridge rail. By 0.174 s, the head of the dummy re-entered the interior of the vehicle.

At 0.246 s, the vehicle lost contact with the rail traveling at an exit speed and angle of 67.6 mi/h and 3.9 degrees, respectively. As the vehicle continued tracking forward after exiting the test installation, the left front of the vehicle impacted a secondary rigid concrete structure, which induced significant additional damage to the front of the vehicle. The vehicle subsequently came to rest 230 ft downstream of impact and 42 ft toward traffic lanes.

[Figures D1 and D2](#) in [Appendix D](#) show sequential photographs of the test period.

Damage to Test Installation

The vehicle contacted the energy-absorbing bridge rail 32 ft-5 inches downstream from the end of the bridge rail and remained in contact with the metal rail element for a distance of 13 ft. The maximum rail deflection was 5.25 inches at joint 2-3. No damage to the concrete wall was evident. [Figure 5.5](#) shows damage to the installation.

Vehicle Damage

A secondary frontal impact of the redirected vehicle with the end of another rigid concrete barrier complicated the damage assessment of the vehicle. The secondary impact occurred on the left side of the vehicle and, therefore, the following damage on the right side of the vehicle was attributed to the initial impact with the bridge rail. The front bumper, hood, right front fender, right front tire and wheel rim, roof over the passenger side, right B-post, right door and door glass, right rear quarter panel, rear bumper, right side floor pan, right side firewall, and right side kickpanel were damaged due to impact with the energy-absorbing bridge rail. Maximum exterior crush to the right side of the vehicle was 16 inches in the side plane at the right front corner at bumper height. Maximum occupant compartment deformation (OCD) on the right side was 9.0 inches in the firewall area. It is believed that the secondary impact likely contributed to the damage in this area, but the OCD measurement was not adjusted for this. Photographs of the vehicle after the test are shown in [Figures 5.6 and 5.7](#). Exterior crush and occupant compartment measurements are documented in [Appendix C](#), [Tables C1 and C2](#).



Figure 5.5. Installation after Test No. 460719-1.



Figure 5.6. Vehicle after Test No. 460719-1.



Figure 5.7. Interior of Vehicle for Test No. 460719-1.

Occupant Risk Factors

Data from the accelerometer, located at the vehicle center of gravity, were digitized for evaluation of occupant risk. In the longitudinal direction, the occupant impact velocity was 40.8 ft/s at 0.072 s, the highest 0.010-s occupant ridedown acceleration was -16.3 G from 0.072 to 0.082 s, and the maximum 0.050-s average acceleration was -16.1 G between 0.032 and 0.082 s. In the lateral direction, the occupant impact velocity was 40.7 ft/s at 0.072 s, the highest 0.010-s occupant ridedown acceleration was -10.0 G from 0.082 to 0.092 s, and the maximum 0.050-s average was -24.0 G between 0.025 and 0.075 s.

Figure 5.8 summarizes these data and other pertinent information from the test. Figures E1 through E7 in Appendix E present vehicle angular displacements and accelerations versus time traces.

Assessment of Test Results

An assessment of the test based on the applicable *MASH* safety evaluation criteria is provided below.

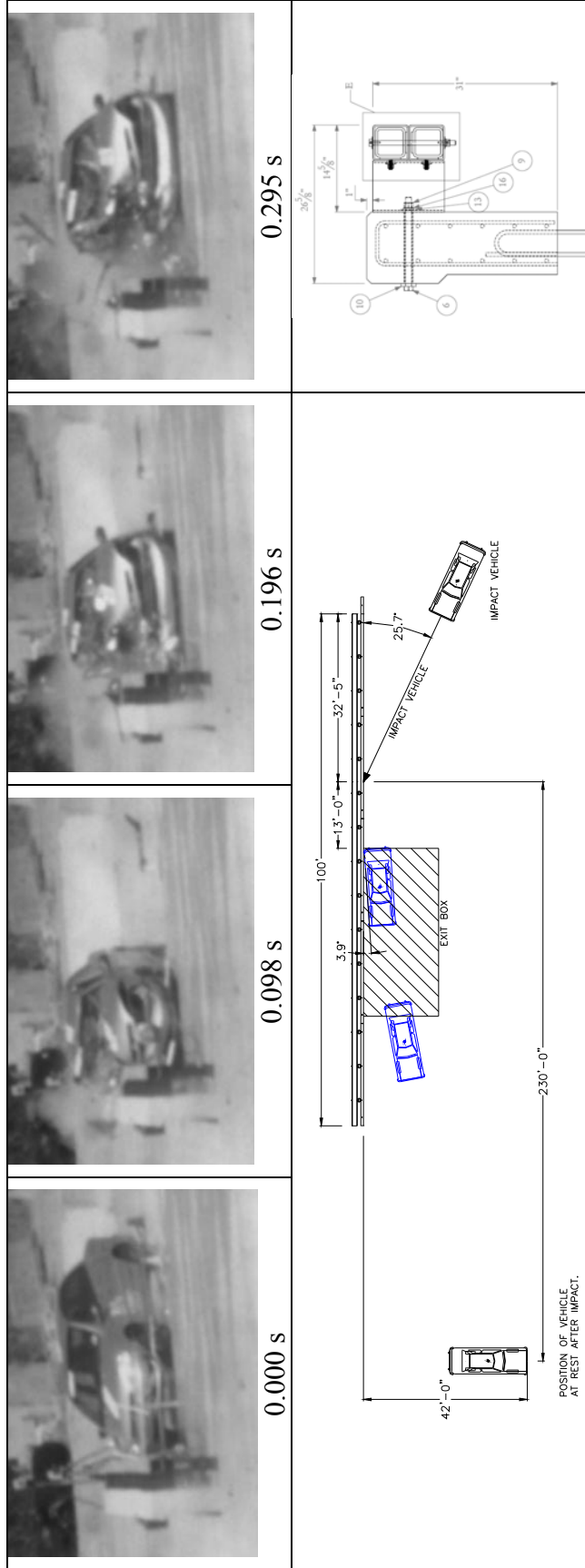
Structural Adequacy

- A. *Test article should contain and redirect the vehicle or bring the vehicle to a controlled stop; the vehicle should not penetrate, underride, or override the installation although controlled lateral deflection of the test article is acceptable.*

Results: The energy-absorbing bridge rail contained and redirected the 1100C vehicle. The vehicle did not penetrate, underride, or override the bridge rail. Maximum dynamic deflection of the metal rail element was 5.25 inches at joint 2-3. (PASS)

Occupant Risk

- D. *Detached elements, fragments, or other debris from the test article should not penetrate or show potential for penetrating the occupant compartment, or present an undue hazard to other traffic, pedestrians, or personnel in a work zone.*
Deformation of, or intrusions into, the occupant compartment should not exceed limits set forth in Section 5.3 and Appendix E of MASH. (roof ≤ 4.0 inches; windshield = 3.0 inches; side windows = no shattering by test article structural member; wheel/foot well/toe pan ≤ 9.0 inches; forward of A-pillar ≤ 12.0 inches; front side door area above seat ≤ 9.0 inches; front side door below seat ≤ 12.0 inches; floor pan/transmission tunnel area ≤ 12.0 inches)



General Information		Impact Conditions		Post-Impact Trajectory	
Test Agency	Texas Transportation Institute	Speed	85.2 mi/h	Stopping Distance	230 ft down traffic
Test No.	406719-1	Angle	25.7 degrees	Location/Orientation	1/3 point
Date	2009-08-07	Exit Conditions		Vehicle Stability	
Test Article		Speed	67.6 mi/h	Maximum Yaw Angle	-40 degrees
Type	Longitudinal Barrier	Angle	3.9 degrees	Maximum Pitch Angle	10 degrees
Name	High-Speed Energy-Absorbing Bridge Rail	Occupant Risk Values		Maximum Roll Angle	12 degrees
Installation Length	100 ft	Impact Velocity		Vehicle Snagging	No
Material or Key Elements	Reinforced concrete parapet; tubular steel rails; collapsible pipe spacers	Longitudinal	24.6 ft/s	Vehicle Pocketing	No
Soil Type and Condition		Lateral	40.7 ft/s	Test Article Deflections	
Test Vehicle		THIV	48.2 km/h	Dynamic	7.5 inches
Type/Designation	1100C	Ridedown Accelerations		Permanent	5.25 inches
Make and Model	2002 Kia Rio	Longitudinal	-16.3 G	Working Width	1.0 ft
Curb	2399 lb	Lateral	-10.0 G	Vehicle Damage	
Test Inertial	2438 lb	PHD	19.0 G	VDS	01RFQ6
Dummy	168 lb	ASI	2.94	CDC	01FREW6
Gross Static	2606 lb	Max. 0.050-s Average		Max. Exterior Deformation	16.0 inches
		Longitudinal	-16.1 G	Max. Occupant Compartment Deformation	9.0 inches
		Lateral	-24.0 G		
		Vertical	-5.0 G		

Figure 5.8. Summary of Results for MASH Test 3-10 on the Energy-Absorbing Bridge Rail.

Occupant Risk (continued)

Results: No detached elements, fragments, or other debris from the bridge rail were present to penetrate or show potential for penetrating the occupant compartment, or to present undue hazard to others in the area. (PASS)
Maximum occupant compartment deformation was 9.0 inches in the right side floor pan/toe pan area. (PASS)

F. *The vehicle should remain upright during and after collision. The maximum roll and pitch angles are not to exceed 75 degrees.*

Results: The 1100C vehicle remained upright during and after the collision event. Maximum roll angle was 13 degrees at 1.7 s, and maximum pitch angle was 10 degrees at 2.00 s. (PASS)

H. *Occupant impact velocities should satisfy the following:*

Longitudinal and Lateral Occupant Impact Velocity

<u>Preferred</u>	<u>Maximum</u>
30 ft/s 40	ft/s

Results: Longitudinal occupant impact velocity was 24.6 ft/s, and lateral occupant impact velocity was 40.7 ft/s. (MARGINAL)

I. *Occupant ridedown accelerations should satisfy the following:*

Longitudinal and Lateral Occupant Ridedown Accelerations

	<u>Preferred</u>		<u>Maximum</u>
15.0	Gs	20.49	Gs

Results: Longitudinal ridedown acceleration was -16.3 G, and lateral ridedown acceleration was -10.0 G. (PASS)

Vehicle Trajectory

For redirective devices, the vehicle shall exit the barrier within the exit box.

Result: The 1100C vehicle exited within the exit box. (PASS)
The vehicle came to rest 230 ft downstream of impact and 42 ft toward traffic lanes.

TEST NO. 460719-2 (MASH TEST DESIGNATION 3-11)

Test Designation and Actual Impact Conditions

MASH test 3-11 involves a 2270P vehicle weighing 5000 lb \pm 100 lb impacting the bridge rail at an impact speed of 62.2 mi/h \pm 2.5 mi/h and an angle of 25 degrees \pm 1.5 degrees. However, for this test, the target impact speed was 85 mi/h. The target impact point was 24 inches upstream of the centerline of the sixth pipe spacer. The Dodge Ram 1500 Quad-Cab pickup used in the test weighed 5006 lb, and the actual impact speed and angle were 86.4 mi/h and 25.3 degrees, respectively. The actual impact point was 24 inches upstream of the centerline of the sixth spacer.

Test Vehicle

A 2002 Dodge Ram 1500 Quad-Cab pickup, shown in [Figures 5.9](#) and [5.10](#), was used for the crash test. Test inertia weight of the vehicle was 5006 lb, and its gross static weight was 5006 lb. The height to the lower edge of the pickup bumper was 13.5 inches, and height to the upper edge of the bumper was 26.0 inches. Height to the center of gravity of the pickup was 28.06 inches. [Figure C2](#) in [Appendix C](#) gives additional dimensions and information on the vehicle. The vehicle was directed into the installation using the cable reverse tow and guidance system, and was released to be free-wheeling and unrestrained just prior to impact.

Weather Conditions

The test was performed on the morning of August 14, 2009. Weather conditions at the time of testing were as follows: Wind speed: 10 mi/h; Wind direction: 192 degrees with respect to the vehicle (vehicle was traveling in a southeasterly direction); Temperature: 88°F, Relative humidity: 59 percent.

Test Description

The 2002 Dodge Ram 1500 Quad-Cab pickup, traveling at an impact speed of 86.4 mi/h, impacted the energy absorbing bridge rail 2 ft upstream of the centerline of the sixth pipe spacer. Shortly after impact, the metal rail began to deflect as the pipe spacers began to collapse. At 0.031 s, the top of the right front passenger door separated from the door frame of the vehicle. At 0.052 s, the windshield began to crack in the lower right corner and the top of the right rear door began to separate from the door frame. At 0.054 s, the vehicle began to redirect, and at 0.062 s, the right front door glass began to shatter. At 0.162 s, the vehicle was parallel to the barrier and was traveling at a speed of 73.1 mi/h. The rear of the vehicle reached its maximum pitch at 0.330 s. At 0.339 s, the vehicle lost contact with the bridge rail traveling at an exit speed and exit angle of 71.6 mi/h and 4.6 degrees, respectively. After losing contact with the rail, the vehicle rolled onto its impact side and then flipped several times before coming to rest. [Figures D3](#) and [D4](#) in [Appendix D](#) show sequential photographs of the test period.



Figure 5.9. Vehicle/Installation Geometrics for Test No. 460719-2.



Figure 5.10. Vehicle before Test No. 460719-2.

Damage to Test Installation

Damage to the bridge rail is shown in [Figures 5.11](#) and [5.12](#). The fifth through eighth pipe spacers between the concrete parapet and the metal rail were deformed. The rail had a maximum permanent deflection of 6.5 inches between the sixth and seventh pipe spacer. Working width was 2.38 ft.

Vehicle Damage

After redirecting and exiting the barrier, the pickup truck rolled over two and one-half times, struck a tree, and subsequently came to rest on its wheels. Damage to the vehicle due to the rollover event was extensive, and it is unclear how much damage is attributable to the secondary impact with the tree. The right side frame rail, left rear spring, the right front upper and lower A-arms and ball joints were deformed, the right front wheel assembly separated at the ball joints, and the right rear wheel assembly separated at the rear axle. The right front door also separated from the truck. Also damaged were the front bumper, hood, grill, radiator and support, fan, water pump, windshield, right side A-B-C posts, right passenger door and glass, roof and rear glass, cargo bed, tailgate, and rear bumper. Maximum exterior crush to the vehicle was estimated to be 20 inches. Maximum occupant compartment deformation was 8.3 inches near the floor pan in the lateral area across the cab from kickpanel to kickpanel. Photographs of the vehicle after the test are shown in [Figures 5.13](#) and [5.14](#). Exterior crush and occupant compartment measurements are documented in [Appendix C](#), [Tables C3](#) and [C4](#).

Occupant Risk Factors

Data from the accelerometer, located at the vehicle center of gravity, were digitized for evaluation of occupant risk. In the longitudinal direction, the occupant impact velocity was 17.4 ft/s at 0.085 s, the highest 0.010-s occupant ridedown acceleration was -7.9 G from 0.091 to 0.101 s, and the maximum 0.050-s average acceleration was -9.0 G between 0.037 and 0.087 s. In the lateral direction, the occupant impact velocity was 31.8 ft/s at 0.085 s, the highest 0.010-s occupant ridedown acceleration was -13.6 G from 0.156 to 0.166 s, and the maximum 0.050-s average was -16.9 G between 0.036 and 0.086 s.

[Figure 5.15](#) presents these data and other pertinent information from the test. [Figures E8](#) through [E14](#) in [Appendix E](#) presents vehicle angular displacements and accelerations versus time traces.



Figure 5.11. After Impact Trajectory Path for Test No. 460719-2.



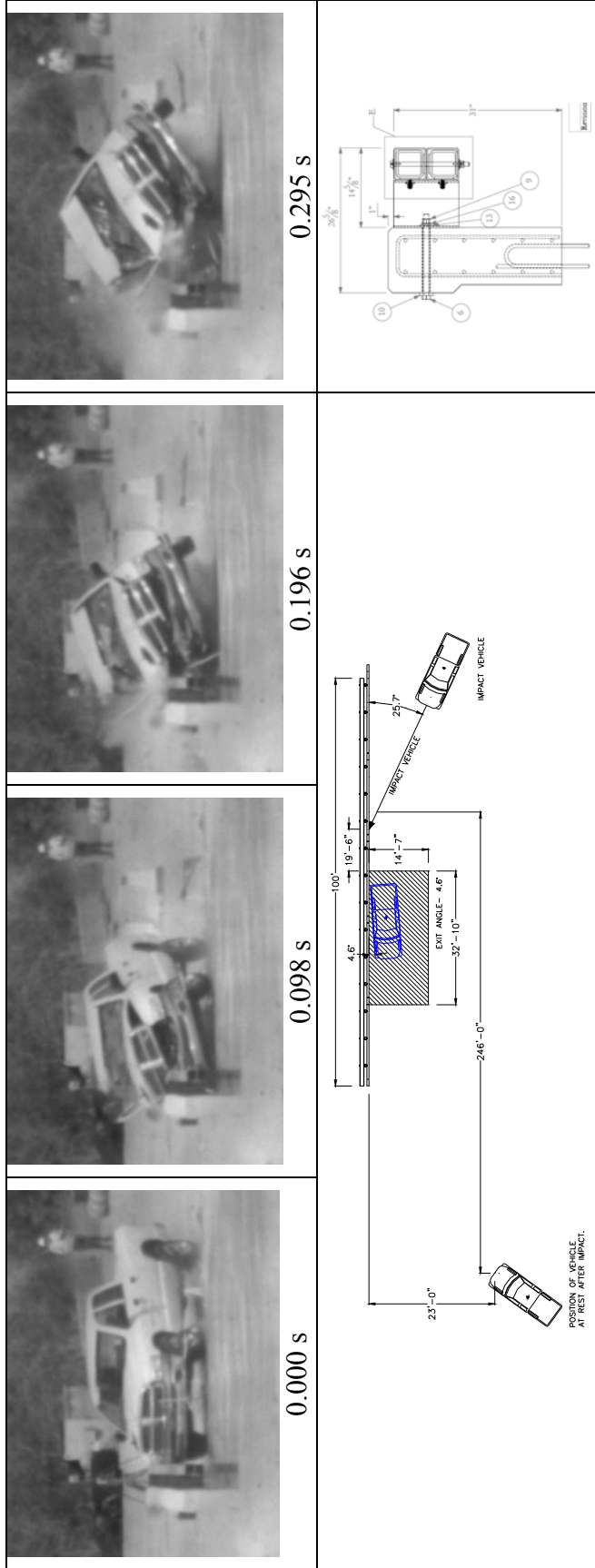
Figure 5.12. Installation after Test No. 460719-2.



Figure 5.13. Vehicle after Test No. 460719-2.



Figure 5.14. Interior of Vehicle for Test No. 460719-2.



General Information	Test Agency Texas Transportation Institute Test No. 406719-2 Date 2009-08-14 Test Article Type Longitudinal Barrier Name Energy-Absorbing Bridge Rail Installation Length High-Speed Energy-Absorbing Bridge Rail Material or Key Elements 100 ft Reinforced concrete parapet; tubular steel rails; collapsible pipe spacers Soil Type and Condition Concrete pavement Test Vehicle Type/Designation 2270P Make and Model 2002 Dodge Ram 1500 Pickup Curb 4759 Test Inertial 5006 Dummy No dummy Gross Static 5006
Impact Conditions	Speed 86.4 mi/h Angle 25.3 degrees Location/Orientation Exit Conditions Speed 71.6 mi/h Angle 4.6 degrees Occupant Risk Values Impact Velocity Longitudinal 17.4 ft/s Lateral 31.8 ft/s THIV 37.9 km/h Ridedown Accelerations Longitudinal -7.9 G Lateral -13.6 G PHS 13.6 G ASI 2.05 Max. 0.050-s Average Longitudinal -9.0 G Lateral -16.9 G Vertical 4.9 G
Post-Impact Trajectory	Stopping Distance 246 ft ds 23 ft twd traffic Vehicle Stability Maximum Yaw Angle -130 deg Maximum Pitch Angle -7 deg Maximum Roll Angle 168 deg Vehicle Snagging No Vehicle Pocketing No Test Article Deflections Dynamic Not obtainable Permanent 6.5 inches Working Width 2.38 ft Vehicle Damage VDS 01RF06 CDC 01FREW6 Max. Exterior Deformation ~20 inches OCDI RF0210000 Max. Occupant Compartment Deformation 8.3 inches

Figure 5.15. Summary of Results for MASH Test 3-11 on the Energy-Absorbing Bridge Rail.

Assessment of Test Results

An assessment of the test based on the applicable *MASH* safety evaluation criteria is provided below.

Structural Adequacy

- B. Test article should contain and redirect the vehicle or bring the vehicle to a controlled stop; the vehicle should not penetrate, underride, or override the installation although controlled lateral deflection of the test article is acceptable.*

Results: The energy-absorbing bridge rail contained and redirected the 2270P vehicle. The vehicle did not penetrate, underride, or override the installation. Maximum deformation of the metal rail was 6.5 inches. (PASS)

Occupant Risk

- D. Detached elements, fragments, or other debris from the test article should not penetrate or show potential for penetrating the occupant compartment, or present an undue hazard to other traffic, pedestrians, or personnel in a work zone.*

Deformation of, or intrusions into, the occupant compartment should not exceed limits set forth in Section 5.3 and Appendix E of MASH. (roof ≤ 4.0 inches; windshield = ≤ 3.0 inches; side windows = no shattering by test article structural member; wheel/foot well/toe pan ≤ 9.0 inches; forward of A-pillar ≤ 12.0 inches; front side door area above seat ≤ 9.0 inches; front side door below seat ≤ 12.0 inches; floor pan/transmission tunnel area ≤ 12.0 inches)

Results: No detached elements, fragments, or other debris from the bridge rail were present to penetrate or to show potential for penetrating the occupant compartment, or to present undue hazard to others in the area. (PASS)
Maximum occupant compartment deformation was 8.3 inches in the lateral area across the cab from kickpanel to kickpanel near the floor pan. (PASS)

- F. The vehicle should remain upright during and after collision. The maximum roll and pitch angles are not to exceed 75 degrees.*

Results: The 2270P vehicle remained upright during the collision event. However, upon exiting the bridge rail, the vehicle rolled several times and came to rest upright. (FAIL)

- I. *Occupant impact velocities should satisfy the following:*
Longitudinal and Lateral Occupant Impact Velocity
- | | |
|------------------|----------------|
| <u>Preferred</u> | <u>Maximum</u> |
| 30 ft/s | 40 ft/s |

Results: Longitudinal occupant impact velocity was 17.4 ft/s, and lateral occupant impact velocity was 31.8 ft/s. (PASS)

- I. *Occupant ridedown accelerations should satisfy the following:*
Longitudinal and Lateral Occupant Ridedown Accelerations
- | | |
|------------------|----------------|
| <u>Preferred</u> | <u>Maximum</u> |
| 15.0 | 20.49 |
| Gs | Gs |

Results: Longitudinal occupant ridedown acceleration was -7.9 G, and lateral occupant ridedown acceleration was -13.6 G. (PASS)

Vehicle Trajectory

For redirective devices, the vehicle shall exit the barrier within the exit box.

Result: The 2270P vehicle exited within the exit box. (PASS)
 The vehicle came to rest 85 ft downstream of impact and 23 ft toward traffic lanes.

CHAPTER 6. FULL-SCALE CRASH TESTING OF THE MODIFIED WOOD POST THRIE BEAM GUARDRAIL

TEST ARTICLE

Design and Construction

The modified wood post thrie beam guardrail incorporates a standard 12-gauge thrie beam rail section mounted at a height of 34 inches on 6-inch x 8-inch x 6 ft-6 inch long wood posts. The posts were spaced on 6 ft-3 inch centers and embedded 43 inches a compacted road base material. The rail was offset from the posts using 6-inch wide x 12-inch deep wood spacer blocks. The length of the spacer blocks was 16 inches, which left the bottom corrugation of the thrie beam rail unsupported. The rail was attached to the blockout and post using a single 5/8-inch diameter x 22-inch long button head bolt through the upper post bolt slot in the thrie beam section. The rail splices were located midspan between posts.

The length of the thrie beam rail section was 150 ft. A 6 ft-3 inch transition section was used to transition the thrie beam to a W-beam rail. A 37.5 ft, wood post ET-PLUS terminal was attached to the transition section. The W-beam rail in the terminal section was tapered down from a height of 30 inches to 27 inches over a distance of 25 ft. The overall length of the installation was 237.5 ft.

A cross section of the modified wood post thrie beam guardrail is shown in [Figure 6.1](#). Photographs of the completed test installation are shown in [Figure 6.2](#). Detailed drawings of the bridge rail are presented in [Appendix F](#).

Material Specifications

The thrie beam and W-beam guardrail conformed to AASHTO M180. The wood posts were Grade 1 southern yellow pine. The posts were installed in soil meeting AASHTO standard specifications for “Materials for Aggregate and Soil Aggregate Subbase, Base and Surface Courses,” designated M147-65(2004), grading B. The guardrail post bolts and rail splice bolts were ASTM A307.

Soil Conditions

No rainfall occurred during the 10 days prior to the test. Moisture content of the AASHTO M147-65(2004), grading B base in which the modified thrie beam guardrail was installed was 6.1 percent.

In accordance with Appendix B of *MASH*, soil strength was measured the day of the crash test (see [Appendix G, Figure G1](#)). During installation of the modified thrie beam guardrail, two W6x16 posts were installed in the immediate vicinity of the barrier utilizing the same fill material and installation procedures used in the previously conducted standard dynamic test (see [Appendix G, Figure G2](#)).

As determined from the test results shown in [Appendix G, Figure G2](#), the minimum post load required for deflections at 5 inches, 10 inches, and 15 inches, measured at a height of 25 inches, is 3940 lb, 5500 lb, and 6540 lb, respectively (90 percent of static load for the initial standard installation). On the day of the test, April 14, 2009, loads on the post at deflections of 5 inches, 10 inches, and 15 inches were 7000 lbf, 9060 lbf, and 10,000 lbf, respectively. The strength of the backfill material met minimum requirements.

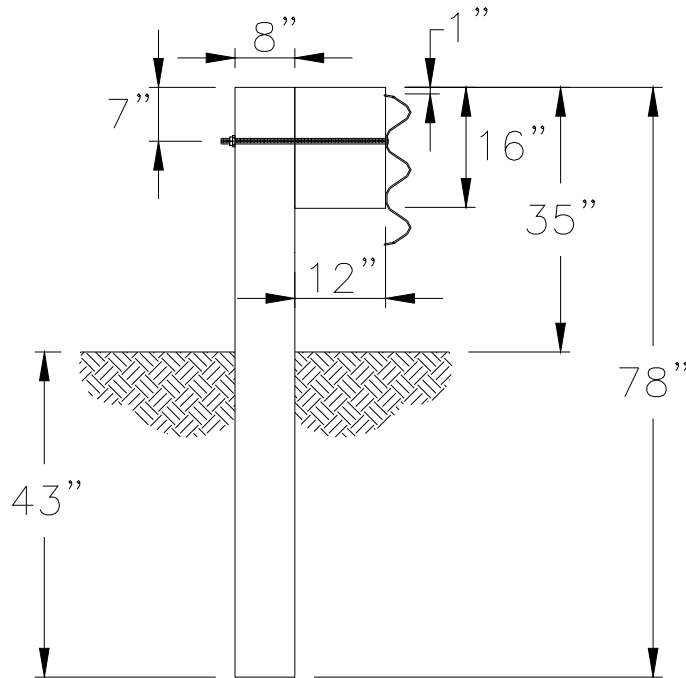


Figure 6.1. Details of the High-Speed Thrie Beam Guardrail.



Figure 6.2. Test Article/Installation before Test No. 470619-3.

TEST NO. 460719-3 (MASH TEST DESIGNATION 3-11)

Test Vehicle

A 2003 Dodge Ram 1500 Quad-Cab pickup, shown in [Figures 6.3](#) and [6.4](#), was used for the crash test. Test inertia weight of the vehicle was 5019 lb, and its gross static weight was 5019 lb. The height to the lower edge of the vehicle bumper was 13.5 inches, and height to the upper edge of the bumper was 26.0 inches. Height to the center of gravity of the pickup was 28.06 inches. [Figure C3](#) in [Appendix C](#) gives additional dimensions and information on the vehicle. The vehicle was directed into the installation using the cable reverse tow and guidance system, and was released to be free-wheeling and unrestrained just prior to impact.

Weather Conditions

The test was performed on the morning of August 21, 2009. No rainfall occurred during the 10 days prior to the test date. Weather conditions at the time of testing were as follows: Wind speed: 5 mi/h; Wind direction: 213 degrees with respect to the vehicle (vehicle was traveling in a northerly direction); Temperature: 88°F, Relative humidity: 66 percent.

Test Description

The 2003 Dodge Ram 1500 Quad-Cab pickup impacted the three beam guardrail at midspan between posts 15 and 16 at an impact speed of 84.1 mi/h and an impact angle of 25.6 degrees. At 0.017 s after impact, the bumper of the vehicle reached post 16, and post 15 began to deflect toward the field side. Post 17 began to move toward the field side at 0.030 s, and post 16 fractured at ground level at 0.031 s. At 0.056 s, post 18 began to move toward the field side and posts 13–15 began to rotate clockwise. Post 17 fractured at ground level at 0.065 s, and the vehicle began to redirect slightly as the vehicle bumper reached post 17 at 0.069 s. At 0.086 s, post 19 began to move toward the field side, and at 0.092 s, post 18 fractured at ground level. The blockout at post 15 separated from the rail at 0.113 s. Between 0.145 s and 0.157 s, the end anchorage failed and released the upstream end of the rail. Post 19 fractured at ground level at 0.157 s. At 0.170 s, the rail separated from post 13, and at 0.177 s, the rail began to pull post 20 toward traffic lanes. At 0.241 s, the left front corner of the vehicle contacted the elbow that had formed at the location of post 20. The rail separated from post 14 at 0.364 s, and the rail wrapped around the side of post 21 at 0.357 s as the vehicle traveled behind the post. The vehicle continued to travel behind the guardrail and came to rest facing the field side 19 ft away from the field side of the guardrail between posts 30 and 31. [Figures D5](#) and [D6](#) in [Appendix D](#) show sequential photographs of the test period.



Figure 6.3. Vehicle/Installation Geometrics for Test No. 460719-3.



Figure 6.4. Vehicle before Test No. 460719-3.

Damage to Test Installation

Damage to the thrie beam guardrail is shown in [Figures 6.5](#) and [6.6](#). Post 1 moved downstream through the soil 1 inch, and post 2 was rotated 30 degrees clockwise and leaning downstream 10 degrees. The anchor bracket connecting the anchor cable to the rail between posts 1 and 2 was pulled out of the rail. Posts 3–5 and 7 were split vertically and the thrie beam rail separated from the posts. Post 6 was split vertically and fractured at ground level. The thrie beam rail separated from posts 8–23, and posts 16–23 were fractured at ground level. The thrie beam rail element was wrapped around post 24, which was leaning downstream at an angle of 6 degrees and had moved upstream through the soil 2.75 inches.

Vehicle Damage

The 2270P vehicle sustained damage to the right upper and lower ball joints, right upper and lower A-arms, right tie rod, and sway bar. Also, the front bumper, hood, right front fender, right front tire and wheel rim, right front door, right rear door, right rear exterior bed, right rear wheel rim, and rear bumper were deformed. The left front fender was dented. Maximum exterior crush to the vehicle was 18 inches in the front plane at the right front corner at bumper height. No deformation or intrusion of the occupant compartment occurred. Photographs of the vehicle are shown in [Figures 6.7](#) and [6.8](#). Exterior crush and occupant compartment measurements are documented in [Appendix C, Tables C5](#) and [C6](#).

Occupant Risk Factors

Data from the accelerometer, located at the vehicle center of gravity, were digitized for evaluation of occupant risk. In the longitudinal direction, the occupant impact velocity was 15.4 ft/s at 0.125 s, the highest 0.010-s occupant ridedown acceleration was -13.2 G from 0.261 to 0.271 s, and the maximum 0.050-s average acceleration was -9.0 G between 0.228 and 0.278 s. In the lateral direction, the occupant impact velocity was 16.1 ft/s at 0.125 s, the highest 0.010-s occupant ridedown acceleration was -5.9 G from 0.259 to 0.269 s, and the maximum 0.050-s average was -5.7 G between 0.034 and 0.084 s.

[Figure 6.9](#) summarizes these data and other pertinent information from the test. [Figures E15](#) through [E21](#) in [Appendix E](#) presents vehicle angular displacements and accelerations versus time traces.



Figure 6.5. After Impact Trajectory Path for Test No. 460719-3.



Figure 6.6. Installation after Test No. 460719-3.



Figure 6.7. Vehicle after Test No. 460719-3.



Figure 6.8. Interior of Vehicle for Test No. 460719-3.

Assessment of Test Results

An assessment of the test based on the applicable *MASH* safety evaluation criteria is provided below.

Structural Adequacy

- A. *Test article should contain and redirect the vehicle or bring the vehicle to a controlled stop; the vehicle should not penetrate, underride, or override the installation although controlled lateral deflection of the test article is acceptable.*

Results: The high-speed thrie beam guardrail did not contain the 2270P vehicle. The vehicle penetrated the rail and came to rest on the field side. (FAIL)

Occupant Risk

- D. *Detached elements, fragments, or other debris from the test article should not penetrate or show potential for penetrating the occupant compartment, or present an undue hazard to other traffic, pedestrians, or personnel in a work zone.*

Deformation of, or intrusions into, the occupant compartment should not exceed limits set forth in Section 5.3 and Appendix E of MASH. (roof ≤ 4.0 inches; windshield = ≤ 3.0 inches; side windows = no shattering by test article structural member; wheel/foot well/toe pan ≤ 9.0 inches; forward of A-pillar ≤ 12.0 inches; front side door area above seat ≤ 9.0 inches; front side door below seat ≤ 12.0 inches; floor pan/transmission tunnel area ≤ 12.0 inches)

Results: Several posts fractured at ground level, but remained relatively close to the installation. This debris did not penetrate or show potential for penetrating the occupant compartment, or to present hazard to others in the area. No occupant compartment deformation occurred. (PASS)

- F. *The vehicle should remain upright during and after collision. The maximum roll and pitch angles are not to exceed 75 degrees.*

Results: The 2270P vehicle remained upright during and after the collision event. (PASS)

- H. *Occupant impact velocities should satisfy the following:*

<u>Longitudinal and Lateral Occupant Impact Velocity</u>	
<u>Preferred</u>	<u>Maximum</u>
30 ft/s	40 ft/s

Results: Longitudinal occupant impact velocity was 15.4 ft/s, and lateral occupant impact velocity was 16.1 ft/s. (PASS)

I. *Occupant ridedown accelerations should satisfy the following:*
Longitudinal and Lateral Occupant Ridedown Accelerations

	<u>Preferred</u>		<u>Maximum</u>
15.0	Gs	20.49	Gs

Results: Longitudinal occupant ridedown acceleration was -13.2 G, and lateral occupant ridedown acceleration was -5.9 G. (PASS)

Vehicle Trajectory

For redirective devices, the vehicle shall exit the barrier within the exit box.

Result: The 2270P vehicle exited toward the field side of the barrier. (N/A)

CHAPTER 7. SUMMARY AND CONCLUSIONS

As TxDOT plans for future expansion of the state's highway network, interest in higher design speeds has been expressed as a means of promoting faster and more efficient travel and movement of goods within the state. TxDOT funded project 0-6071 as part of a proactive consideration of safety on these high-speed facilities. This project began the process of developing roadside safety hardware suitable for use on high-speed highways. The impact conditions selected for the design, testing, and evaluation of this high-speed hardware include a speed of 85 mi/h and an angle of 25 degrees for barrier impacts. The design vehicles are those specified by the pending AASHTO *Manual for Assessing Safety Hardware (MASH)* and include a 5000-lb, ½-ton, 4-door pickup truck and a 2425-lb passenger car.

After evaluation of several barrier systems using finite element simulation, two designs were selected for further evaluation through full-scale crash testing. These included an energy absorbing bridge rail concept and a modified wood post three beam guardrail.

The 85 mi/h impact simulations of the energy absorbing bridge rail predicted marginal performance for both the small car and pickup truck. The results showed a high vehicle roll angle during redirection, which indicated the possibility of vehicle instability and rollover. The simulated small passenger car impact indicated an occupant impact velocity near the maximum acceptable value of 12 m/s and significant occupant compartment deformation. However, considering the challenge of accommodating these severe impact conditions and in absence of any obvious failure for either vehicle, TxDOT elected to approve some full-scale crash tests.

ENERGY ABSORBING BRIDGE RAIL

The energy-absorbing bridge rail contained and redirected the 1100C vehicle. The 1100C vehicle remained upright during and after the collision event. Maximum roll angle was 13 degrees at 1.7 s, and maximum pitch angle was 10 degrees at 2.00 s. Maximum occupant compartment deformation was 9.0 inches in the right side floor pan/toe pan area, which is the allowable limit for this area recommended in *MASH*. Longitudinal occupant impact velocity was 24.6 ft/s, and lateral occupant impact velocity was 40.7 ft/s. The maximum limit according to *MASH* is 40 ft/s, which was slightly exceeded in the lateral direction. It is noted that under NCHRP Report 350, a value of 41 ft/s (12.49 m/s) was considered acceptable by FHWA. Longitudinal and lateral ridedown accelerations were -16.3 G and -10.0 G, respectively, both of which are below the recommended threshold of 20 G. As summarized in [Table 7.1](#), the performance of the energy absorbing bridge rail was considered marginal.

In a subsequent test, the energy-absorbing bridge rail contained and redirected the 2270P vehicle. However, upon exiting the bridge rail, the vehicle rolled over. As summarized in [Table 7.2](#), this outcome is unacceptable. This stability issue is discussed further in [Chapter 8](#). It is of interest to note that the occupant compartment deformation and occupant risk indices were within the limits specified in *MASH*.

MODIFIED WOOD POST THRIE BEAM GUARDRAIL

A performance assessment of the modified wood post thrie beam guardrail is presented in [Table 7.3](#). As shown in this table, the 2270P vehicle was not successfully contained and redirected. Failure of the upstream anchorage permitted the vehicle to penetrate behind the guardrail. Although the outcome of the test was unacceptable, it is not necessarily an indictment of the modified wood post thrie beam guardrail system. Further discussion and recommendations regarding this system are presented in [Chapter 8](#).

Table 7.1. Performance Evaluation Summary for MASH Test 3-10 on the Energy-Absorbing Bridge Rail.

Test Agency: Texas Transportation Institute		Test No.: 406719-1	Test Date: 2009-08-07
MASH Test 3-10 Evaluation Criteria		Test Results	Assessment
Structural Adequacy			
<i>A. Test article should contain and redirect the vehicle or bring the vehicle to a controlled stop; the vehicle should not penetrate, underride, or override the installation although controlled lateral deflection of the test article is acceptable</i>		The energy-absorbing bridge rail contained and redirected the 1100C vehicle. The vehicle did not penetrate, underride, or override the bridge rail. Maximum dynamic deflection of the metal rail element was 5.25 inches at joint 2-3.	Pass
Occupant Risk			
<i>D. Detached elements, fragments, or other debris from the test article should not penetrate or show potential for penetrating the occupant compartment, or present an undue hazard to other traffic, pedestrians, or personnel in a work zone.</i>		No detached elements, fragments, or other debris from the bridge rail were present to penetrate or show potential for penetrating the occupant compartment, or to present undue hazard to others in the area.	Pass
<i>Deformations of, or intrusions into, the occupant compartment should not exceed limits set forth in Section 5.3 and Appendix E of MASH.</i>		Maximum occupant compartment deformation was 9.0 inches in the right side floor pan/toe pan area.	Pass
<i>F. The vehicle should remain upright during and after collision. The maximum roll and pitch angles are not to exceed 75 degrees.</i>		The 1100C vehicle remained upright during and after the collision event. Maximum roll angle was 13 degrees at 1.7 s and maximum pitch angle was 10 degrees at 2.00 s.	Pass
<i>H. Longitudinal and lateral occupant impact velocities should fall below the preferred value of 30 ft/s, or at least below the maximum allowable value of 40 ft/s.</i>		Longitudinal occupant impact velocity was 24.6 ft/s, and lateral occupant impact velocity was 40.7 ft/s.	Marginal
<i>I. Longitudinal and lateral occupant ridedown accelerations should fall below the preferred value of 15.0 Gs, or at least below the maximum allowable value of 20.49 Gs.</i>		Longitudinal ridedown acceleration was -16.3 G, and lateral ridedown acceleration was -10.0 G.	Pass
Vehicle Trajectory			
<i>It is preferable that the vehicle leave the barrier within the "exit box."</i>		The vehicle exited the barrier within the exit box and came to rest 230 ft downstream of impact and 42 ft toward traffic lanes.	Pass

Table 7.2. Performance Evaluation Summary for MASH Test 3-11 on the Energy-Absorbing Bridge Rail.

Test Agency: Texas Transportation Institute		Test No.: 406719-2	Test Date: 2009-08-14
MASH Test 3-11 Evaluation Criteria		Test Results	Assessment
Structural Adequacy			
<i>A. Test article should contain and redirect the vehicle or bring the vehicle to a controlled stop; the vehicle should not penetrate, underride, or override the installation although controlled lateral deflection of the test article is acceptable</i>		The energy-absorbing bridge rail contained and redirected the 2270P vehicle. The vehicle did not penetrate, underride, or override the installation. Maximum deformation of the metal rail was 6.5 inches.	Pass
Occupant Risk			
<i>D. Detached elements, fragments, or other debris from the test article should not penetrate or show potential for penetrating the occupant compartment, or present an undue hazard to other traffic, pedestrians, or personnel in a work zone.</i>		No detached elements, fragments, or other debris from the bridge rail were present to penetrate or to show potential for penetrating the occupant compartment, or to present undue hazard to others in the area.	Pass
<i>Deformations of, or intrusions into, the occupant compartment should not exceed limits set forth in Section 5.3 and Appendix E of MASH.</i>		Maximum occupant compartment deformation was 8.3 inches in the lateral area across the cab from kickpanel to kickpanel near the floor pan.	Pass
<i>F. The vehicle should remain upright during and after collision. The maximum roll and pitch angles are not to exceed 75 degrees.</i>		The 2270P vehicle remained upright during the collision event. However, upon exiting the bridge rail, the vehicle rolled several times before coming to rest upright.	Fail
<i>H. Longitudinal and lateral occupant impact velocities should fall below the preferred value of 30 ft/s, or at least below the maximum allowable value of 40 ft/s.</i>		Longitudinal occupant impact velocity was 17.4 ft/s, and lateral occupant impact velocity was 31.8 ft/s.	Pass
<i>I. Longitudinal and lateral occupant ridedown accelerations should fall below the preferred value of 15.0 Gs, or at least below the maximum allowable value of 20.49 Gs.</i>		Longitudinal occupant ridedown acceleration was -7.9 G, and lateral occupant ridedown acceleration was -13.6 G.	Pass
Vehicle Trajectory			
<i>It is preferable that the vehicle leave the barrier within the "exit box."</i>		The 2270P vehicle exited within the exit box and came to rest 85 ft downstream of impact and 23 ft toward traffic lanes.	Pass

Table 7.3. Performance Evaluation Summary for MASH Test 3-11 on the Thrie Beam Guardrail.

Test Agency: Texas Transportation Institute		Test No.: 406719-3	Test Date: 2009-08-22
MASH Test 3-11 Evaluation Criteria		Test Results	Assessment
Structural Adequacy			
<i>A. Test article should contain and redirect the vehicle or bring the vehicle to a controlled stop; the vehicle should not penetrate, underride, or override the installation although controlled lateral deflection of the test article is acceptable</i>		The high-speed thrie beam guardrail did not contain the 2270P vehicle. The vehicle penetrated the rail and came to rest on the field side.	Fail
Occupant Risk			
<i>D. Detached elements, fragments, or other debris from the test article should not penetrate or show potential for penetrating the occupant compartment, or present an undue hazard to other traffic, pedestrians, or personnel in a work zone.</i>		Several posts fractured at ground level, but remained relatively close to the installation. This debris did not penetrate or show potential for penetrating the occupant compartment, or to present hazard to others in the area.	Pass
<i>Deformations of, or intrusions into, the occupant compartment should not exceed limits set forth in Section 5.3 and Appendix E of MASH.</i>		No occupant compartment deformation occurred.	Pass
<i>F. The vehicle should remain upright during and after collision. The maximum roll and pitch angles are not to exceed 75 degrees.</i>		The 2270P vehicle remained upright during and after the collision event.	Pass
<i>H. Longitudinal and lateral occupant impact velocities should fall below the preferred value of 30 ft/s, or at least below the maximum allowable value of 40 ft/s.</i>		Longitudinal occupant impact velocity was 15.4 ft/s, and lateral occupant impact velocity was 16.1 ft/s.	Pass
<i>I. Longitudinal and lateral occupant ridedown accelerations should fall below the preferred value of 15.0 Gs, or at least below the maximum allowable value of 20.49 Gs.</i>		Longitudinal occupant ridedown acceleration was -13.2 G, and lateral occupant ridedown acceleration was -5.9 G.	Pass
Vehicle Trajectory			
<i>It is preferable that the vehicle leave the barrier within the "exit box."</i>		The 2270P vehicle penetrated the guardrail.	N/A

CHAPTER 8. IMPLEMENTATION STATEMENT

The goal of this research project was to identify roadside safety hardware suitable for use on highways with very high design speed. For purposes of this project, a roadway design speed of 100 mi/h was selected and the corresponding design impact speed for the evaluation and testing of roadside safety devices was taken to be 85 mi/h based on research conducted under project 0-5544.

This impact speed results in an impact severity far outside the normal design range. Therefore, conventional engineering design practice was of limited value. Finite element simulation was used as a tool to evaluate the impact performance of selected barrier designs. Although some performance concerns related to the very high-speed impacts were noted, a decision was made in conjunction with TxDOT personnel to test two systems: an energy absorbing bridge rail and a modified wood post thrie beam guardrail. The simulation results indicated that these two systems had a reasonable probability of meeting the required performance criteria. The tests were also designed to develop an enhanced understanding of vehicle and hardware performance at very high impact speeds and serve as a means of validating simulation models. Validity of the models could not be established during the initial phase of this research due to the absence of testing under these severe impact conditions.

The energy absorbing bridge rail and modified wood post thrie beam guardrail failed to meet all of the evaluation criteria recommended in the new *AASHTO Manual for Assessing Safety Hardware (MASH)*. New or modified designs are required to address these performance issues before implementation can be addressed. Recommendations for further research and development of these systems are discussed below.

BRIDGE RAIL

Simulation analyses identified performance issues with common concrete barriers profiles under high-speed impact conditions. Although the results varied for the different profiles evaluated, the concerns were generally related to vehicle stability, occupant risk, and occupant compartment deformation.

Since TxDOT engineers desired to retain a concrete rail if possible, researchers recommended that a more flexible metal rail be attached to the traffic face of a concrete parapet to help manage the energy of the impacting vehicle. The idea was to absorb some of the energy of the impacting vehicle prior to the vehicle engaging the rigid concrete barrier system to help moderate occupant impact velocity and occupant compartment deformation while maintaining vehicle stability.

The design evolved to include dual tubular steel rail elements attached to the face of a vertical concrete parapet by means of energy dissipating spacer pipes. The energy absorbing bridge rail design met the *MASH* performance evaluation criteria when impacted by a 2425-lb passenger car at 85 mi/h. However, a subsequent test with a 5000-lb pickup truck was

unsuccessful due to rollover of the vehicle after it exited the barrier. It was noted that the occupant risk and occupant compartment deformation criteria were met. Therefore, if the stability problem can be addressed, a satisfactory high-speed bridge rail solution appears achievable.

The pipe spacers are designed to help control energy dissipation through their plastic deformation. It was noted that at least one of the pipe spacers was completely collapsed during the pickup truck impact. After this collapse, the rail system imparted a significant impulse to the pickup truck that induced instability as it completed its redirection and exited the barrier system. Increasing the rail height through the addition of a third tubular section or providing separation between the two existing rail elements is a possible solution that can be explored. In addition to providing a higher reaction point that can impart a greater restoring moment, the addition of a third tubular steel rail would provide more contact surface area and better load distribution on the vehicle. However, increasing the rail height and stiffness raises concerns related to small passenger car impacts because it can aggravate already marginal performance in terms of occupant impact velocity and occupant compartment deformation and would increase the potential for an occupant's head to contact the rail during impact.

Another potential means of improving vehicle stability and achieving acceptable impact performance is to incorporate larger diameter pipe spacers. If complete collapse of the spacer pipes can be avoided or delayed, the impulse on the pickup truck can be reduced and stability will be improved. The concept is to provide more collapse distance without significantly changing the stiffness of the rail system. Therefore, the impact performance with the small car should not degrade. The disadvantage of this modification is that it will increase the lateral "footprint" of the barrier and require additional deck space to install.

GUARDRAIL

It was observed in the high-speed simulations of the standard modified steel post three beam guardrail that the steel blockouts deformed and collapsed. This led to significant interaction between the front wheel assembly of the impacting vehicle and the guardrail support posts that led to the vehicle climbing over the rail.

The researchers proposed some modifications to mitigate this behavior. It was recommended that the steel posts and the blockouts be replaced with wood posts and wood blockouts. The objective was to eliminate vehicle climb by preventing collapse of the blockouts and changing the failure mode of the posts. The impact simulation of this modified wood post three beam guardrail predicted stable containment and redirection of the pickup truck.

During the full-scale crash test, the upstream end anchorage failed and released the rail. This allowed the pickup truck to penetrate behind the guardrail system. The terminal system was not explicitly modeled in the simulation. The length of the guardrail installation was believed to be sufficient to limit the forces reaching the anchor assembly.

Unfortunately, the failure of the anchorage precluded a complete evaluation of the modified wood post thrie beam guardrail design. The guardrail performed as intended until the time of anchor failure. The vehicle was being redirected and there was no evidence of vehicle pocketing. However, no conclusions regarding the ability of the guardrail to accommodate high-speed impact conditions can be drawn without further testing.

If the need for a high-speed guardrail system persists, the researchers recommend that the modified wood post thrie beam system be further tested in combination with a modified anchorage system with increased capacity. The weak-post W-beam barrier also showed promise for high-speed vehicle containment and could be further evaluated in any subsequent research.

REFERENCES

1. H. E. Ross, Jr., D. L. Sicking, R. A. Zimmer and J. D. Michie. *Recommended Procedures for the Safety Performance Evaluation of Highway Features*, National Cooperative Highway Research Program Report 350, Transportation Research Board, National Research Council, Washington, D.C., 1993.
2. American Association of State Highway and Transportation Officials. *Manual for Assessing Safety Hardware*. AASHTO, Washington, DC, October 2009.
3. K. Fitzpatrick, K. Zimmerman, R. Bligh, S. Chrysler, and B. Blaschke. *Criteria for High Speed Design Facilities*. Research Report 0-5544-1, Texas Transportation Institute, College Station, TX. March 2007.
4. N.M. Sheikh, R. Ferdous, R.P. Bligh, A. Abu-Odeh. *Analysis of Roadside Safety Devices for Use on Very High-Speed Roadways*. Research Report 0-6071-1, Texas Transportation Institute, College Station, TX. September 2009.
5. J. O. Hallquist. *LS-DYNA Theory Manual*. Livermore Software Technology Corporation, Livermore, CA. March 2006

APPENDIX A. CRASH TEST AND DATA ANALYSIS PROCEDURES

The crash test and data analysis procedures were in accordance with guidelines presented in *MASH*. Brief descriptions of these procedures are presented as follows.

ELECTRONIC INSTRUMENTATION AND DATA PROCESSING

The test vehicle was instrumented with three solid-state angular rate transducers to measure roll, pitch, and yaw rates; a triaxial accelerometer near the vehicle center of gravity (C.G.) to measure longitudinal, lateral, and vertical acceleration levels; and a backup biaxial accelerometer in the rear of the vehicle to measure longitudinal and lateral acceleration levels. These accelerometers were ENDEVCO[®] Model 2262CA, piezoresistive accelerometers with a ± 100 G range.

The accelerometers are strain gauge type with a linear millivolt output proportional to acceleration. Angular rate transducers are solid state, gas flow units designed for high-“g” service. Signal conditioners and amplifiers in the test vehicle increase the low-level signals to a ± 2.5 volt maximum level. The signal conditioners also provide the capability of a resistive calibration (R-cal) or shunt calibration for the accelerometers and a precision voltage calibration for the rate transducers. The electronic signals from the accelerometers and rate transducers are transmitted to a base station by means of a 15-channel, constant bandwidth, Inter-Range Instrumentation Group (I.R.I.G.), FM/FM telemetry link for recording and for display. Calibration signals from the test vehicle are recorded before the test and immediately afterwards. A crystal-controlled time reference signal is simultaneously recorded with the data. Wooden dowels actuate pressure-sensitive switches on the bumper of the impacting vehicle prior to impact by wooden dowels to indicate the elapsed time over a known distance to provide a measurement of impact velocity. The initial contact also produces an “event” mark on the data record to establish the instant of contact with the installation.

The multiplex of data channels, transmitted on one radio frequency, is received and demultiplexed onto a TEAC[®] instrumentation data recorder. After the test, the data are played back from the TEAC[®] recorder and digitized. A proprietary software program (WinDigit) converts the analog data from each transducer into engineering units using the R-cal and pre-zero values at 10,000 samples per second per channel. WinDigit also provides Society of Automotive Engineers (SAE) J211 class 180 phaseless digital filtering and vehicle impact velocity.

All accelerometers are calibrated annually according to the SAE J211 4.6.1 by means of an ENDEVCO[®] 2901, precision primary vibration standard. This device and its support instruments are returned to the factory annually for a National Institute of Standards Technology (NIST) traceable calibration. The subsystems of each data channel are also evaluated annually, using instruments with current NIST traceability, and the results are factored into the accuracy of the total data channel, per SAE J211. Calibrations and evaluations are made any time data are suspect.

The Test Risk Assessment Program (TRAP) uses the data from WinDigit to compute occupant/compartiment impact velocities, time of occupant/compartiment impact after vehicle impact, and the highest 10-millisecond (ms) average ridedown acceleration. WinDigit calculates change in vehicle velocity at the end of a given impulse period. In addition, WinDigit computes maximum average accelerations over 50-ms intervals in each of the three directions. For reporting purposes, the data from the vehicle-mounted accelerometers are filtered with a 60-Hz digital filter, and acceleration versus time curves for the longitudinal, lateral, and vertical directions are plotted using TRAP.

TRAP uses the data from the yaw, pitch, and roll rate transducers to compute angular displacement in degrees at 0.0001-s intervals and then plots yaw, pitch, and roll versus time. These displacements are in reference to the vehicle-fixed coordinate system with the initial position and orientation of the vehicle-fixed coordinate systems being initial impact.

ANTHROPOMORPHIC DUMMY INSTRUMENTATION

An Alderson Research Laboratories Hybrid II, 50th percentile male anthropomorphic dummy, restrained with lap and shoulder belts, was placed in the driver's position of the 1100C vehicle. The dummy was uninstrumented. Use of a dummy in the 2270P vehicle is optional according to *NCHRP Report 350*, and there was no dummy used in the tests with the 2000P vehicle.

PHOTOGRAPHIC INSTRUMENTATION AND DATA PROCESSING

Photographic coverage of the test included three high-speed cameras: one overhead with a field-of-view perpendicular to the ground and directly over the impact point; one placed behind the installation at an angle; and a third placed to have a field-of-view parallel to and aligned with the installation at the downstream end. A flash bulb activated by pressure-sensitive tape switches was positioned on the impacting vehicle to indicate the instant of contact with the installation and was visible from each camera. The films from these high-speed cameras were analyzed on a computer-linked Motion Analyzer to observe phenomena occurring during the collision and to obtain time-event, displacement, and angular data. A 16-mm movie cine, a BetaCam, a VHS-format video camera and recorder, and still cameras were used to record and document conditions of the test vehicle and installation before and after the test.

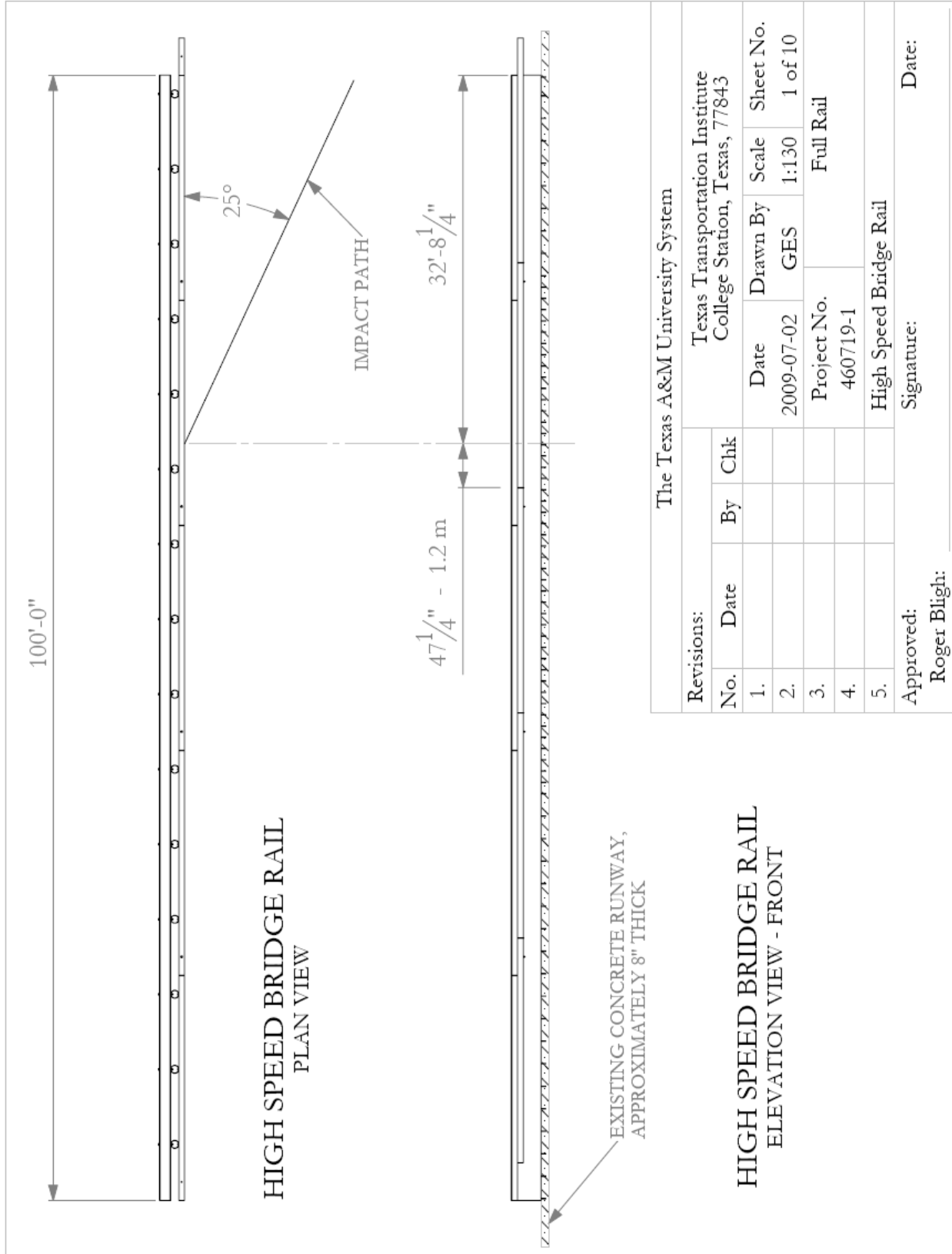
TEST VEHICLE PROPULSION AND GUIDANCE

The test vehicle was towed into the test installation using a steel cable guidance and reverse tow system. A steel cable for guiding the test vehicle was tensioned along the path, anchored at each end, and threaded through an attachment to the front wheel of the test vehicle. An additional steel cable was connected to the test vehicle, passed around a pulley near the impact point, through a pulley on the tow vehicle, and then anchored to the ground such that the tow vehicle moved away from the test site. A 2-to-1 speed ratio between the test and tow vehicle

existed with this system. Just prior to impact with the installation, the test vehicle was released to be free-wheeling and unrestrained. The vehicle remained free-wheeling, i.e., no steering or braking inputs, until the vehicle cleared the immediate area of the test site, at which time the vehicle's brakes were activated to bring it to a safe and controlled stop.

APPENDIX B. DETAILS OF THE HIGH-SPEED ENERGY-ABSORBING BRIDGE RAIL

T:\2008-2009\460719-1 High Speed Bridge Rail\SolidWorks\Drawings\Full Assembly



The Texas A&M University System

Revisions:		Texas Transportation Institute College Station, Texas, 77843			
No.	Date	By	Chk	Scale	Sheet No.
1.				1:130	1 of 10
2.	2009-07-02	GES		1:130	1 of 10
3.				Full Rail	
4.				Project No. 460719-1	
5.				High Speed Bridge Rail	

Approved: Signature: _____ Date: _____
 Roger Bligh:

#	PART NUMBER	QTY.	PAGE
17	Parapet Sturup #4	205	5
18	Rebar, # 5 - 20'	60	
19	Rebar, # 5 - 13' 11"	12	
20	Deck Sturup #5	74	5
21	Rebar, # 5 - 17"	74	
22	Sleeve, 3" x 1 1/2" - 11 gauge A36	15	4

PARTS LIST - CONCRETE

#	PART NAME	QTY.	PAGE
1	Pipe Spacer, 8" schedule 40 A53	15	8
2	Rail Tube, 6" x 6" x 1/4" x 19' 11 1/2" A500 steel	10	9
3	Splice Tube	8	10
4	Bolt, 1/4 -20 x 1 1/2" Gr. 5	8	
5	Bolt, 3/4 -10 x 14" A325	4	
6	HBOLT 1.0000-8x10x2.5-N	15	
7	HNUT 0.6250-11-D-N	30	
8	HNUT 0.7500-10-D-N	4	
9	HNUT 1.0000-8-D-N	15	
10	Washer, 2 1/2" x 2 1/2" x 1/2" plate A36 steel	15	8
11	Washer, 5/8" Flat	30	
12	Regular FW 0.75	8	
13	Regular FW 1	15	
14	Regular LW 0.625	30	
15	Regular LW 0.75	4	
16	Regular LW 1	15	

PARTS LIST - RAIL

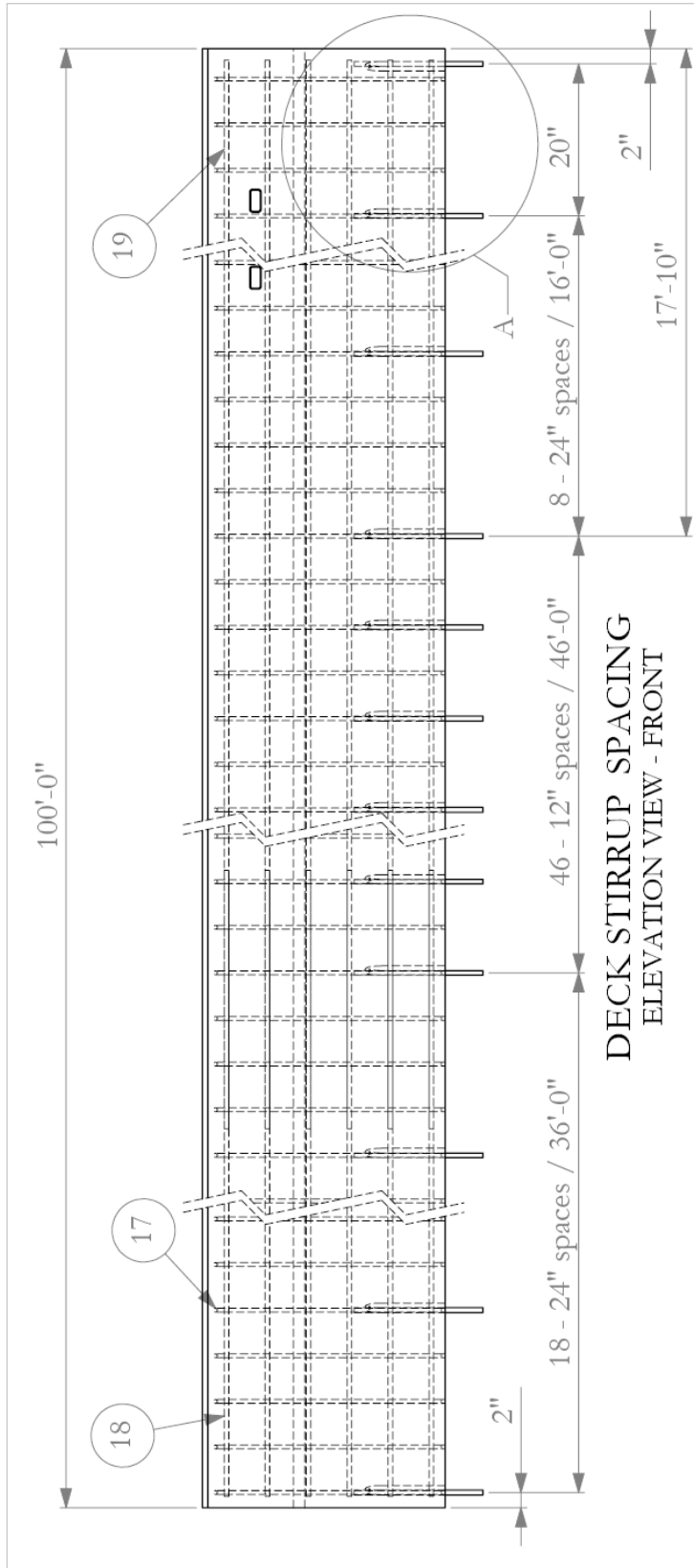
1. CONCRETE SHALL BE 3600 PSI.
2. ALL REBAR - GRADE 60
3. REBAR LAP LENGTH - 34"
4. 13' 11" REBAR (19) - LONGITUDINAL AT END OF PARAPET.

The Texas A&M University System							
Revisions:							
No.	Date	By	Chk	Date	Drawn By	Scale	Sheet No.
1.				2009-07-02	GES	1:500	2 of 10
2.							
3.							
4.							
5.							

Texas Transportation Institute
College Station, Texas, 77843

Project No. 460719-1
High Speed Bridge Rail

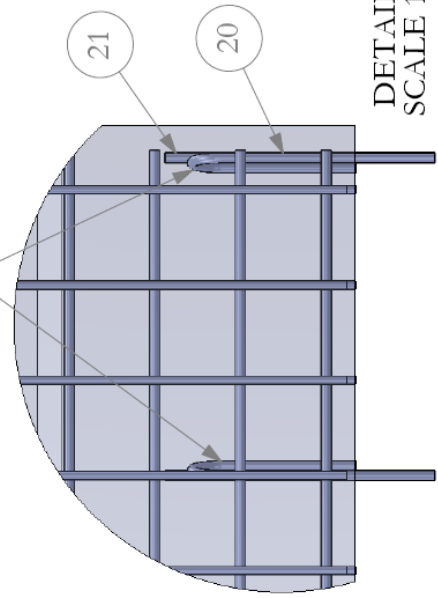
Parts List



**DECK STIRRUP SPACING
ELEVATION VIEW - FRONT**

DECK STIRRUPS (20) TURNED TO AVOID 17" #5 REBAR (21)

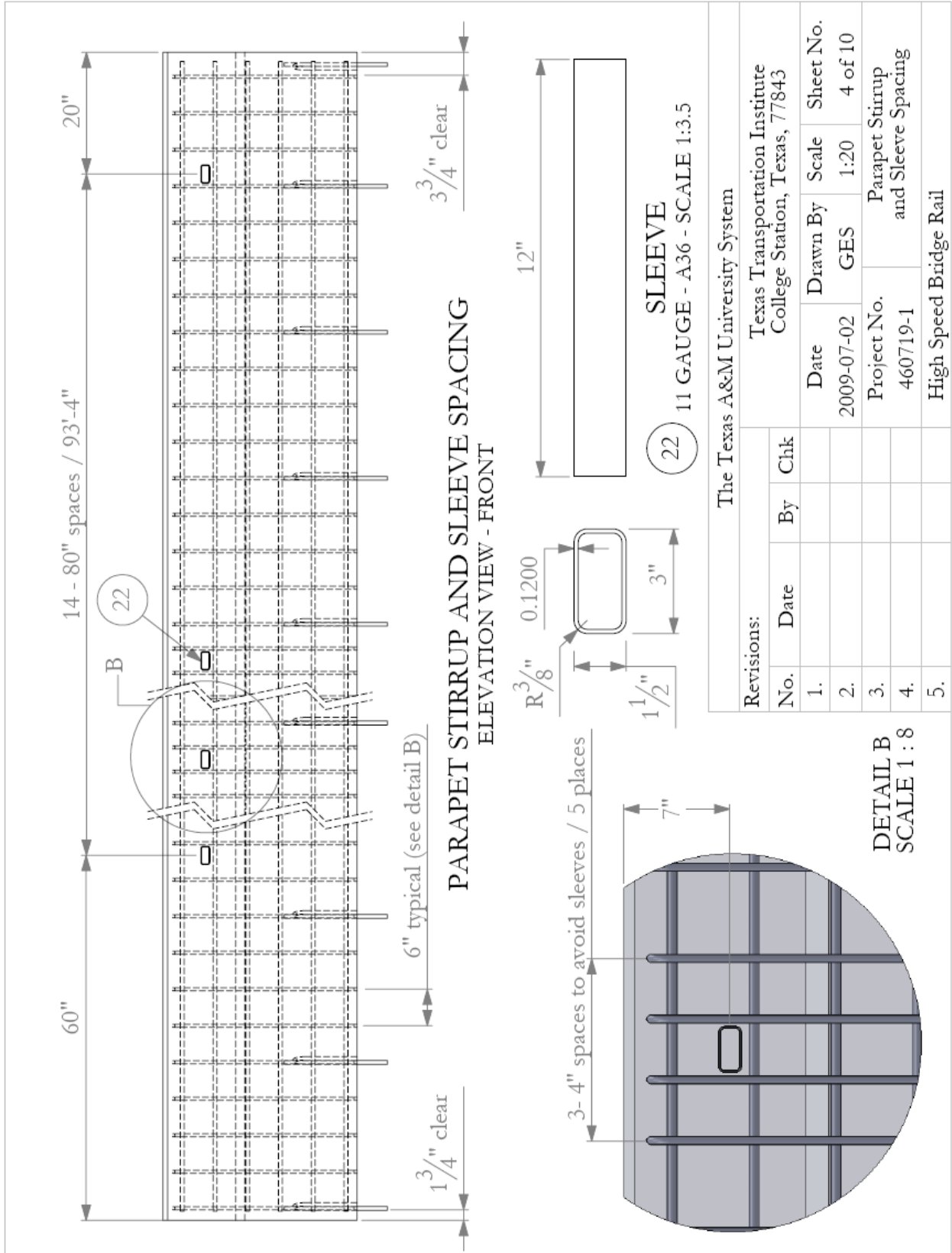
DECK STIRRUPS AND 17" #5 BARS IN 3/4" x 5" HOLES DRILLED IN CONCRETE, ANCHORED WITH HILTI RE500 EPOXY.



**DETAIL A
SCALE 1 : 10**

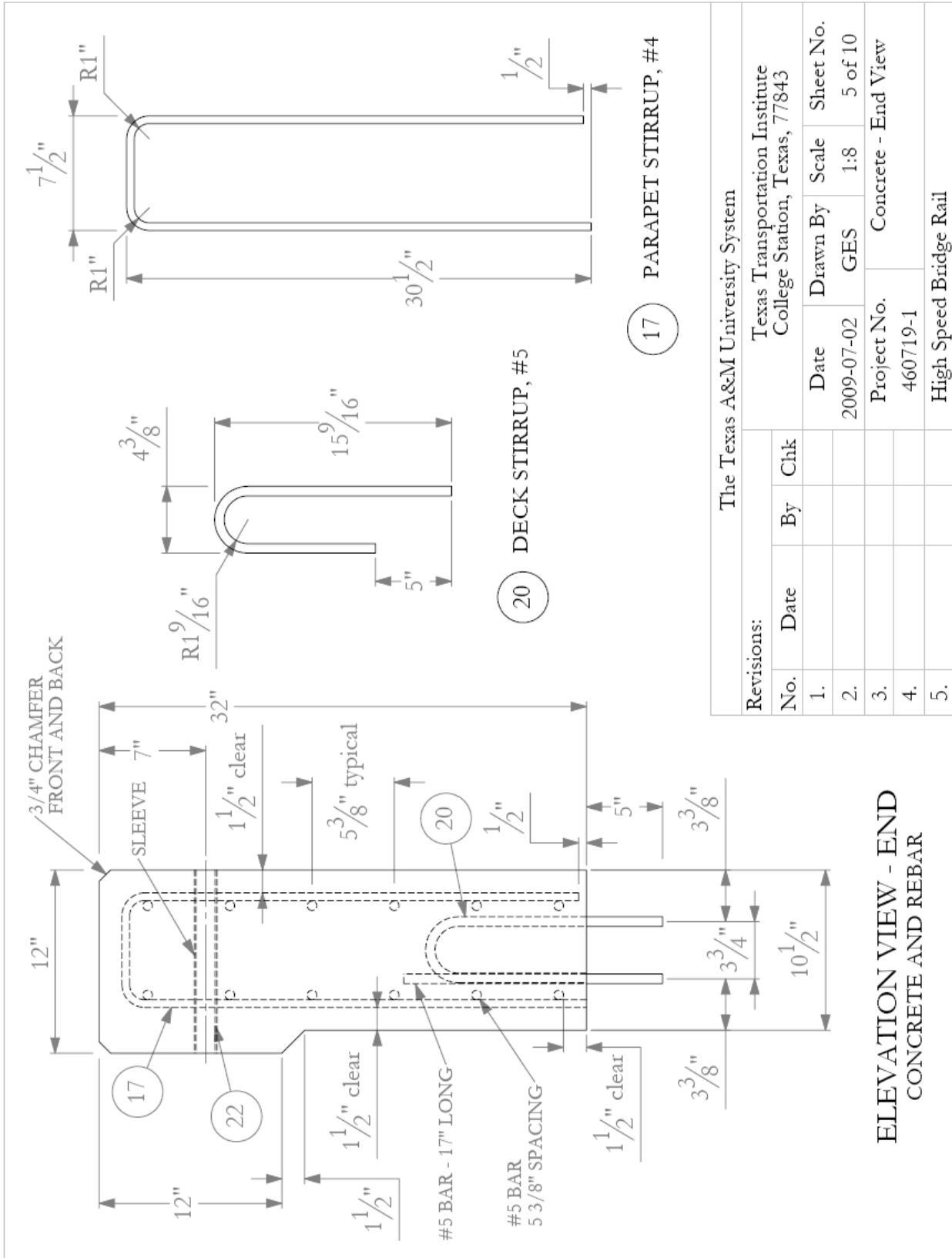
Revisions:				
No.	Date	By	Chk	
1.				
2.				
3.				
4.				
5.				

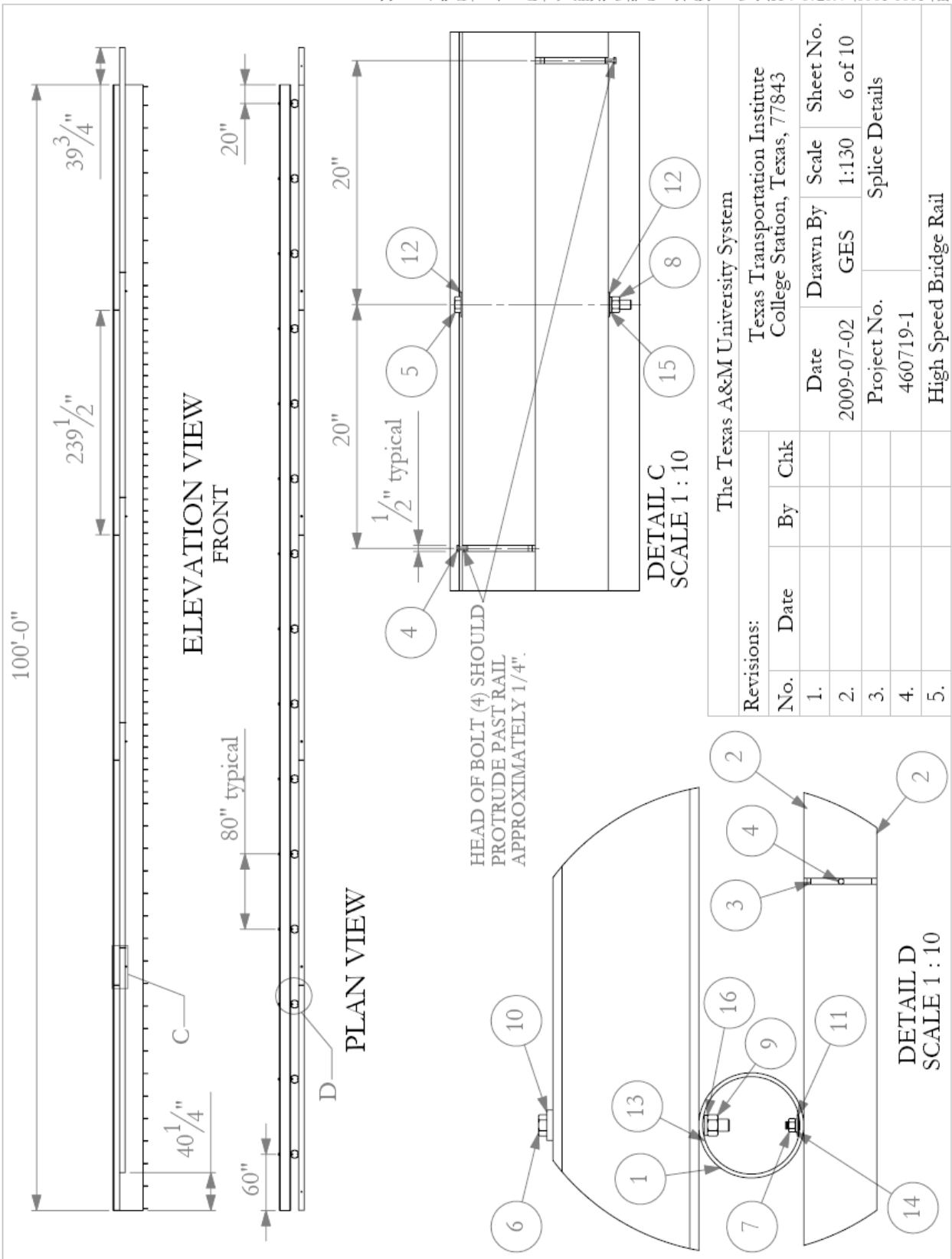
The Texas A&M University System				
Texas Transportation Institute College Station, Texas, 77843		Date	Drawn By	Scale
		2009-07-02	GES	1:20
Project No.	Deck StIRRUP Spacing and Rebar Parts			
460719-1				
High Speed Bridge Rail				

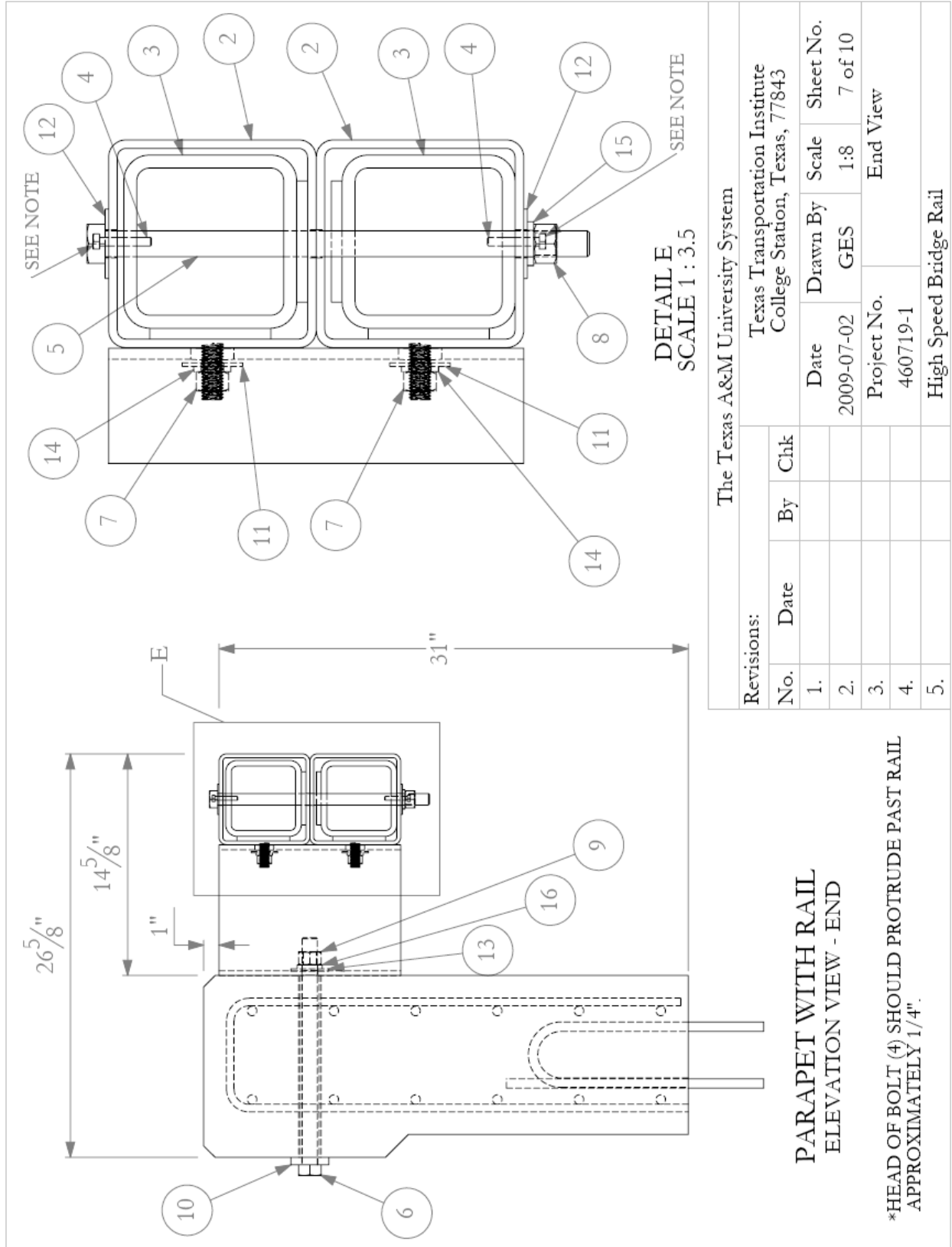


The Texas A&M University System

Revisions:		Texas Transportation Institute College Station, Texas, 77843		Date	Drawn By	Scale	Sheet No.
No.	Date	By	Chk	2009-07-02	GES	1:20	4 of 10
1.							
2.							
3.							
4.							
5.							
				Project No.	Parapet Stirrup and Sleeve Spacing		
				460719-1	High Speed Bridge Rail		





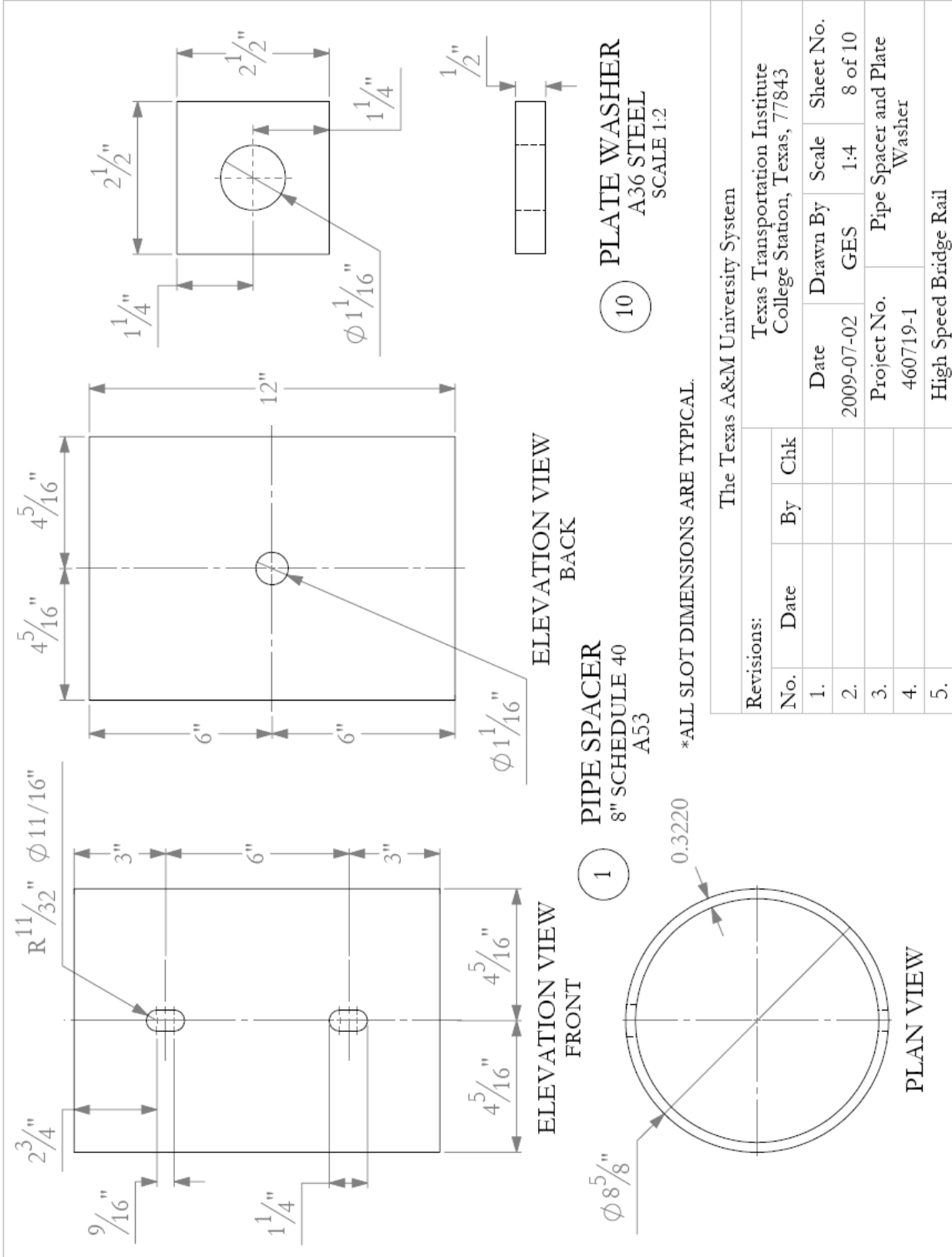


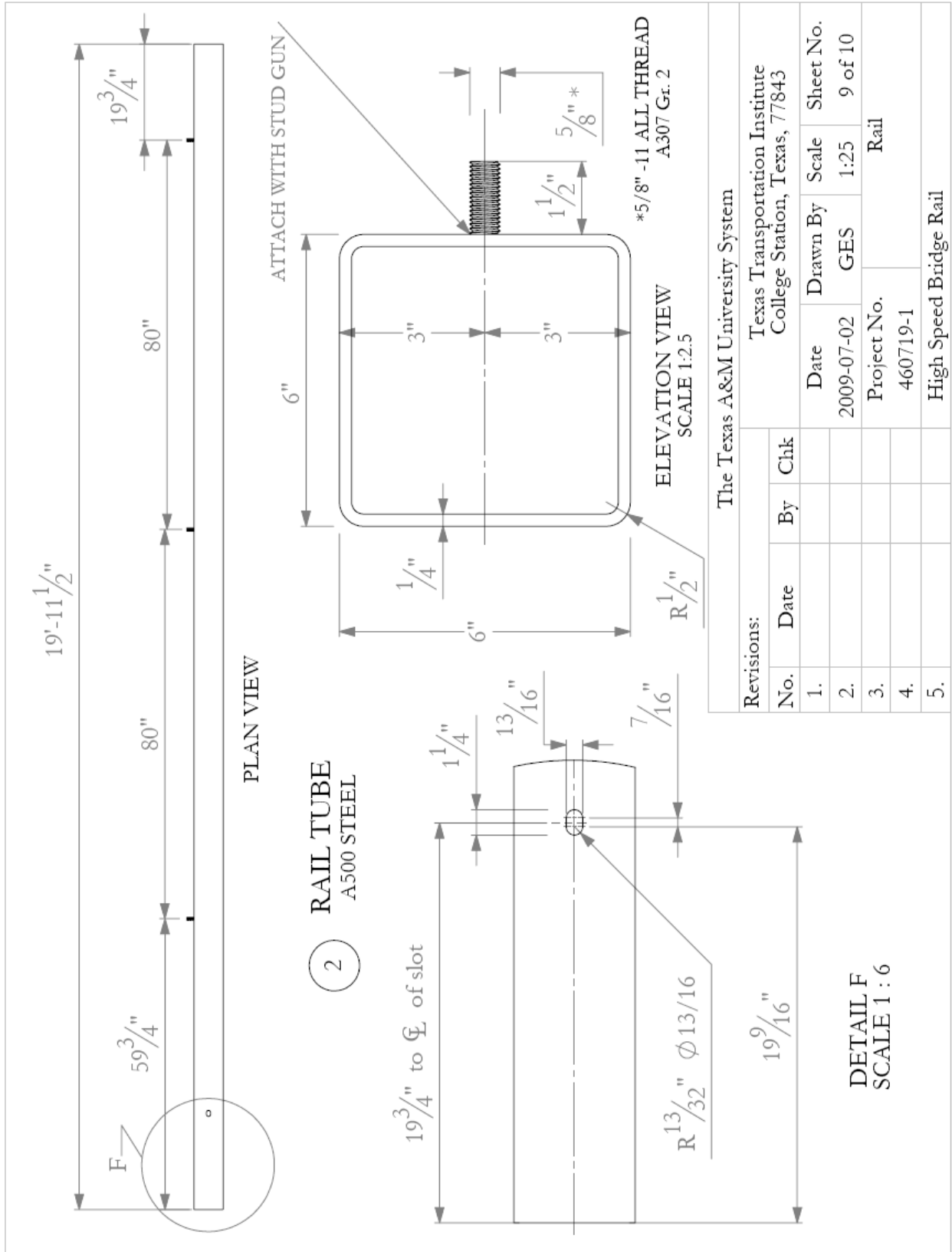
The Texas A&M University System

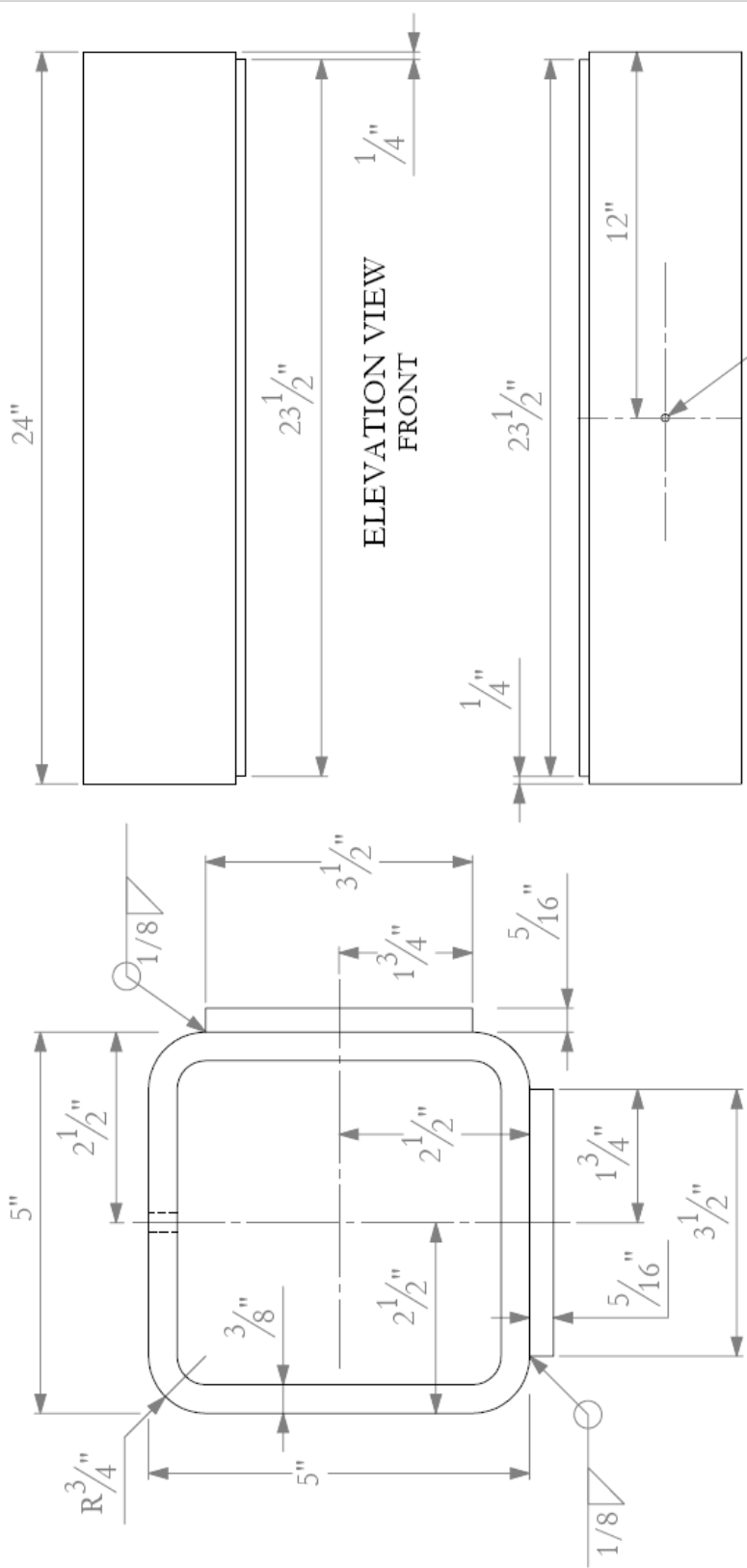
Revisions:		Texas Transportation Institute College Station, Texas, 77843	
No.	Date	By	Chk
1.			
2.	2009-07-02	GES	
3.			
4.			
5.			

Date	Drawn By	Scale	Sheet No.
2009-07-02	GES	1:8	7 of 10

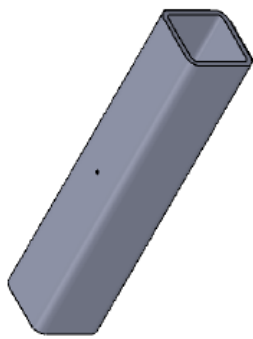
Project No. 460719-1
End View
High Speed Bridge Rail







3 **SPLICE TUBE**
5" x 5" TUBE - A500
5/16" STRAP - A36



ISOMETRIC VIEW
SCALE 1:10

The Texas A&M University System

Revisions:		Texas Transportation Institute College Station, Texas, 77843		
No.	Date	By	Chk	Sheet No.
1.	2009-07-24	GES	RB	10 of 10
2.	2009-07-02	GES		1:5
3.				Splice Tube
4.				460719-1
5.				High Speed Bridge Rail

APPENDIX C. TEST VEHICLE PROPERTIES AND INFORMATION

Date: 2009-08-07 Test No.: 460719-1 VIN No.: KNADC123126132882

Year: 2002 Make: Kia Model: Rio

Tire Inflation Pressure: 29 psi Odometer: 117041 Tire Size: P185/65R14

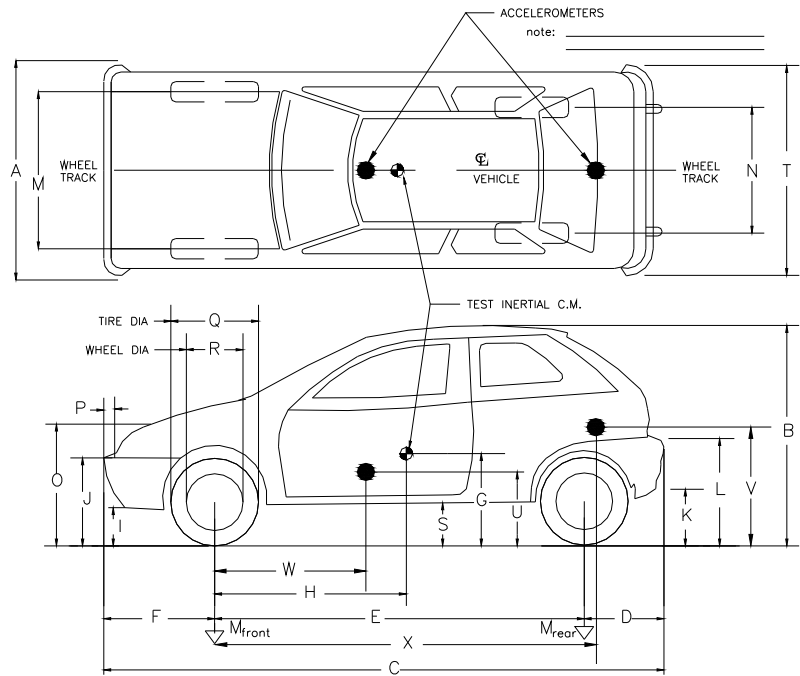
Describe any damage to the vehicle prior to test: _____

• Denotes accelerometer location.

NOTES: _____

Engine Type: 4 cylinder
 Engine CID: 1.5 liter
 Transmission Type:
 Auto or Manual
 FWD RWD 4WD
 Optional Equipment:

Dummy Data:
 Type: 95th percentile male
 Mass: 168 lb
 Seat Position: Passenger Side



Geometry: inches

A	<u>62.50</u>	F	<u>32.00</u>	K	<u>12.00</u>	P	<u>3.25</u>	U	<u>15.50</u>
B	<u>56.12</u>	G	<u> </u>	L	<u>24.25</u>	Q	<u>22.50</u>	V	<u>21.50</u>
C	<u>164.25</u>	H	<u>36.17</u>	M	<u>56.50</u>	R	<u>15.50</u>	W	<u>39.50</u>
D	<u>37.00</u>	I	<u>8.50</u>	N	<u>57.00</u>	S	<u>8.62</u>	X	<u>110.50</u>
E	<u>95.25</u>	J	<u>22.75</u>	O	<u>28.00</u>	T	<u>63.00</u>		

Wheel Center Ht Front 10.75 Wheel Center Ht Rear 11.12

RANGE LIMIT: A = 65 ±3 inches; C = 168 ±8 inches; E = 98 ±5 inches; F = 35 ±4 inches; G = 39 ±4 inches;
 O = 24 ±4 inches; M+N/2 = 56 ±2 inches

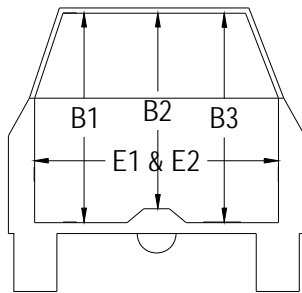
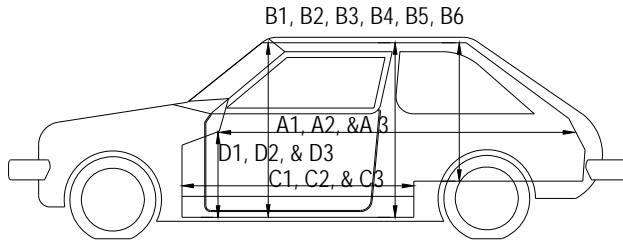
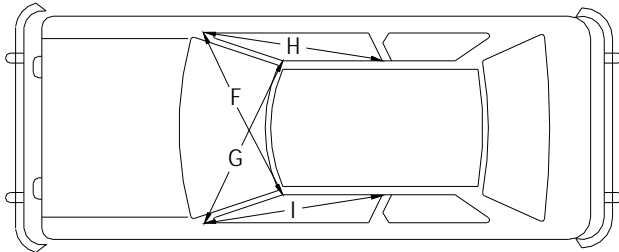
GVWR Ratings:	Mass: lb	Curb	Test Inertial	Gross Static
Front <u>1691</u>	M_{front}	<u>1494</u>	<u>1511</u> Allowable	<u>1593</u> Allowable
Back <u>1559</u>	M_{rear}	<u>905</u>	<u>922</u> Range	<u>1013</u> Range =
Total <u>3250</u>	M_{Total}	<u>2399</u>	<u>2438</u> 2420 ±55 lb	<u>2606</u> 2585 ±55 lb

Mass Distribution:
 lb LF: 786 RF: 725 LR: 460 RR: 467

Figure C1. Vehicle Properties for Test No. 406719-1.

Table C2. Occupant Compartment Measurements for Test No. 460719-1.

Date: 2009-08-07 Test No.: 460719-1 VIN No.: KNADC123126132882
 Year: 2002 Make: Kia Model: Rio



OCCUPANT COMPARTMENT DEFORMATION MEASUREMENT

	Before (inches)	After (inches)
A1	67.25	57.00
A2	64.50	55.75
A3	67.50	61.00
B1	39.50	44.00
B2	35.50	39.50
B3	39.12	44.75
B4	34.88	36.75
B5	35.12	36.75
B6	34.88	35.50
C1	26.62	13.00
C2	-----	-----
C3	26.25	17.25
D1	10.25	13.75
D2	-----	-----
D3	9.12	8.75
E1	49.44	49.00
E2	51.00	49.00
F	49.00	45.00
G	49.00	53.00
H	37.00	30.50
I	37.00	32.00
J*	50.25	44.25

*Lateral area across the cab from driver's side kickpanel to passenger's side kickpanel.

Date: 2009-08-14 Test No.: 460719-2 VIN No.: 3D7HA18N22G161086

Year: 2002 Make: Dodge Model: Ram 1500 Quad-Cab

Tire Size: 245/70R17 Tire Inflation Pressure: 44 psi

Tread Type: Highway Odometer: 98140

Note any damage to the vehicle prior to test: _____

- Denotes accelerometer location.

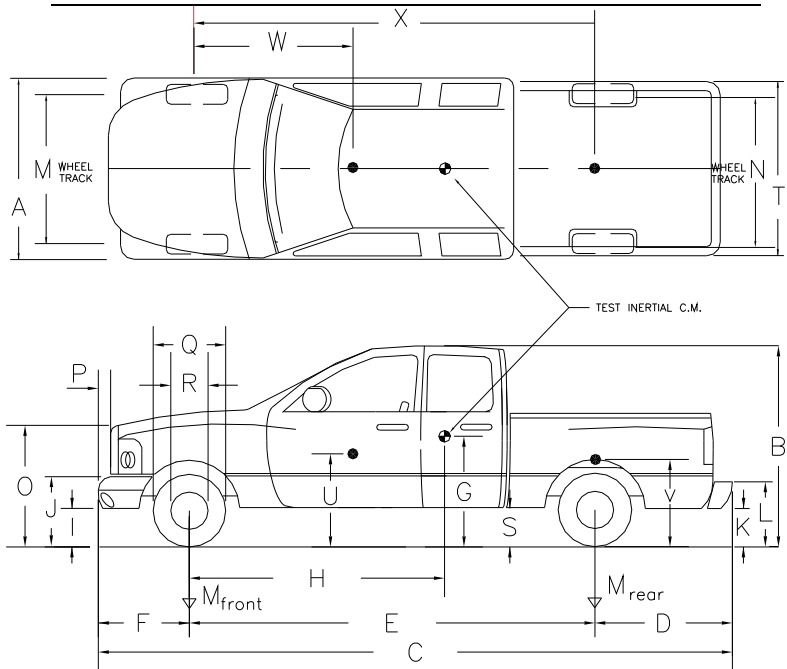
NOTES: _____

Engine Type: V-8
 Engine CID: 4.7 Liter

Transmission Type:
 Auto or _____ Manual
 FWD RWD 4WD

Optional Equipment: _____

Dummy Data:
 Type: No Dummy
 Mass: _____
 Seat Position: _____



Geometry: inches

A	<u>77.00</u>	F	<u>39.00</u>	K	<u>20.50</u>	P	<u>3.00</u>	U	<u>27.50</u>
B	<u>73.25</u>	G	<u>28.06</u>	L	<u>28.75</u>	Q	<u>29.50</u>	V	<u>33.00</u>
C	<u>227.00</u>	H	<u>62.36</u>	M	<u>68.25</u>	R	<u>18.50</u>	W	<u>59.50</u>
D	<u>47.50</u>	I	<u>13.50</u>	N	<u>67.25</u>	S	<u>14.25</u>	X	<u>140.50</u>
E	<u>140.50</u>	J	<u>26.00</u>	O	<u>44.75</u>	T	<u>75.50</u>		

Wheel Center Ht Front	<u>14.12</u>	Wheel Well Clearance (FR)	<u>6.12</u>	Frame Ht (FR)	<u>16.62</u>
Wheel Center Ht Rear	<u>14.25</u>	Wheel Well Clearance (RR)	<u>11.25</u>	Frame Ht (RR)	<u>24.25</u>

RANGE LIMIT: A=78 ±2 inches; C=237 ±13 inches; E=148 ±12 inches; F=39 ±3 inches; G = > 28 inches; H = 63 ±4 inches; O=43 ±4 inches; M+N/2=67 ±1.5 inches

GVWR Ratings:	Mass: lb	Curb	Test Inertial	Gross Static
Front <u>3650</u>	M_{front}	<u>2713</u>	<u>2784</u> Allowable	Allowable
Back <u>3900</u>	M_{rear}	<u>2046</u>	<u>2222</u> Range	Range
Total <u>6650</u>	M_{Total}	<u>4759</u>	<u>5006</u> 5000 ±110 lb	5000 ±110 lb

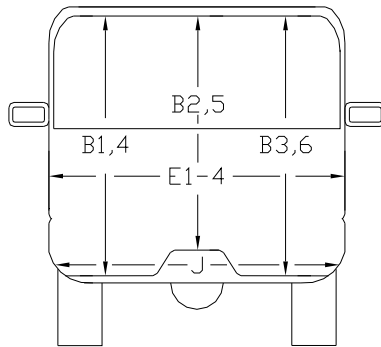
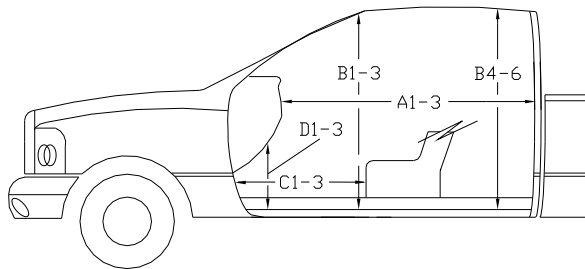
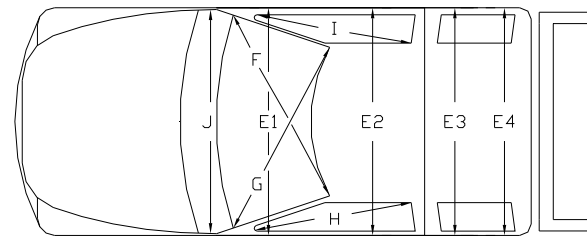
Mass Distribution:
 lb LF: 1411 RF: 1373 LR: 1071 RR: 1151

Figure C2. Vehicle Properties for Test No. 460719-2.

Table C4. Occupant Compartment Measurements for Test No. 460719-2.

Date: 2009-08-14 Test No.: 460719-2 VIN No.: 3D7HA18N22G161086
 Year: 2002 Make: Dodge Model: Ram 1500

OCCUPANT COMPARTMENT DEFORMATION MEASUREMENT



	Before (inches)	After (inches)
A1	64.50	64.25
A2	64.25	63.50
A3	65.25	63.25
B1	44.50	48.75
B2	39.38	71.69
B3	45.25	47.25
B4	42.18	43.31
B5	42.50	43.44
B6	42.19	38.50
C1	29.50	-----
C2	-----	-----
C3	27.25	26.00
D1	12.75	-----
D2	2.62	N/A
D3	11.62	14.75
E1	62.50	N/A
E2	64.75	N/A
E3	64.50	N/A
E4	64.12	62.38
F	60.00	59.00
G	60.00	57.00
H	39.75	N/A
I	39.75	37.25
J*	24.56	16.25

*Lateral area across the cab from driver's side kickpanel to passenger's side kickpanel.

Date: 2009-08-21 Test No.: 460719-3 VIN No.: 1K7HA18NX3S140902

Year: 2003 Make: Dodge Model: Ram 1500 Quad-Cab

Tire Size: 245/70R17 Tire Inflation Pressure: 35 psi

Tread Type: Highway Odometer: 177426

Note any damage to the vehicle prior to test: _____

● Denotes accelerometer location.

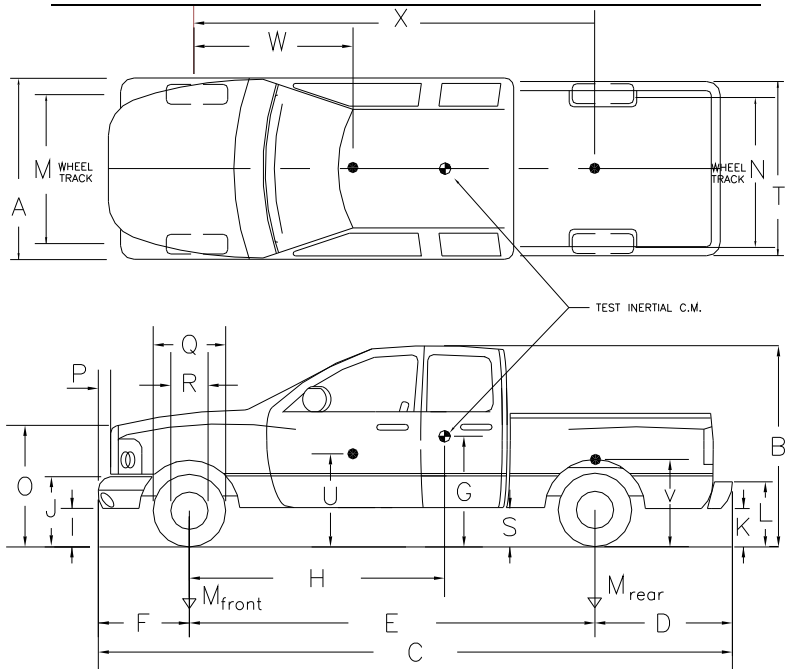
NOTES: _____

Engine Type: V8
 Engine CID: 4.7 liter

Transmission Type:
 Auto or _____ Manual
 FWD RWD 4WD

Optional Equipment: _____

Dummy Data:
 Type: No dummy
 Mass: _____
 Seat Position: _____



Geometry: inches

A	<u>77.00</u>	F	<u>39.00</u>	K	<u>20.50</u>	P	<u>3.00</u>	U	<u>27.50</u>
B	<u>73.25</u>	G	<u>28.02</u>	L	<u>28.75</u>	Q	<u>29.50</u>	V	<u>33.00</u>
C	<u>227.00</u>	H	<u>62.98</u>	M	<u>68.25</u>	R	<u>18.50</u>	W	<u>59.50</u>
D	<u>47.50</u>	I	<u>13.50</u>	N	<u>67.25</u>	S	<u>14.25</u>	X	<u>140.50</u>
E	<u>140.50</u>	J	<u>26.00</u>	O	<u>44.75</u>	T	<u>75.50</u>		

Wheel Center Ht Front	<u>14.12</u>	Wheel Well Clearance (FR)	<u>6.12</u>	Frame Ht (FR)	<u>16.62</u>
Wheel Center Ht Rear	<u>14.25</u>	Wheel Well Clearance (RR)	<u>11.25</u>	Frame Ht (RR)	<u>24.24</u>

RANGE LIMIT: A=78 ±2 inches; C=237 ±13 inches; E=148 ±12 inches; F=39 ±3 inches; G = > 28 inches; H = 63 ±4 inches; O=43 ±4 inches; M+N/2=67 ±1.5 inches

GVWR Ratings:	Mass: lb	Curb	Test Inertial	Gross Static
Front <u>3650</u>	M_{front}	<u>2780</u>	<u>2769</u> Allowable	Allowable
Back <u>6900</u>	M_{rear}	<u>1989</u>	<u>2250</u> Range	Range
Total <u>6650</u>	M_{Total}	<u>4769</u>	<u>5019</u> 5000 ±110 lb	5000 ±110 lb

Mass Distribution:
 lb LF: 1398 RF: 1371 LR: 1113 RR: 1137

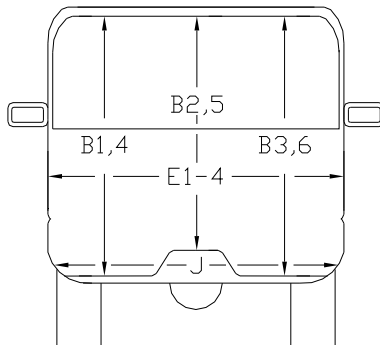
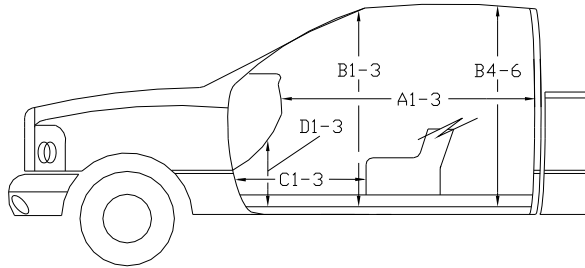
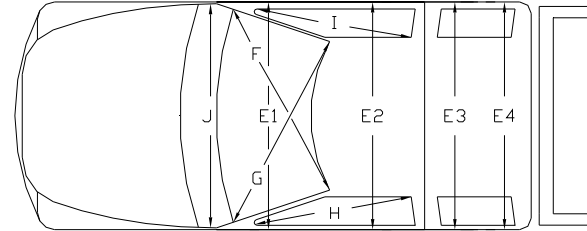
Figure C3. Vehicle Properties for Test No. 460719-3.

Table C6. Occupant Compartment Measurements for Test No. 460719-3.

Date: 2009-08-21 Test No.: 460719-3 VIN No.: 1K7HA18NX3S140902

Year: 2003 Make: Dodge Model: Ram 1500 Quad-Cab

OCCUPANT COMPARTMENT DEFORMATION MEASUREMENT



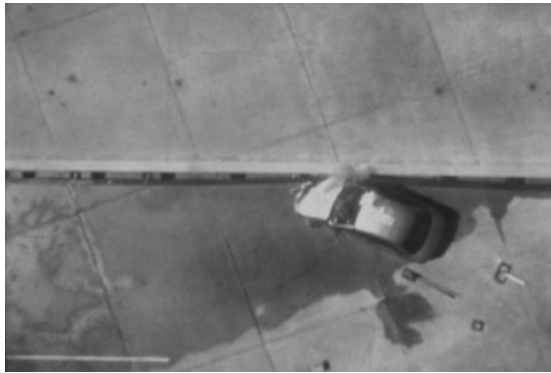
	Before (inches)	After (inches)
A1	64.44	64.44
A2	64.50	64.50
A3	65.12	65.12
B1	45.25	45.25
B2	39.25	39.25
B3	45.50	45.50
B4	52.25	52.25
B5	42.75	42.75
B6	42.75	42.75
C1	29.75	29.75
C2	-----	-----
C3	27.75	27.75
D1	12.75	12.75
D2	2.50	2.50
D3	11.62	11.62
E1	62.50	62.50
E2	64.50	64.50
E3	64.31	64.31
E4	64.00	64.00
F	59.50	59.50
G	59.50	59.50
H	39.00	39.00
I	39.00	39.00
J*	62.12	62.12

*Lateral area across the cab from driver's side kickpanel to passenger's side kickpanel.

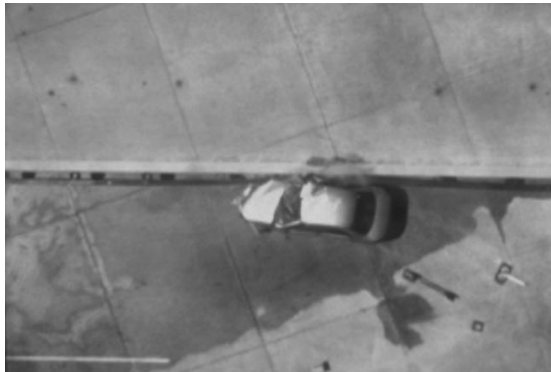
APPENDIX D. SEQUENTIAL PHOTOGRAPHS



0.000 s



0.049 s



0.098 s



0.147 s



Figure D1. Sequential Photographs for Test No. 460719-1 (Overhead and Frontal Views).



0.196 s



0.246 s



0.295 s



0.344 s



**Figure D1. Sequential Photographs for Test No. 460719-1
(Overhead and Frontal Views) (Continued).**



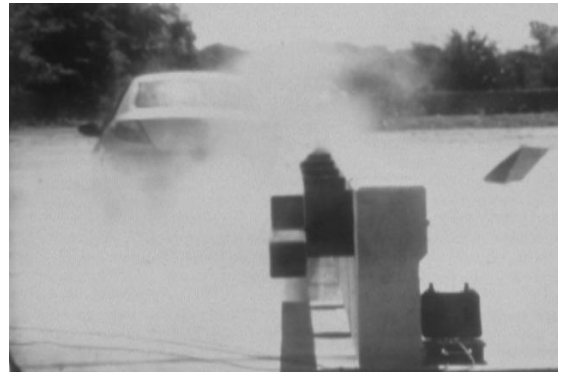
0.000 s



0.196 s



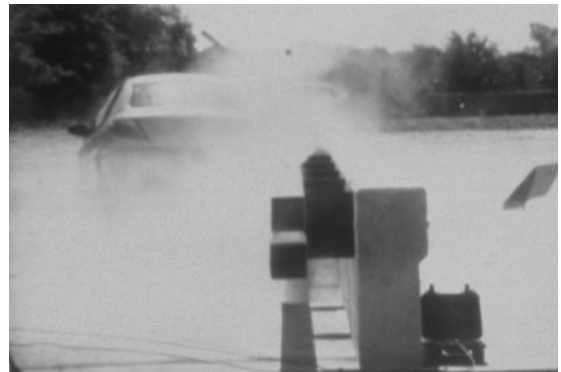
0.049 s



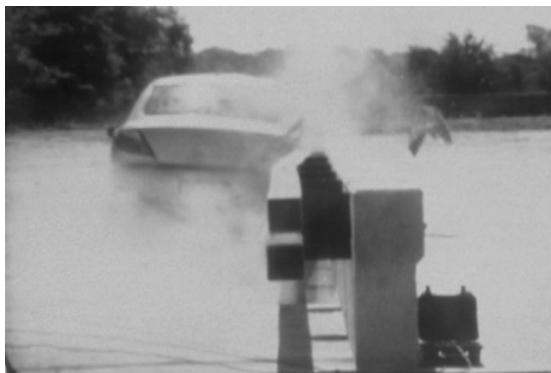
0.246 s



0.098 s



0.295 s



0.147 s



0.344 s

Figure D2. Sequential Photographs for Test No. 460719-1 (Rear View).



0.000 s



0.049 s



0.098 s



0.147 s



Figure D3. Sequential Photographs for Test 460719-2 (Overhead and Frontal Views).



0.196 s



0.246 s



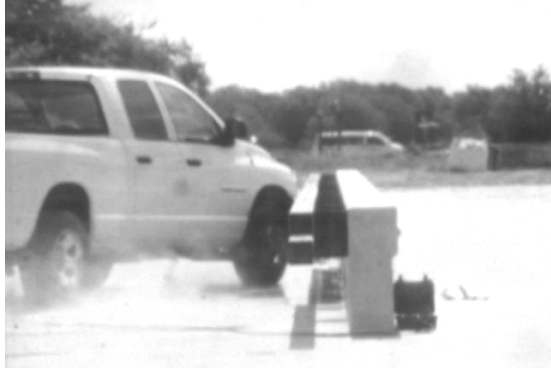
0.295 s



0.344 s



**Figure D3. Sequential Photographs for Test 460719-2
(Overhead and Frontal Views) (Continued).**



0.000 s



0.049 s



0.098 s



0.147 s



0.196 s



0.246 s



0.295 s



0.344 s

**Figure D4. Sequential Photographs for Test 460719-2
(Rear View).**



0.000 s



0.049 s



0.098 s



0.148 s



**Figure D5. Sequential Photographs for Test No. 460719-3
(Overhead and Frontal Views).**



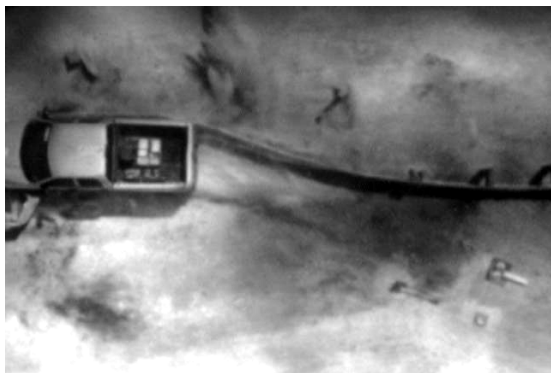
0.197 s



0.246 s



0.295 s



0.344 s



**Figure D5. Sequential Photographs for Test No. 460719-3
(Overhead and Frontal Views) (Continued).**



0.000 s



0.197 s



0.049 s



0.246 s



0.098 s



0.295 s



0.148 s



0.344 s

**Figure D6. Sequential Photographs for Test No. 460719-3
(Rear View).**

APPENDIX E. VEHICLE ANGULAR DISPLACEMENTS AND ACCELERATIONS

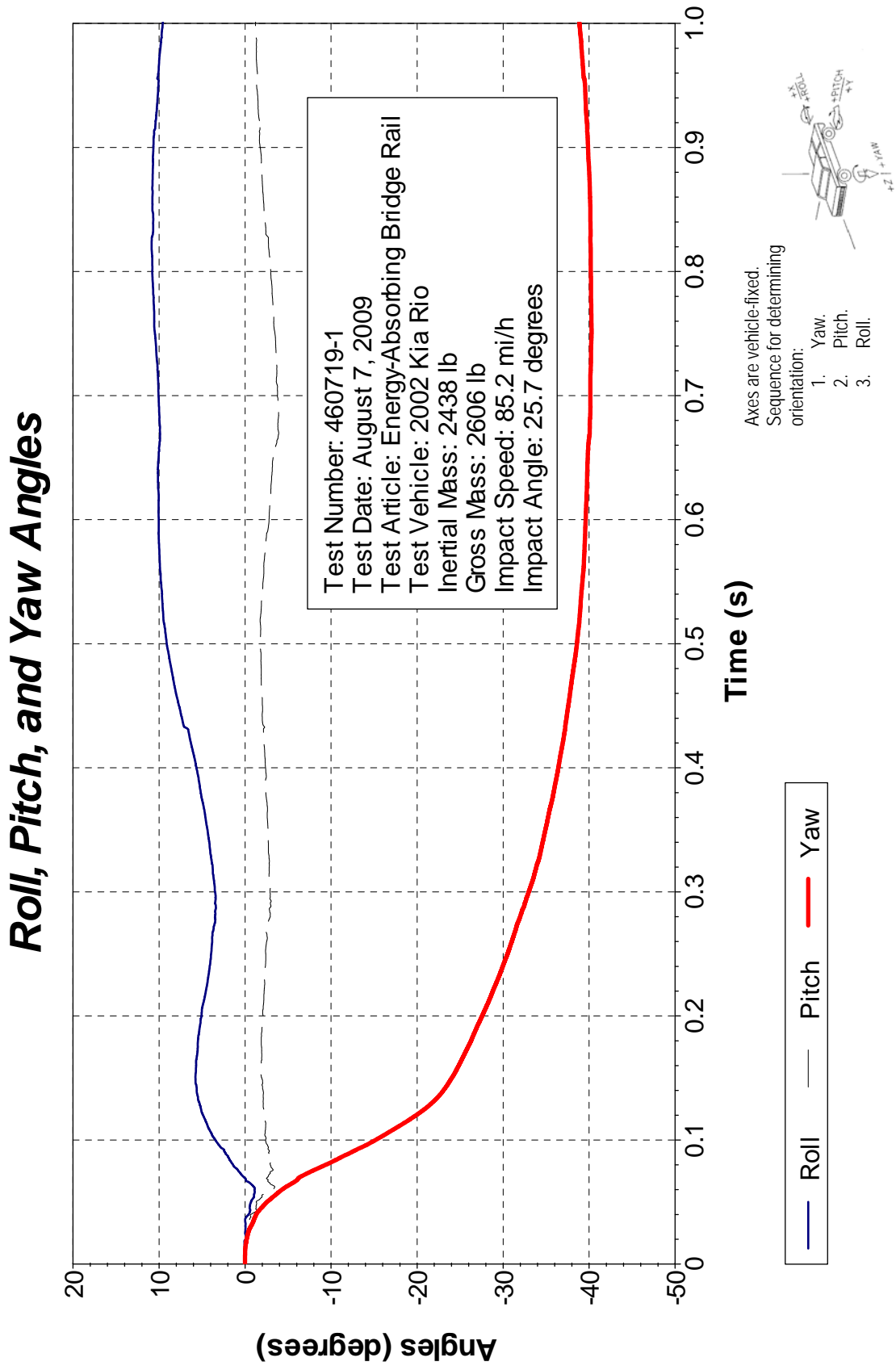


Figure E1. Vehicle Angular Displacements for Test No. 460719-1.

X Acceleration at CG

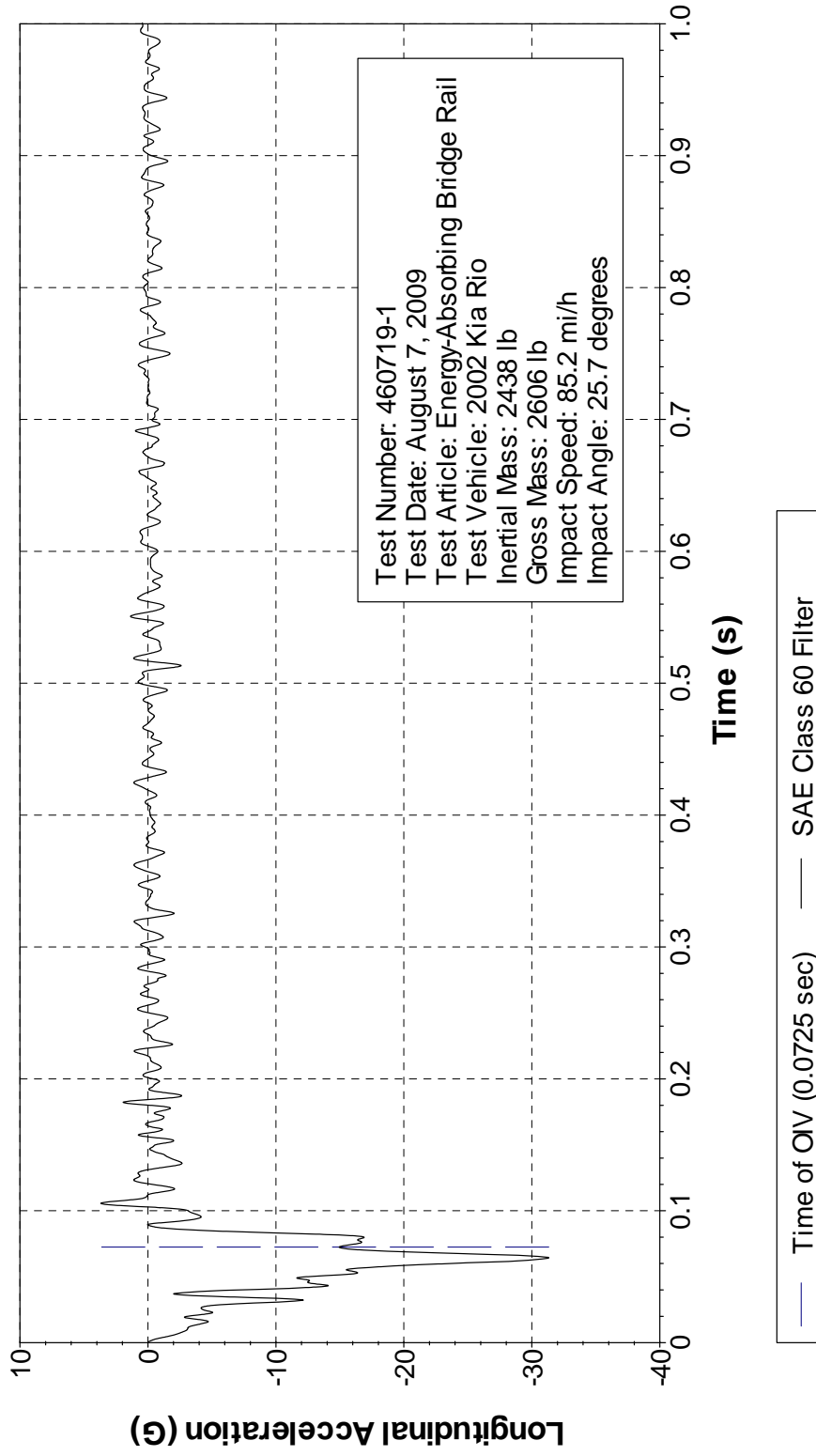


Figure E2. Vehicle Longitudinal Accelerometer Trace for Test No. 460719-1 (Accelerometer Located at Center of Gravity).

Y Acceleration at CG

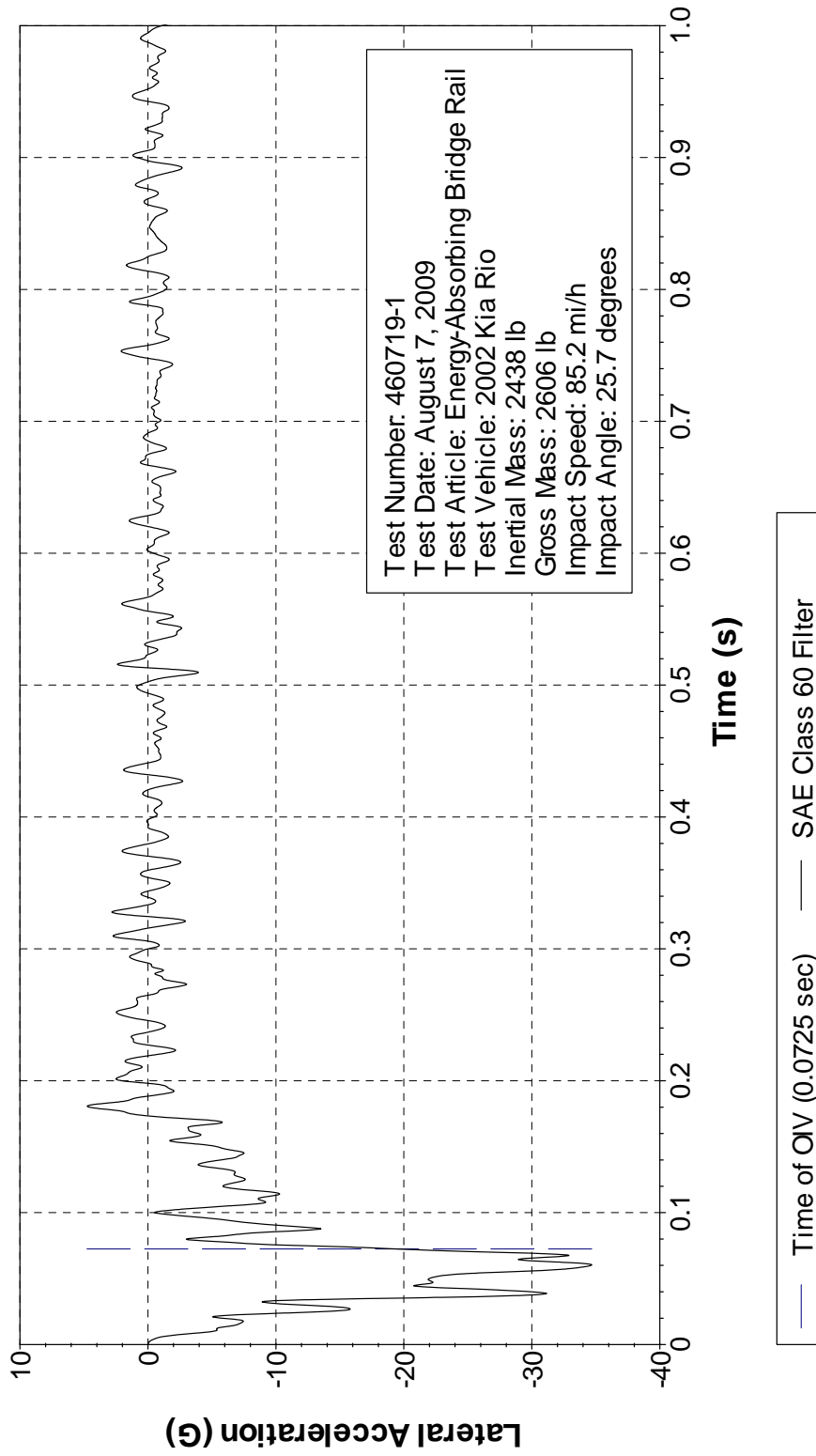
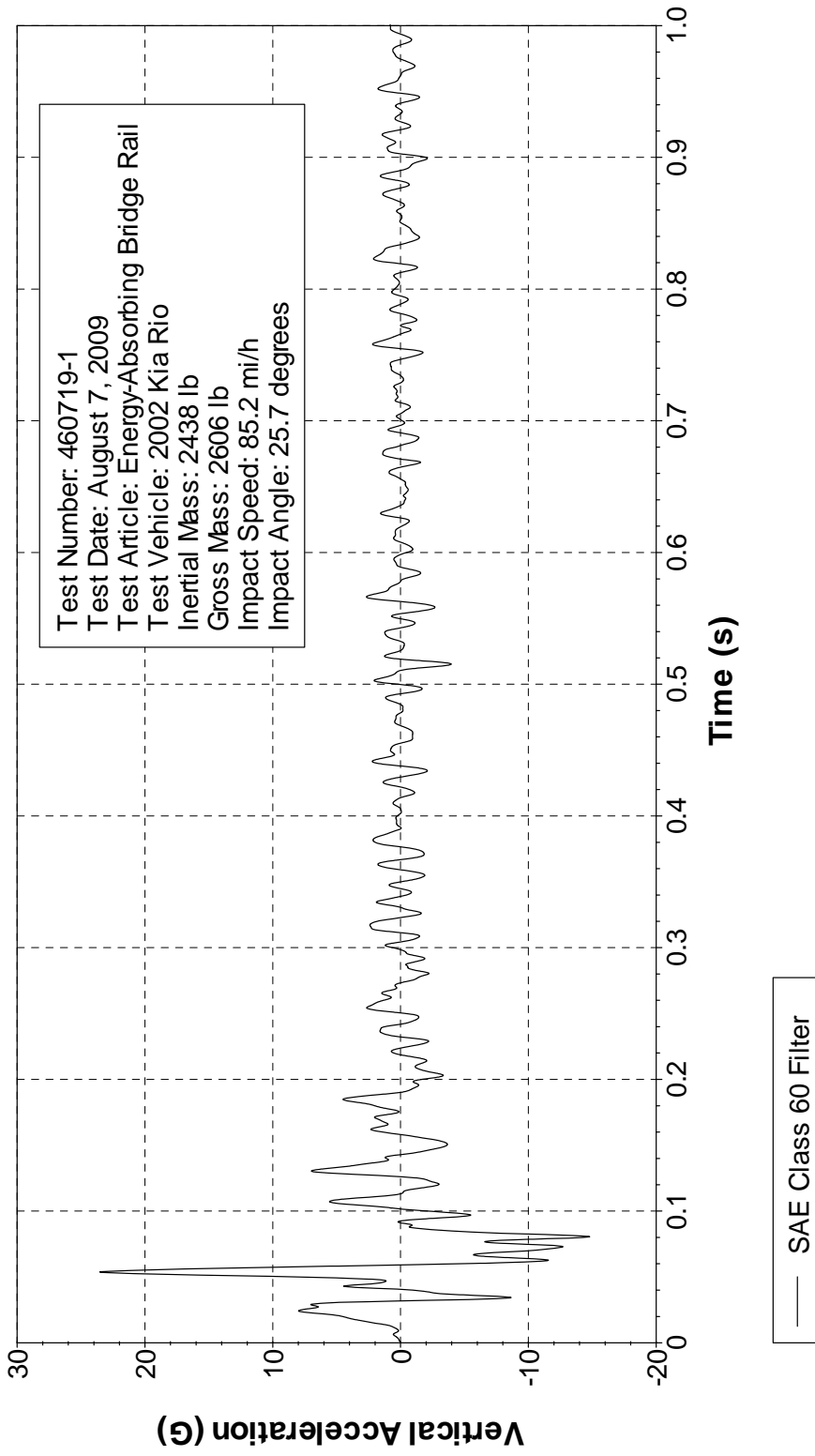


Figure E3. Vehicle Lateral Accelerometer Trace for Test No. 460719-1 (Accelerometer Located at Center of Gravity).

Z Acceleration at CG



**Figure E4. Vehicle Vertical Accelerometer Trace for Test No. 460719-1
(Accelerometer Located at Center of Gravity).**

X Acceleration over Rear Axle

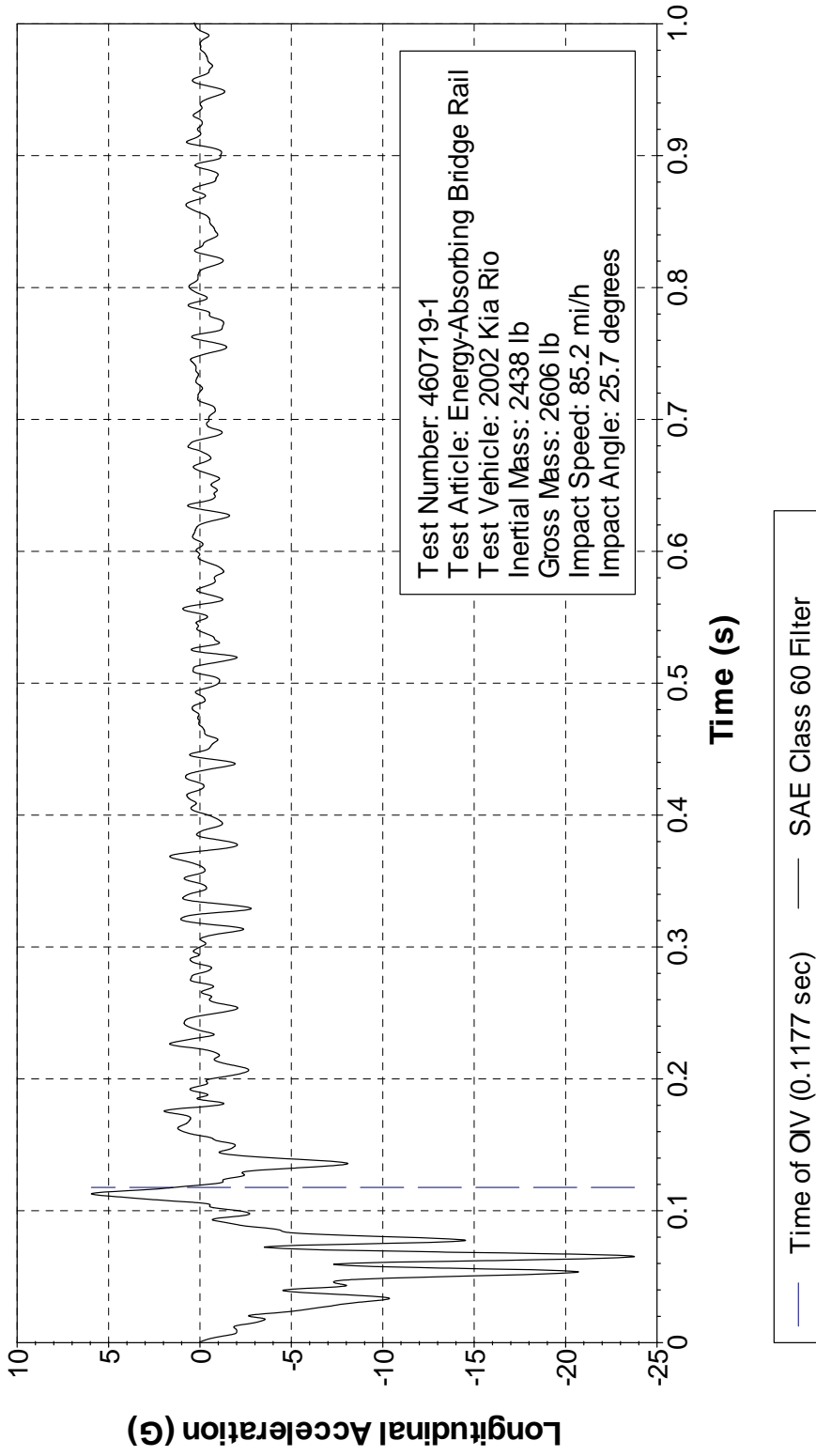


Figure E5. Vehicle Longitudinal Accelerometer Trace for Test No. 460719-1 (Accelerometer Located over Rear Axle).

Y Acceleration over Rear Axle

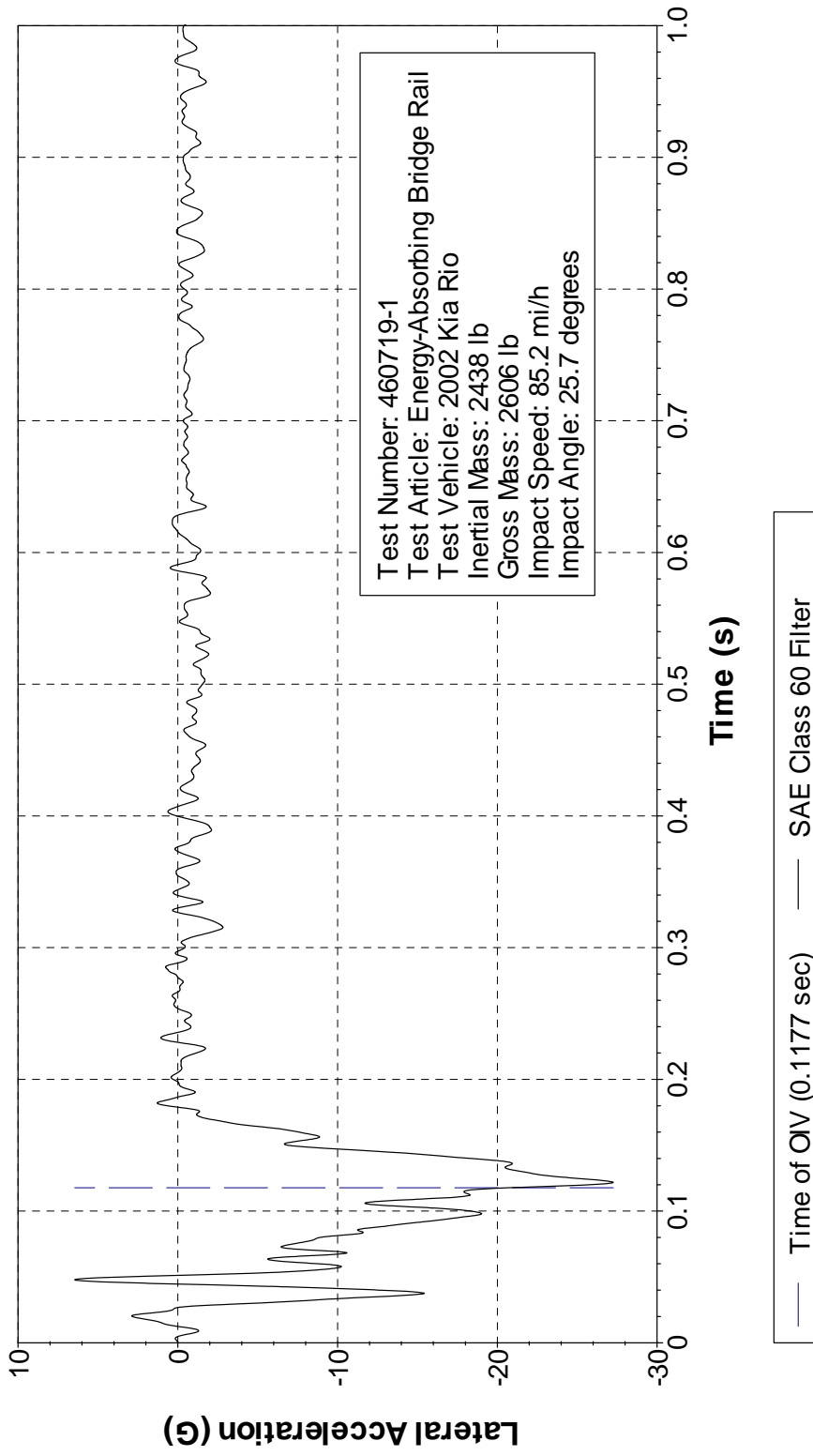
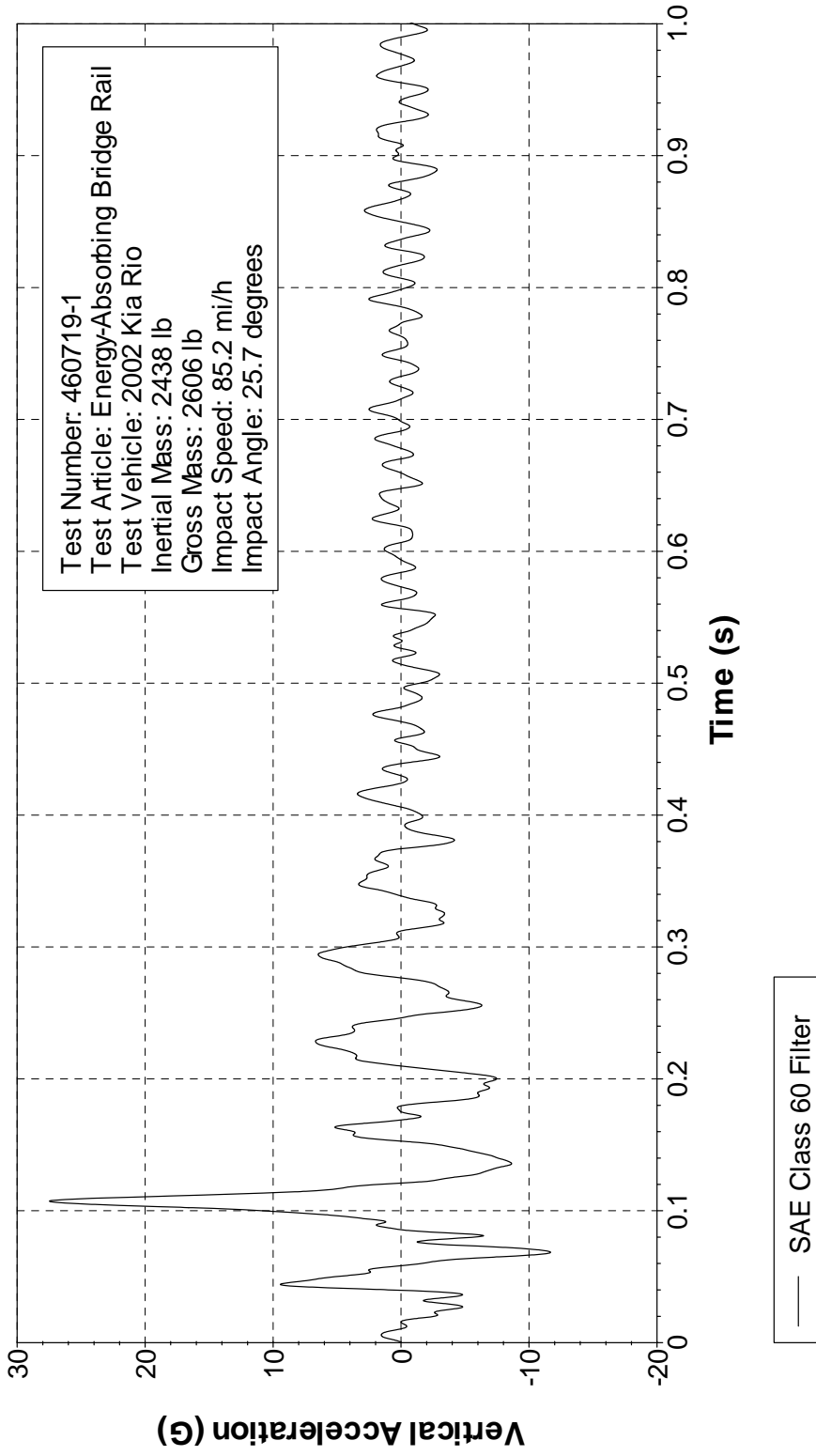


Figure E6. Vehicle Lateral Accelerometer Trace for Test No. 460719-1
(Accelerometer Located over Rear Axle).

Z Acceleration over Rear Axle



**Figure E7. Vehicle Vertical Accelerometer Trace for Test No. 460719-1
(Accelerometer Located over Rear Axle).**

Roll, Pitch, and Yaw Angles

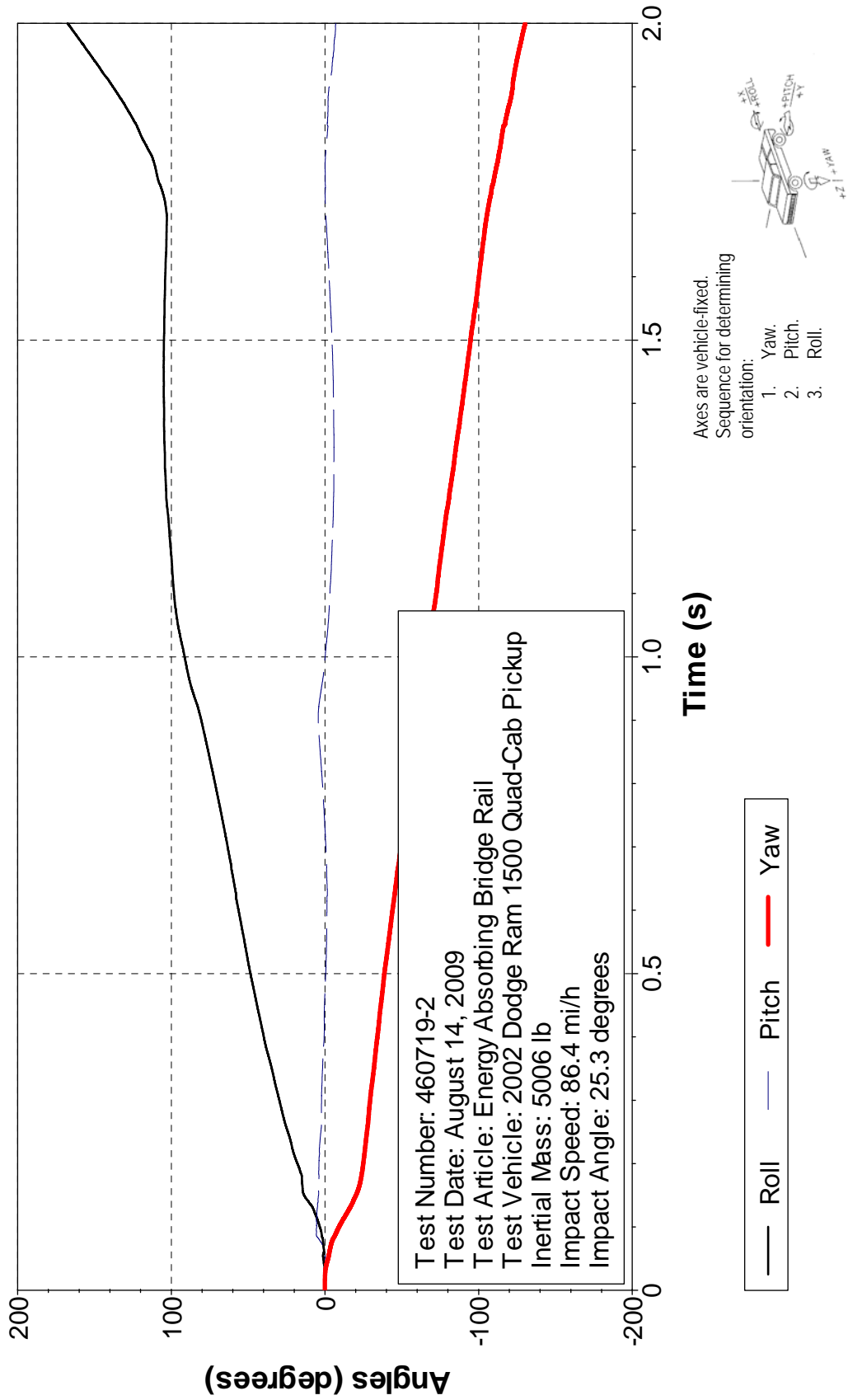
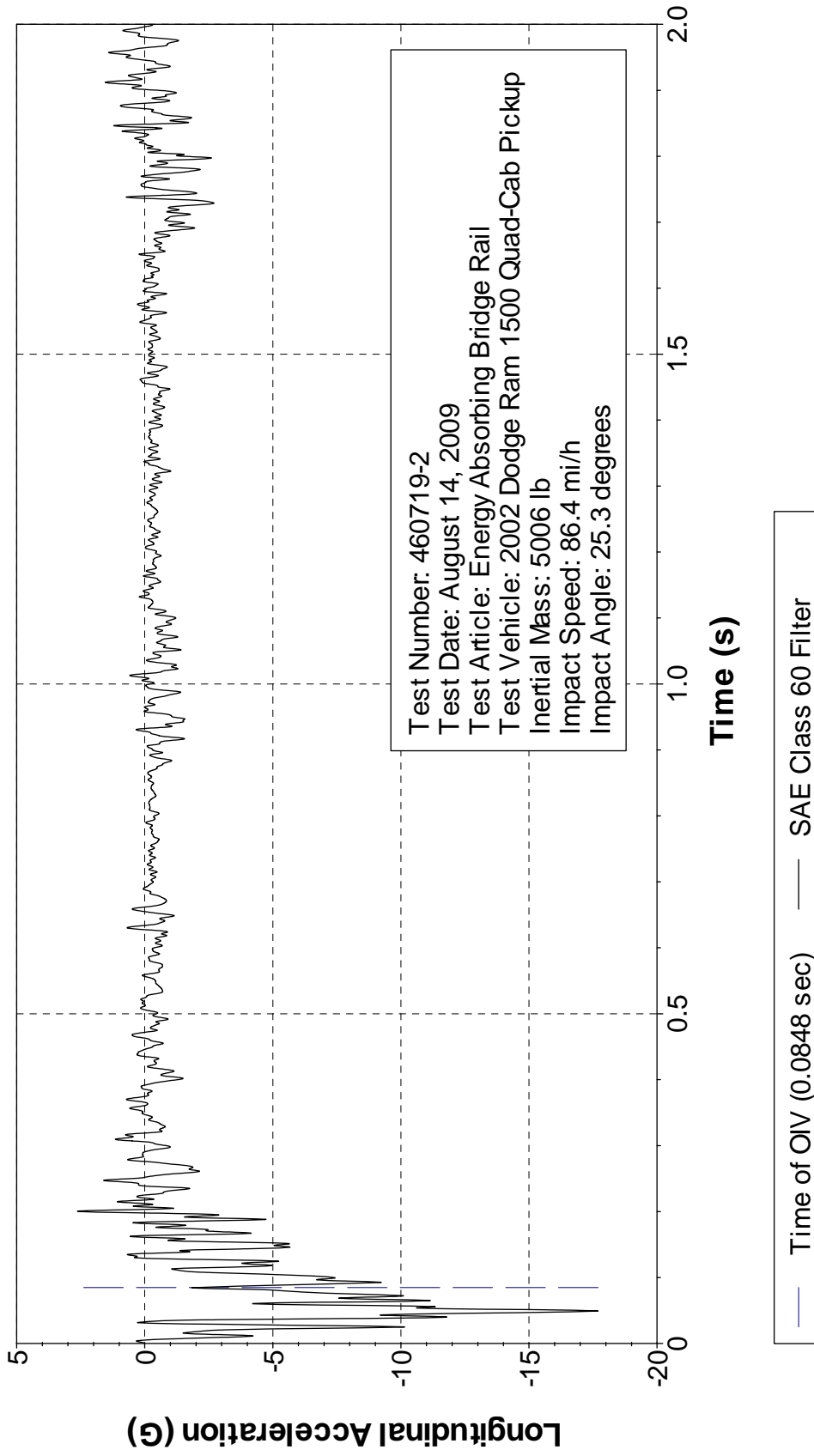


Figure E8. Vehicle Angular Displacements for Test No. 460719-2.

X Acceleration at CG



**Figure E9. Vehicle Longitudinal Accelerometer Trace for Test No. 460719-2
(Accelerometer Located at Center of Gravity).**

Y Acceleration at CG

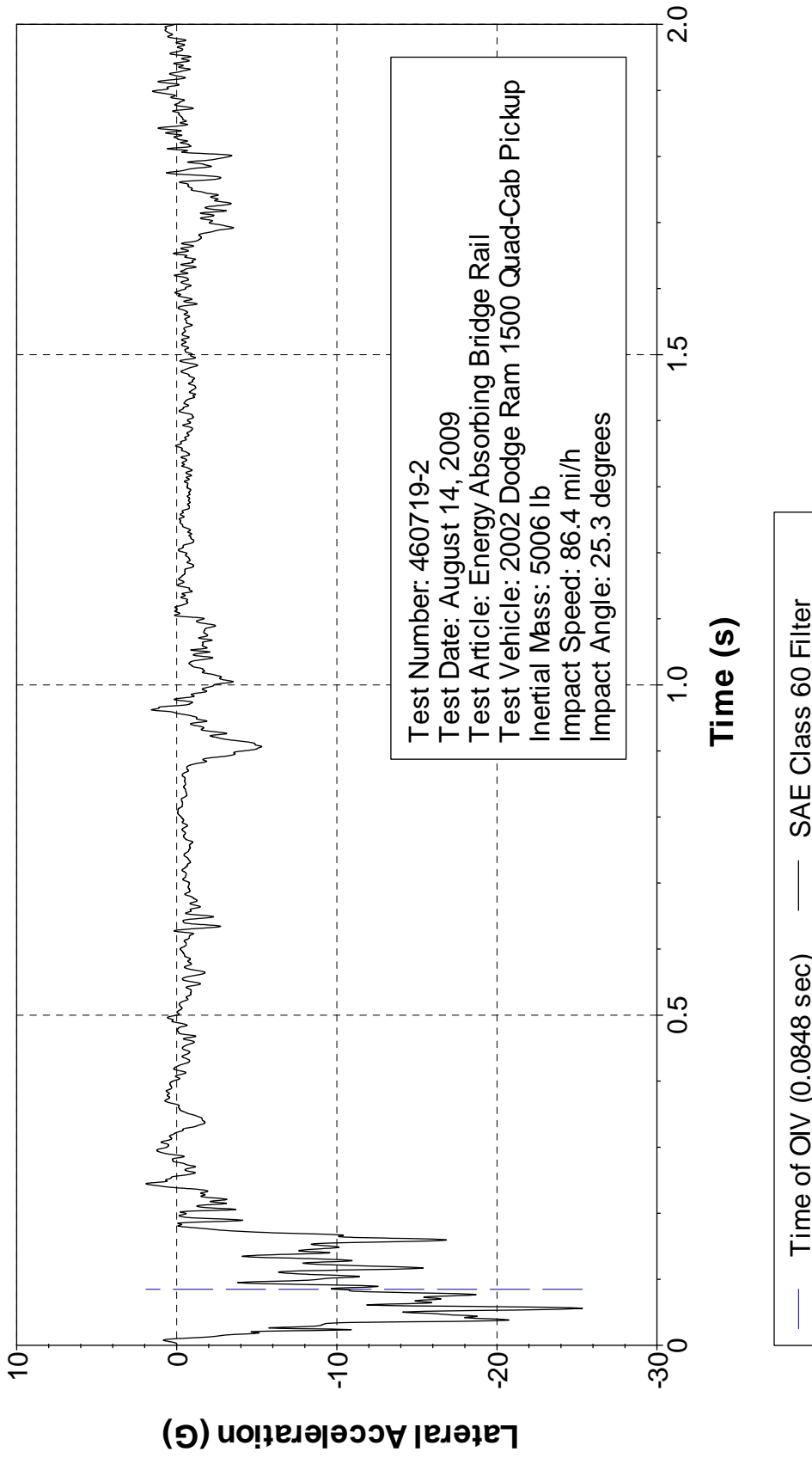


Figure E10. Vehicle Lateral Accelerometer Trace for Test No. 460719-2 (Accelerometer Located at Center of Gravity).

Z Acceleration at CG

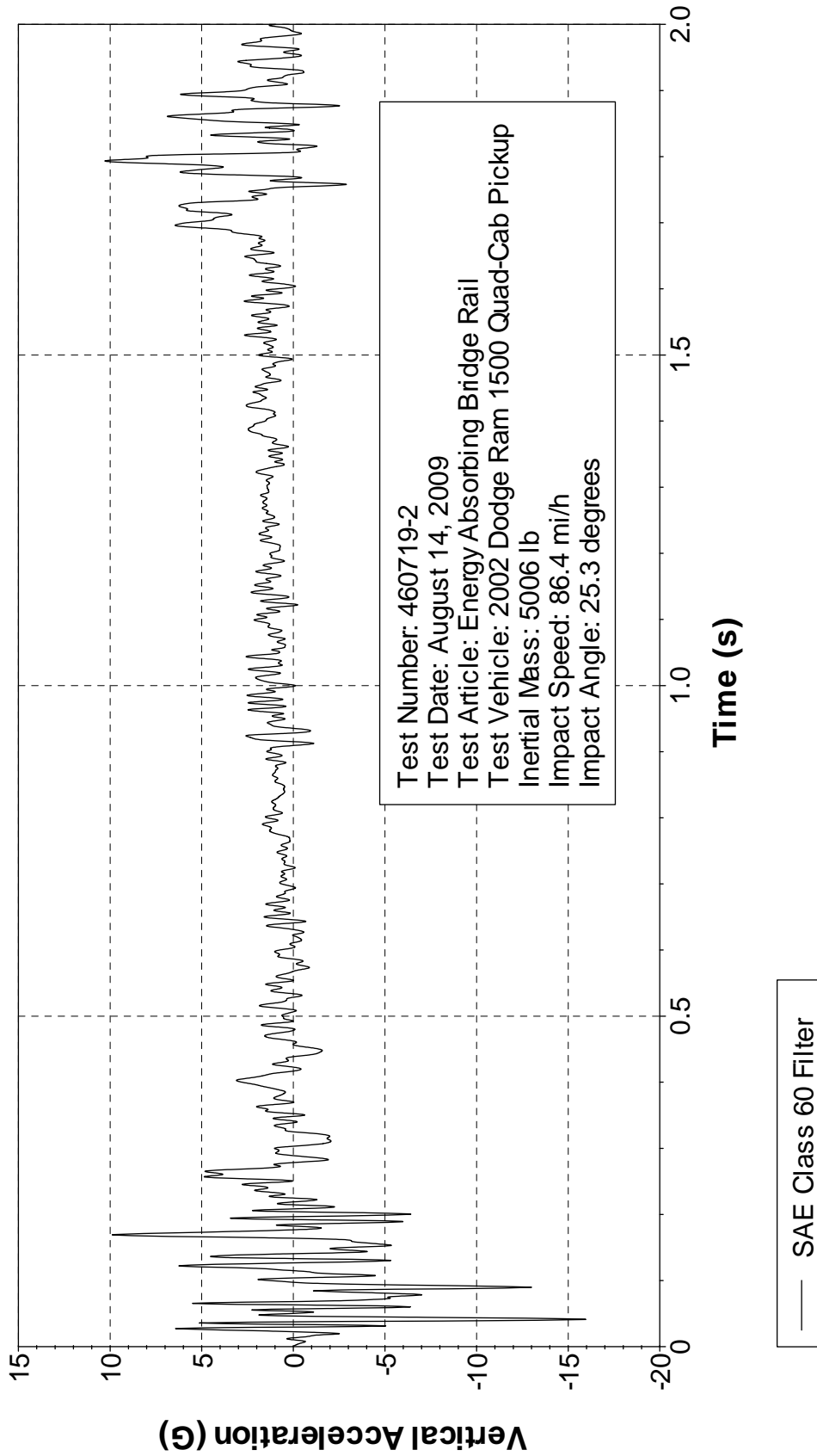


Figure E11. Vehicle Vertical Accelerometer Trace for Test No. 460719-2 (Accelerometer Located at Center of Gravity).

X Acceleration over Rear Axle

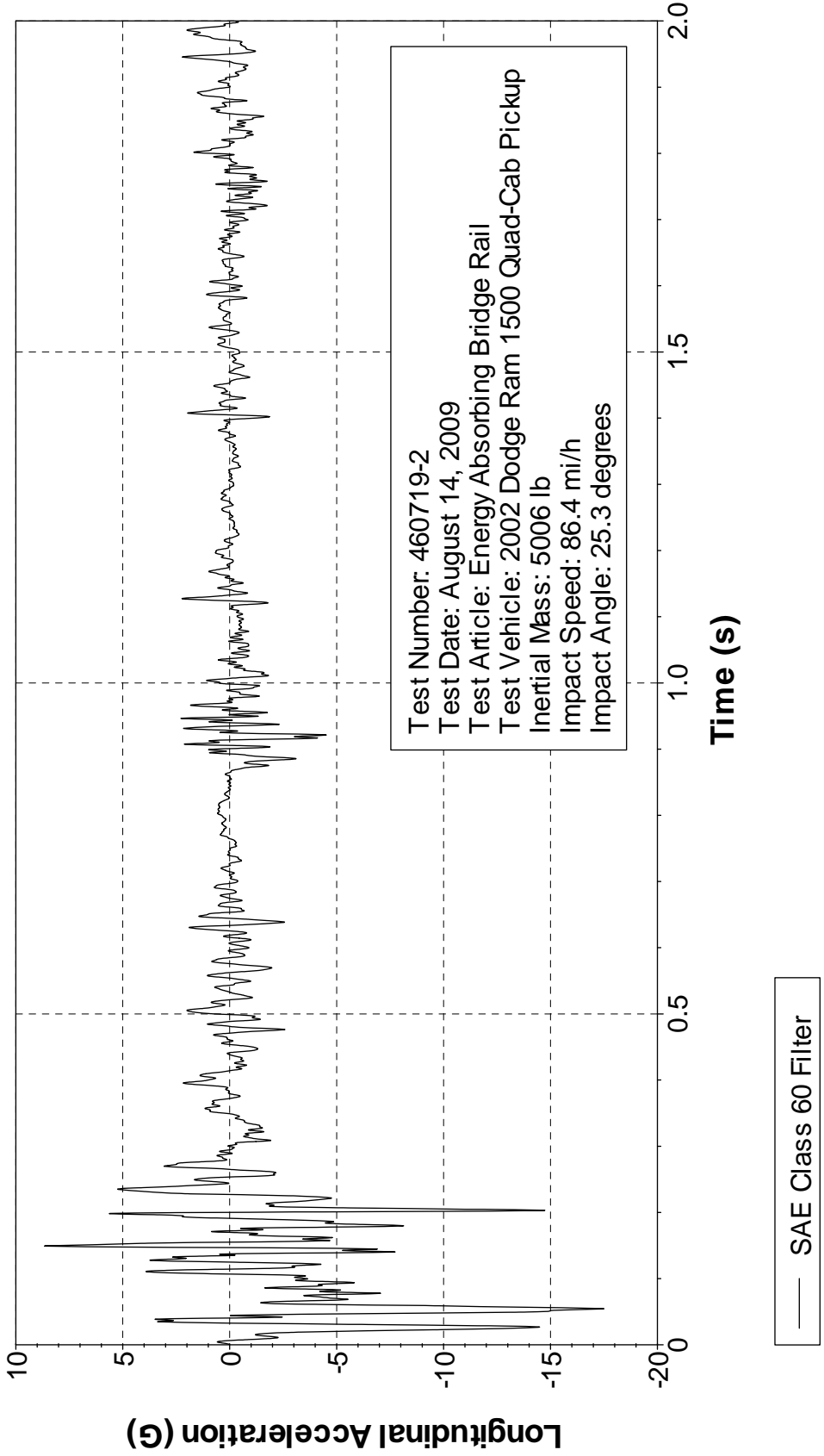
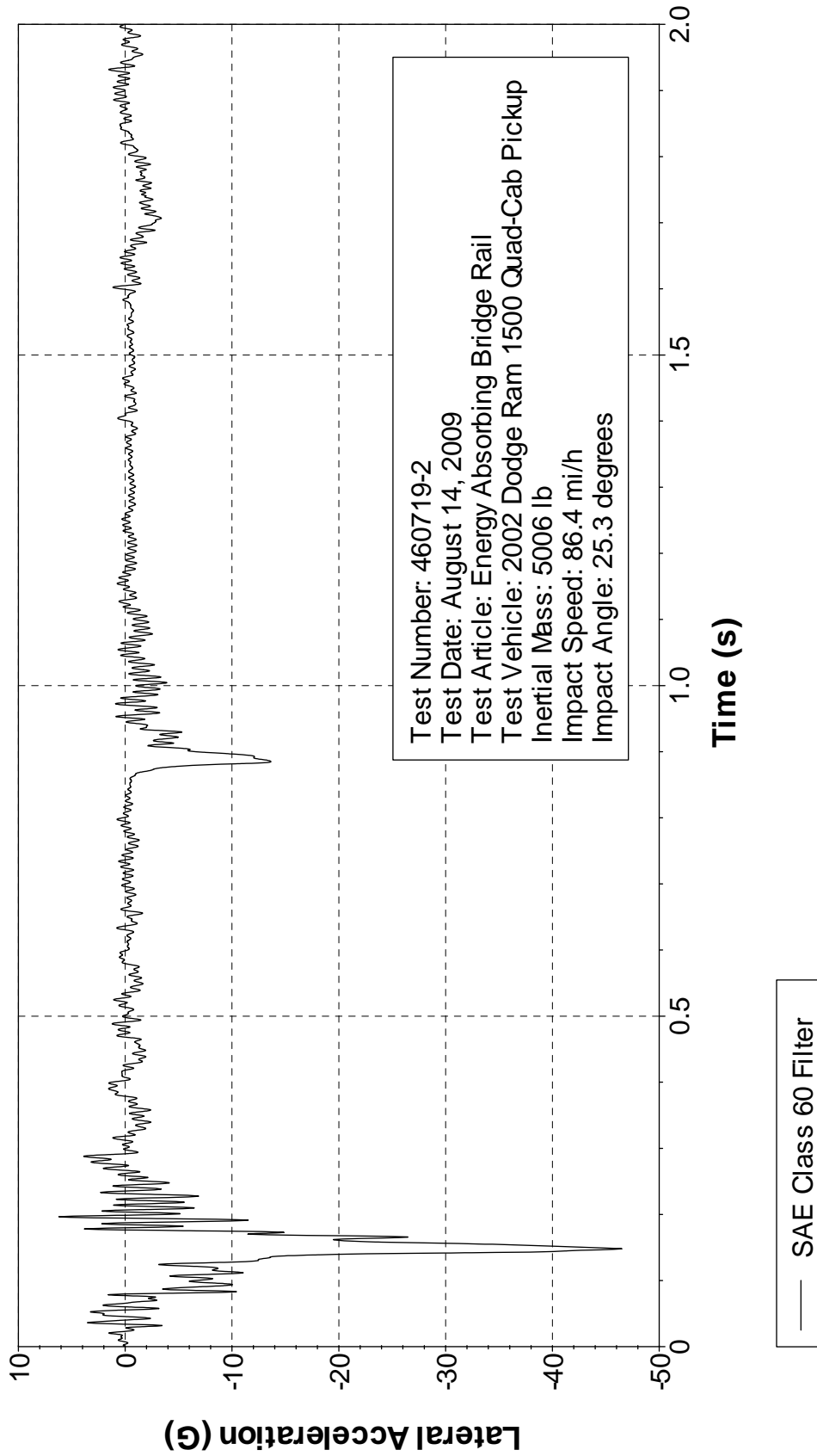


Figure E12. Vehicle Longitudinal Accelerometer Trace for Test No. 460719-2 (Accelerometer Located over Rear Axle).

Y Acceleration over Rear Axle



**Figure E13. Vehicle Lateral Accelerometer Trace for Test No. 460719-2
(Accelerometer Located over Rear Axle).**

Z Acceleration over Rear Axle

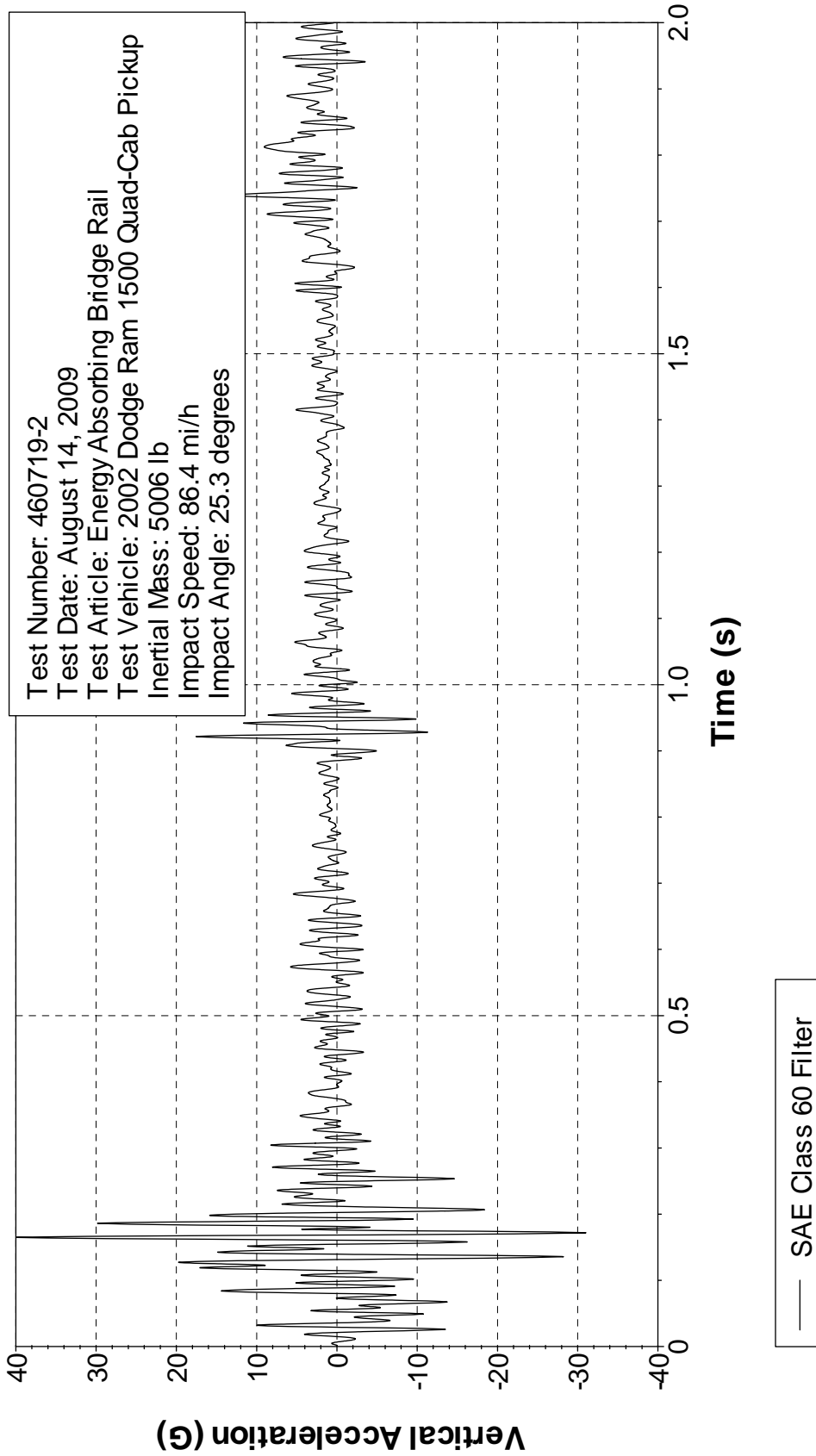


Figure E14. Vehicle Vertical Accelerometer Trace for Test No. 460719-2 (Accelerometer Located over Rear Axle).

Roll, Pitch, and Yaw Angles

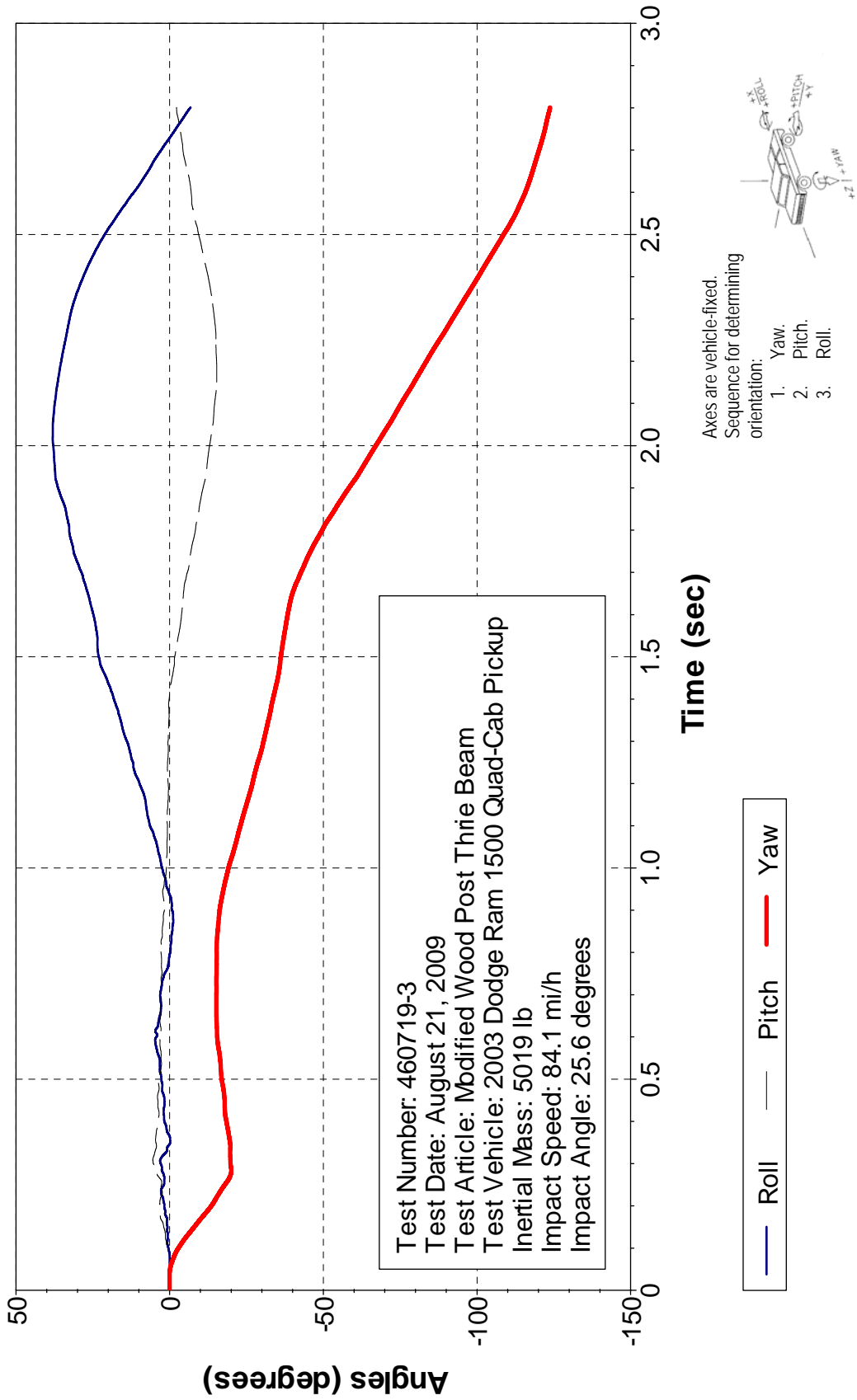
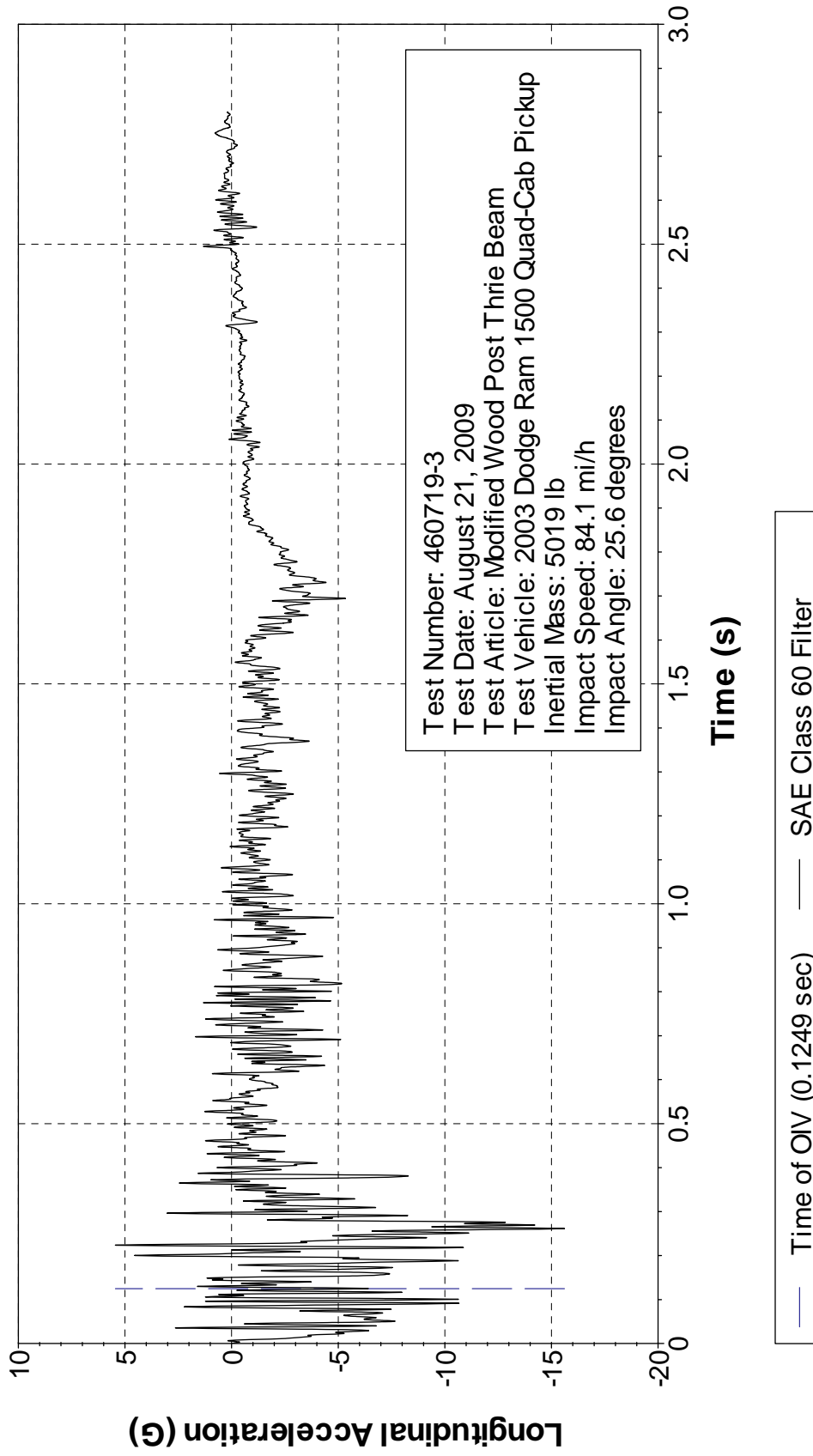


Figure E15. Vehicle Angular Displacements for Test No. 460719-3.

X Acceleration at CG



**Figure E16. Vehicle Longitudinal Accelerometer Trace for Test No. 460719-3
(Accelerometer Located at Center of Gravity).**

Y Acceleration at CG

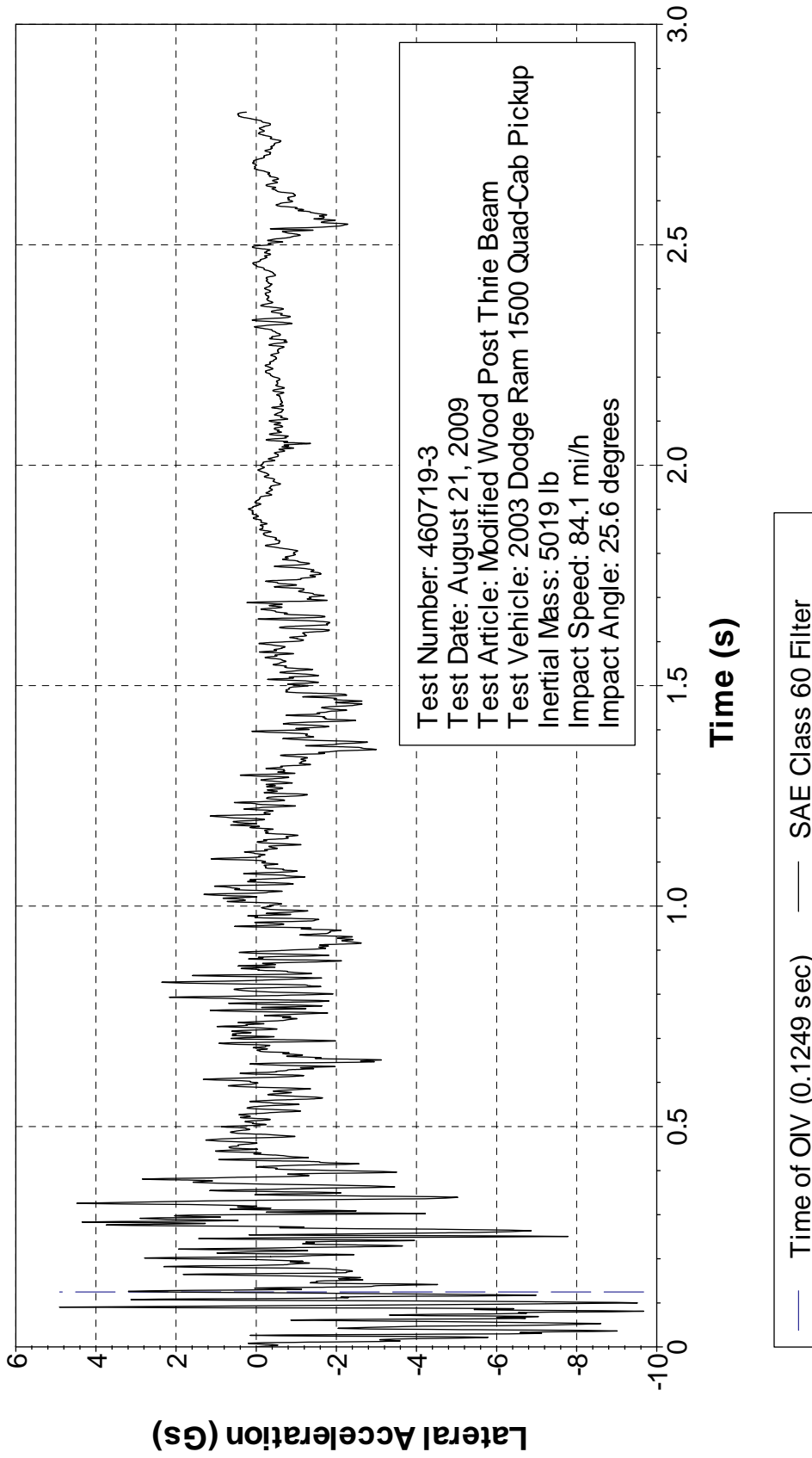


Figure E17. Vehicle Lateral Accelerometer Trace for Test No. 460719-3 (Accelerometer Located at Center of Gravity).

Z Acceleration at CG

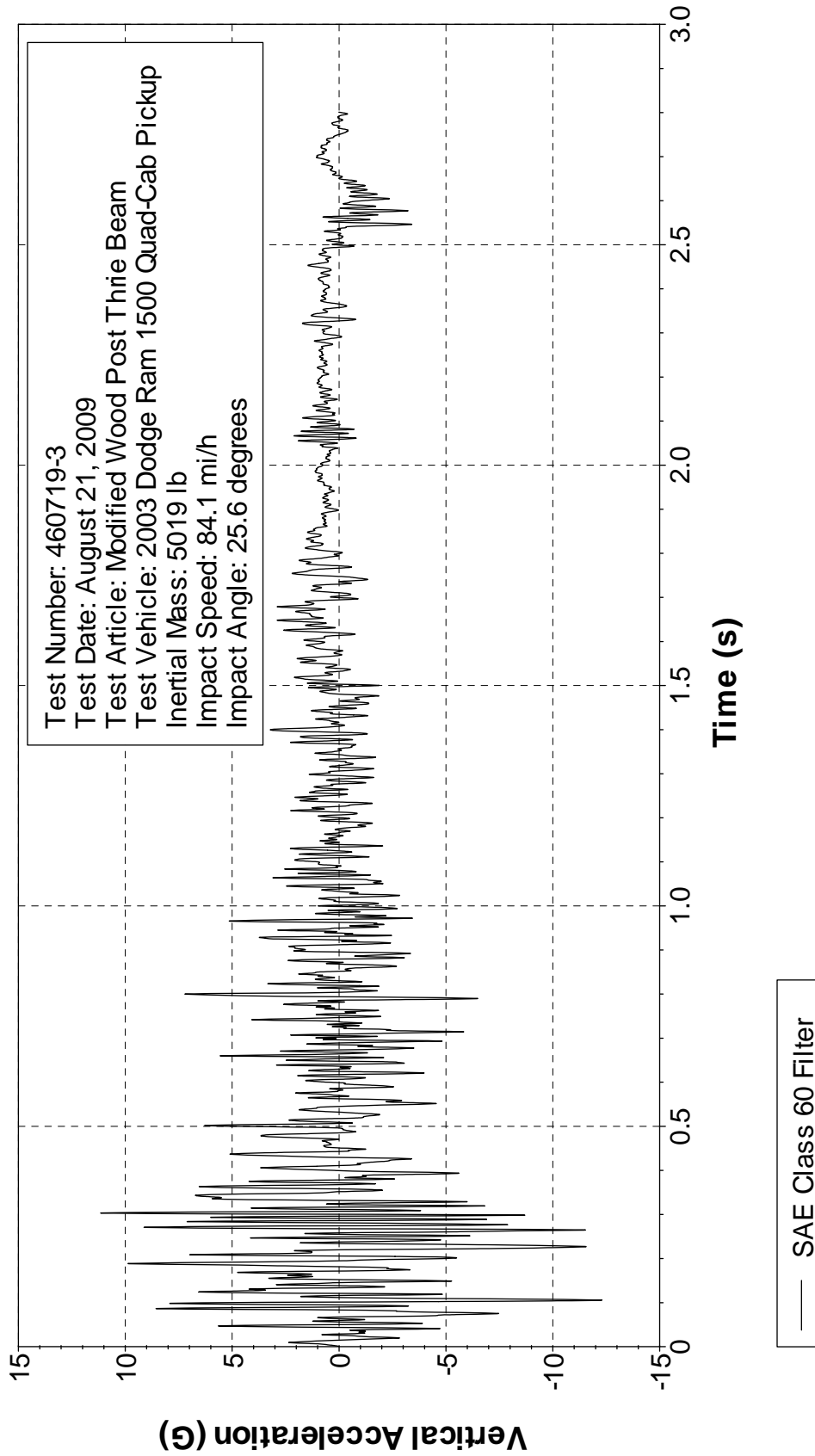


Figure E18. Vehicle Vertical Accelerometer Trace for Test No. 460719-3 (Accelerometer Located at Center of Gravity).

X Acceleration over Rear Axle

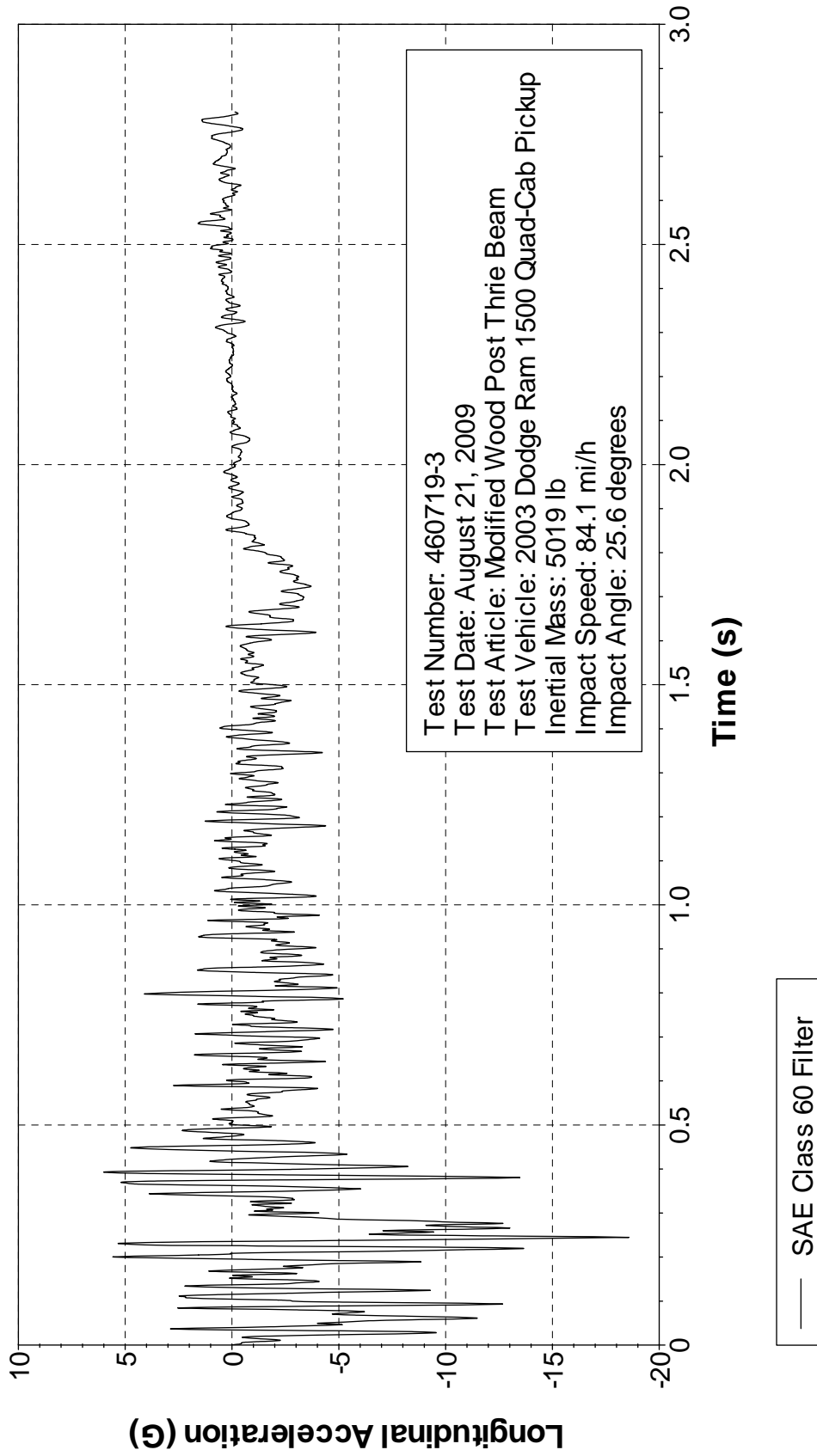


Figure E19. Vehicle Longitudinal Accelerometer Trace for Test No. 460719-3
(Accelerometer Located over Rear Axle).

Y Acceleration over Rear Axle

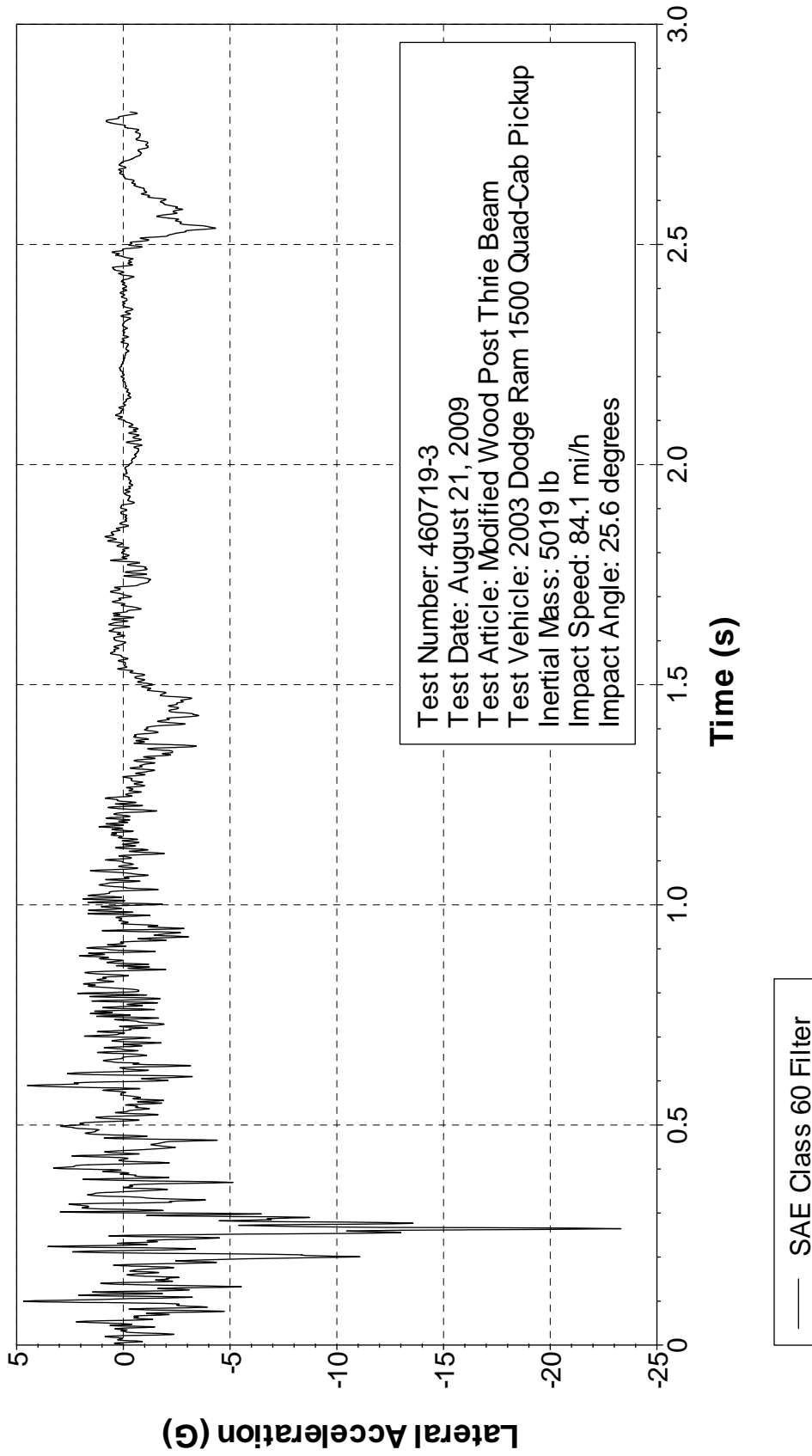


Figure E20. Vehicle Lateral Accelerometer Trace for Test No. 460719-3 (Accelerometer Located over Rear Axle).

Z Acceleration over Rear Axle

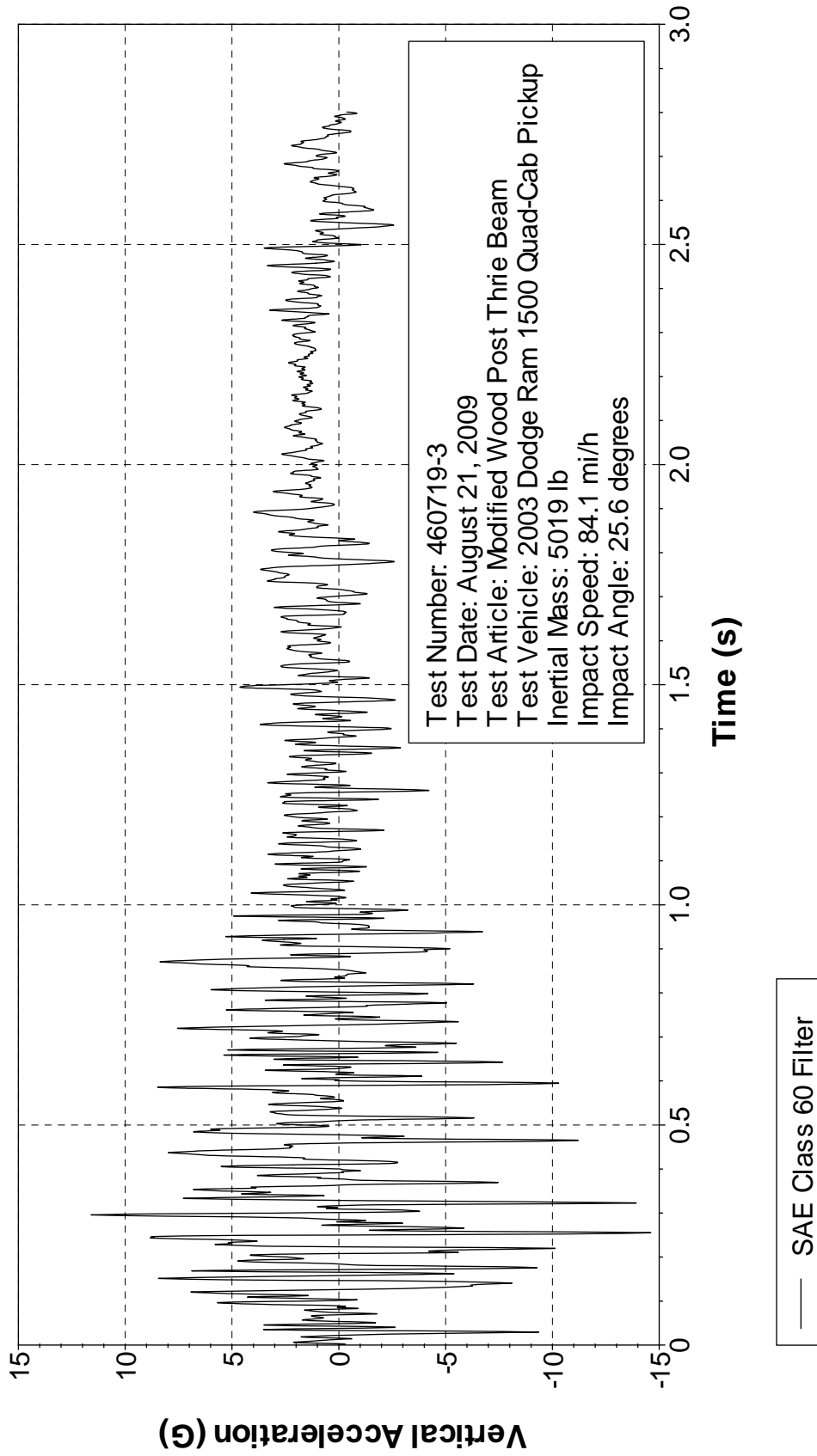
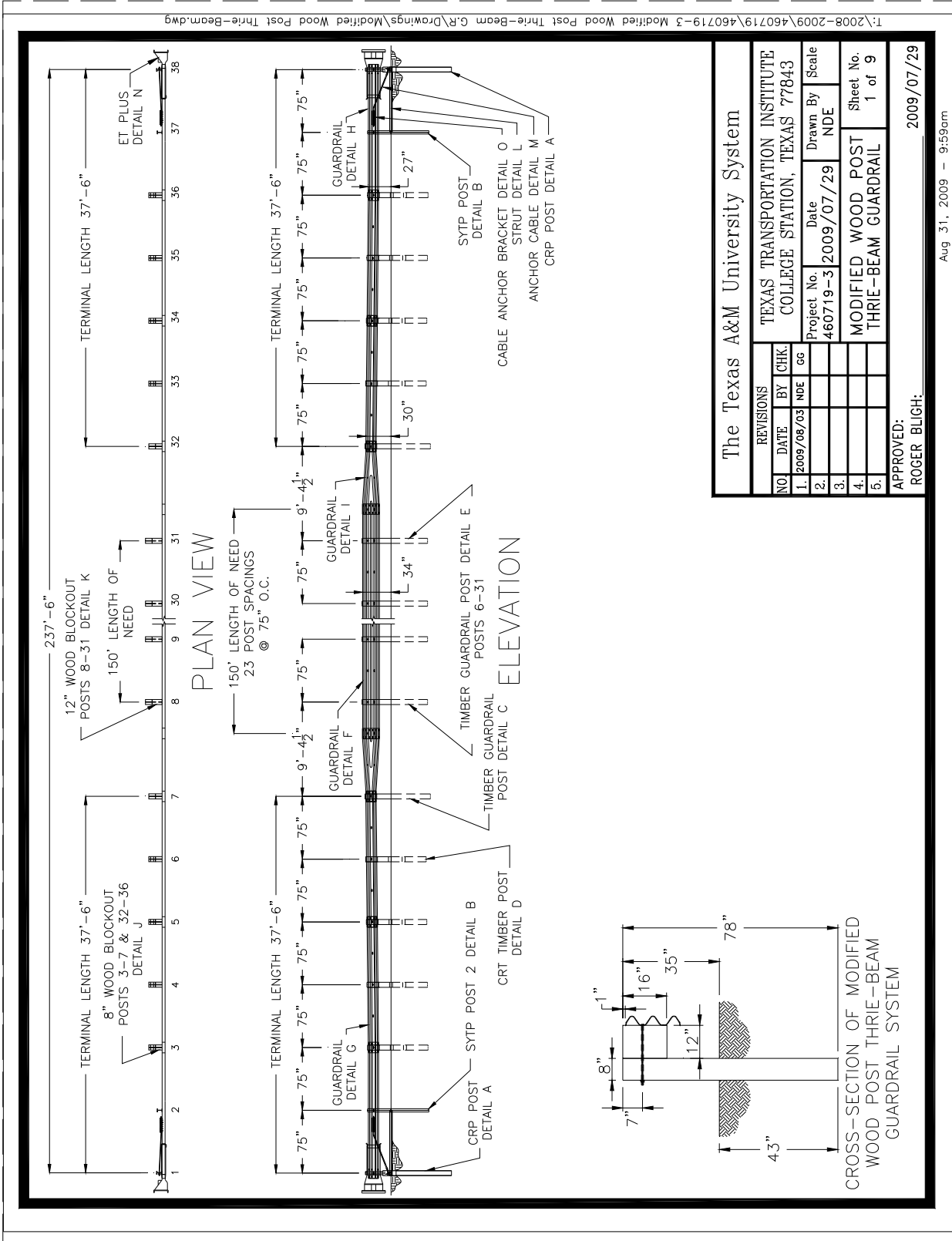


Figure E21. Vehicle Vertical Accelerometer Trace for Test No. 460719-3
(Accelerometer Located over Rear Axle).

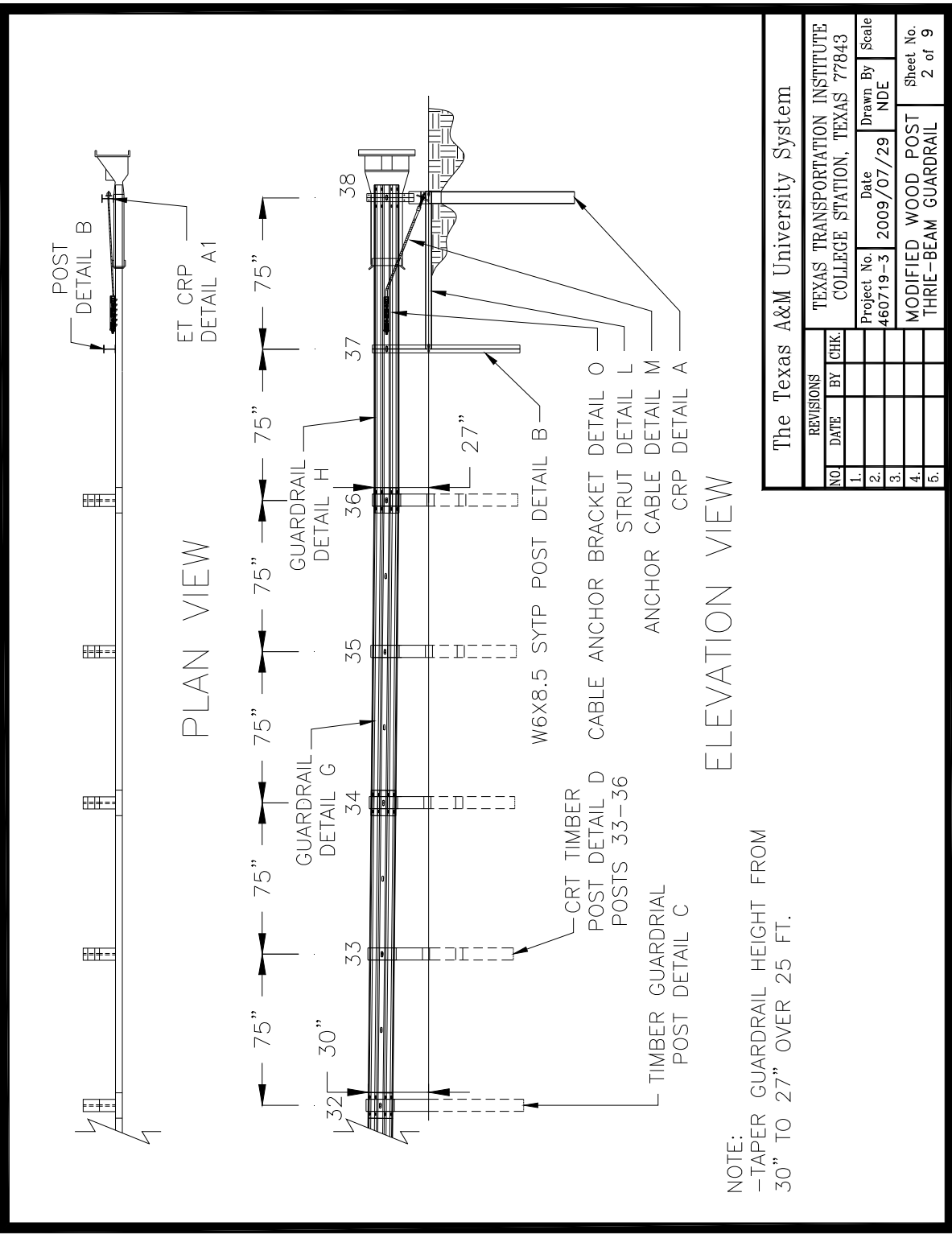
APPENDIX F. DETAILS OF THE HIGH-SPEED THRIE BEAM GUARDRAIL



T:\2008-2009\460719\460719-3 Modified Wood Post Thrie-Beam.GR\Drawings\Modified Wood Post Thrie-Beam.dwg

The Texas A&M University System			
TEXAS TRANSPORTATION INSTITUTE COLLEGE STATION, TEXAS 77843			
Project No.	Date	Drawn By	Scale
460719-3	2009/07/29	NDE	
Sheet No.			1 of 9
MODIFIED WOOD POST THRIE-BEAM GUARDRAIL			
APPROVED:			2009/07/29
ROGER BLUGH:			

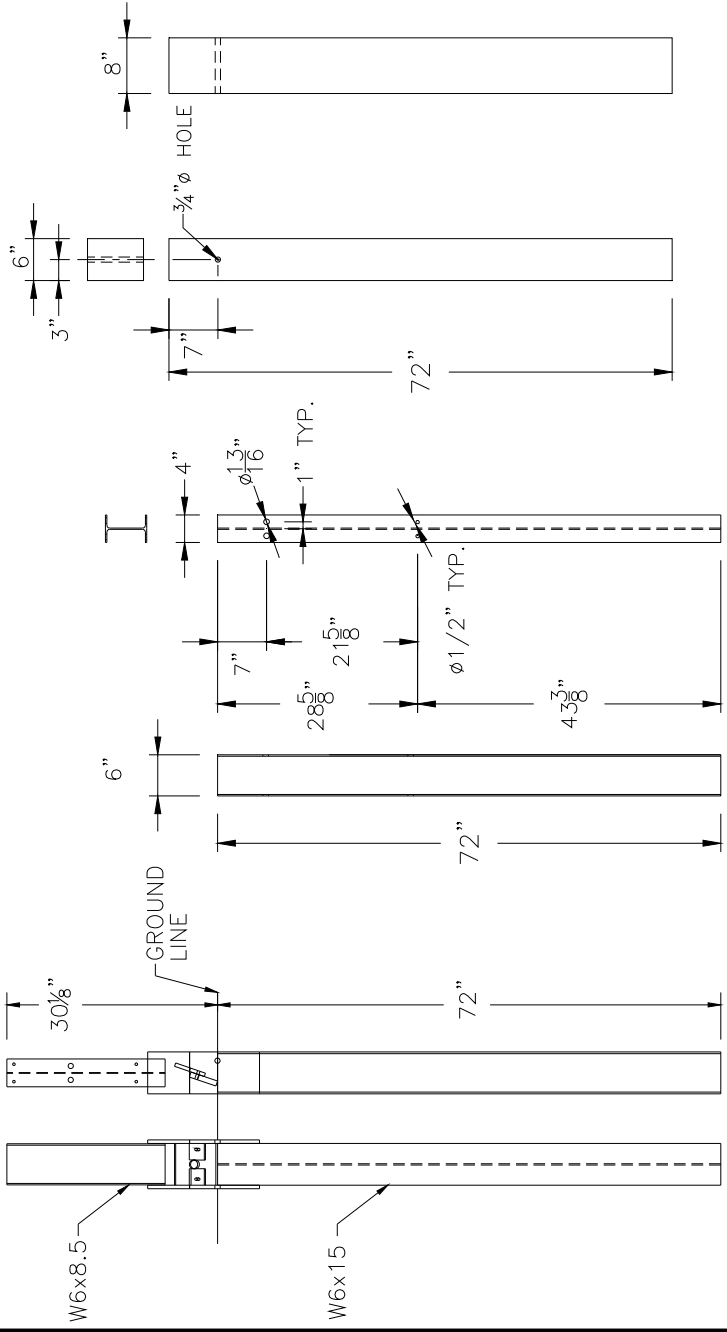
NO.	DATE	BY	CHK
1.	2009/08/03	NDE	gg
2.			
3.			
4.			
5.			



NOTE:
 -TAPER GUARDRAIL HEIGHT FROM
 30" TO 27" OVER 25 FT.

The Texas A&M University System					
TEXAS TRANSPORTATION INSTITUTE COLLEGE STATION, TEXAS 77843					
Project No.		Date		Drawn By / Scale	
460719-3		2009/07/29		NDE	
MODIFIED WOOD POST THRIE-BEAM GUARDRAIL				Sheet No. 2 of 9	
REVISIONS					
NO.	DATE	BY	CHK		
1.					
2.					
3.					
4.					
6.					

Aug 31, 2009 - 10:03am



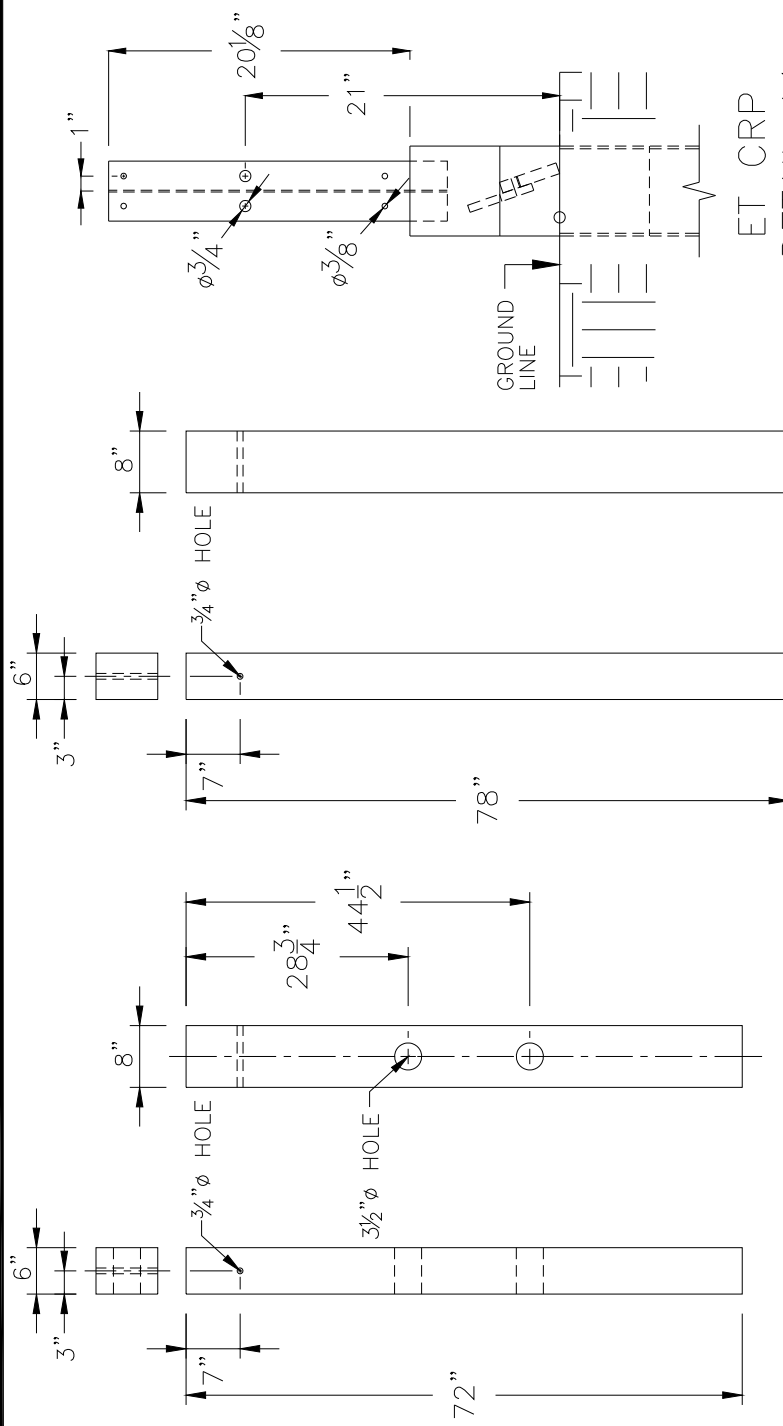
STANDARD CRP WITH 20° OFFSET
 DETAIL A

SYTP-W6X8.5
 DETAIL B

TIMBER GUARDRAIL POST
 DETAIL C (AASHTO-AGC-
 ARTBA #PDE02)

The Texas A&M University System					
TEXAS TRANSPORTATION INSTITUTE COLLEGE STATION, TEXAS 77843					
Project No.		Date		Drawn By / Scale	
460719-3		2009/07/29		NDE	
MODIFIED WOOD POST THRIE-BEAM GUARDRAIL				Sheet No. 3 of 9	
REVISIONS					
NO.	DATE	BY	CHK		
1.					
2.					
3.					
4.					
5.					
6.					

Aug 31, 2009 - 10:05am



CRT TIMBER GUARDRAIL POST
DETAIL D
(AASHTO-AGC-ARTBA #PDE09)

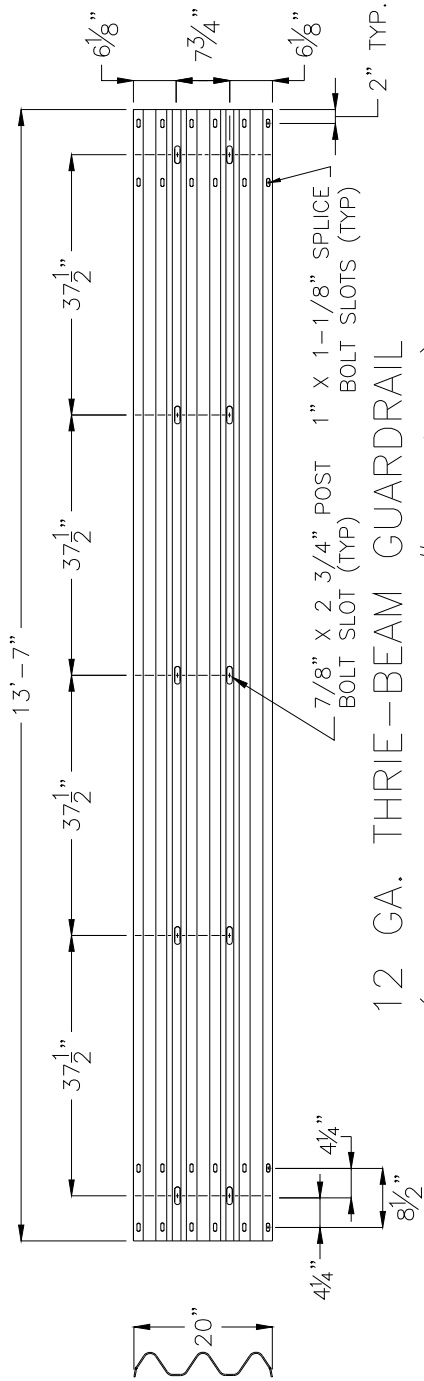
TIMBER GUARDRAIL POST
DETAIL E
(AASHTO-AGC-ARTBA #PDE03)

ET CRP
DETAIL A1

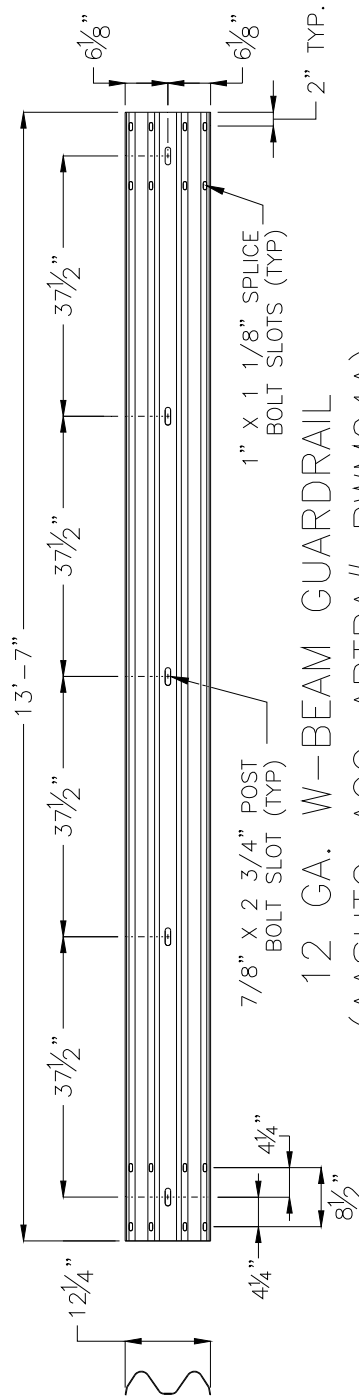
The Texas A&M University System	
TEXAS TRANSPORTATION INSTITUTE COLLEGE STATION, TEXAS 77843	
Project No.	Date
460719-3	2009/07/29
Drawn By	Scale
NDE	
Sheet No.	4 of 9

REVISIONS	
NO.	DATE
1.	
2.	
3.	
4.	
5.	
6.	

Aug 31, 2009 - 10:07am



12 GA. THRIE-BEAM GUARDRAIL
(AASHTO-AGC-ARTBA# RTM04A)
DETAIL F



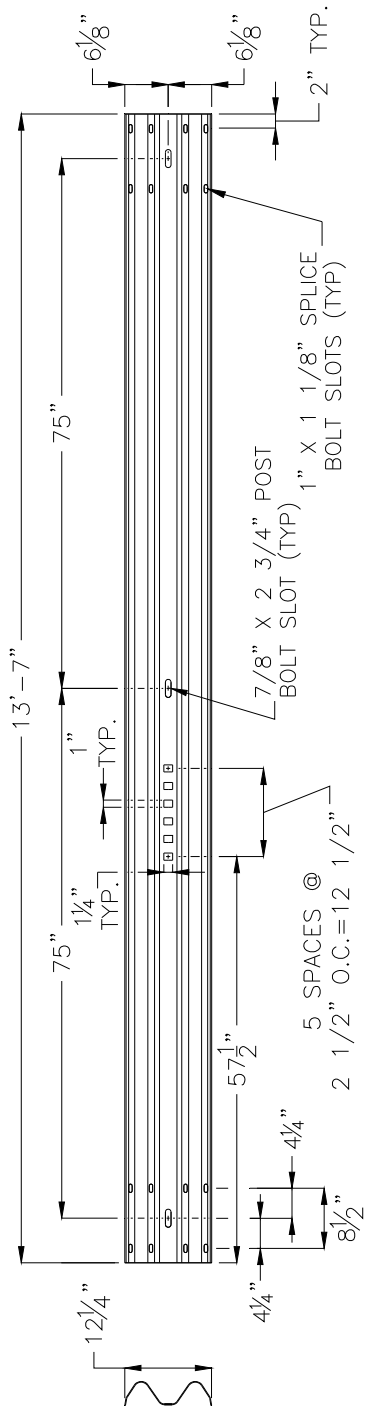
12 GA. W-BEAM GUARDRAIL
(AASHTO-AGC-ARTBA# RWM04A)
DETAIL G

The Texas A&M University System

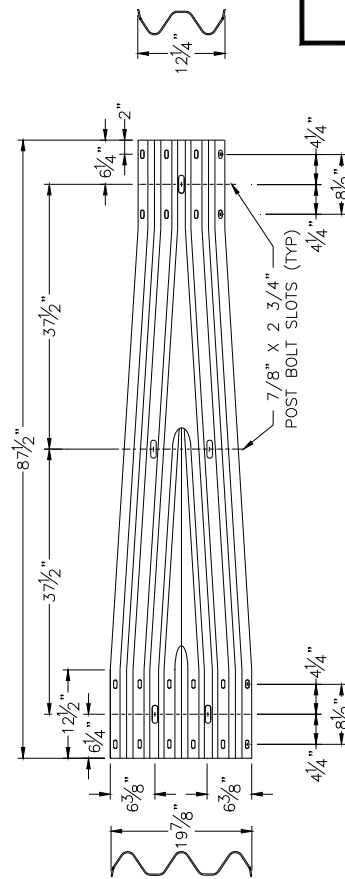
REVISIONS		TEXAS TRANSPORTATION INSTITUTE	
NO.	DATE	BY	CHK
1.			
2.			
3.			
4.			
5.			

Project No.		Date		Drawn By		Scale	
460719-3		2009/07/29		NDE			
MODIFIED WOOD POST THRIE-BEAM GUARDRAIL				Sheet No.			
				5 of 9			

Aug 31, 2009 - 10:08am



12 GA. W-BEAM END TERMINAL
GUARDRAIL DETAIL H

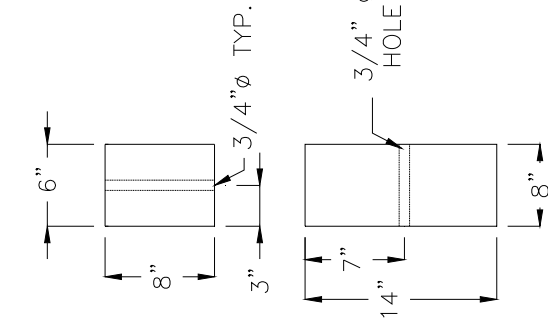


12 GA. THRIE-BEAM TRANSITION
(AASHTO-AGC-ARTBA# RWTO1A)
DETAIL I

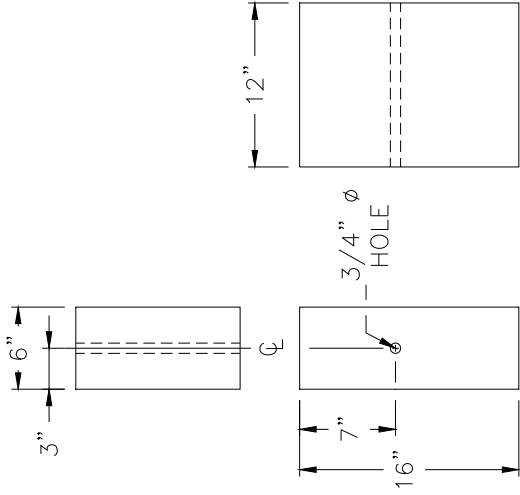
The Texas A&M University System		TEXAS TRANSPORTATION INSTITUTE	
		COLLEGE STATION, TEXAS 77843	
Project No.	Date	Drawn By	Scale
460719-3	2009/07/29	NDE	
MODIFIED WOOD POST		Sheet No.	
THRIE-BEAM GUARDRAIL		6 of 9	

Aug 31, 2009 - 10:09am

T:\2008-2009\460719\460719-3 Modified Wood Post Thrie-Beam G.R\Drawings\Modified Wood Post Thrie-Beam.dwg



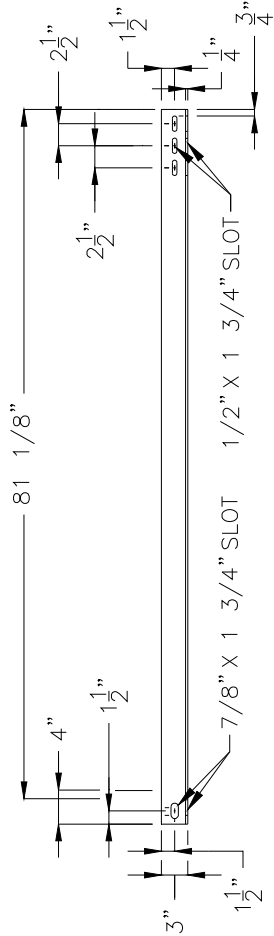
8" W-BEAM WOOD
BLOCKOUT DETAIL J
(AASHTO-AGC-ARTBA# PDB01)



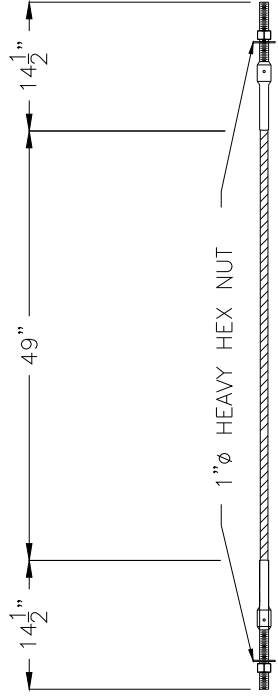
12" THRIE-BEAM
WOOD BLOCKOUT
DETAIL K

The Texas A&M University System					
TEXAS TRANSPORTATION INSTITUTE COLLEGE STATION, TEXAS 77843					
Project No.		Date		Drawn By / Scale	
460719-3		2009/07/29		NDE	
MODIFIED WOOD POST THRIE-BEAM GUARDRAIL				Sheet No. 7 of 9	
REVISIONS					
NO.	DATE	BY	CHK		
1.	2009/08/03	NDE	GG		
2.					
3.					
4.					
5.					
6.					

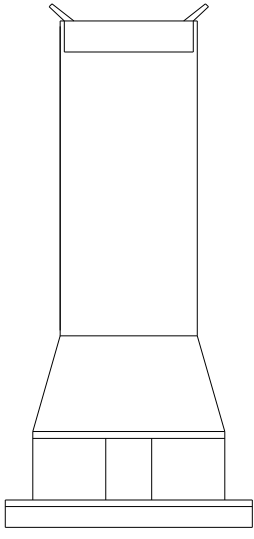
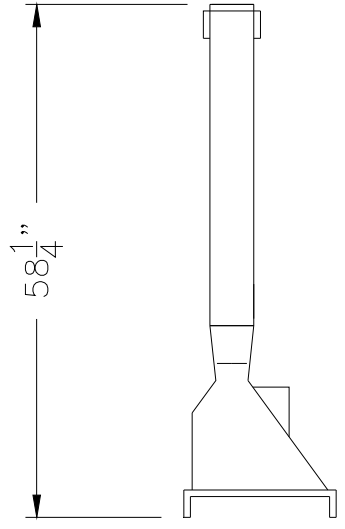
Aug 31, 2009 - 10:10am



3" X 3" X 1/4"
STRUT DETAIL L



ANCHOR BRACKET CABLE
DETAIL M

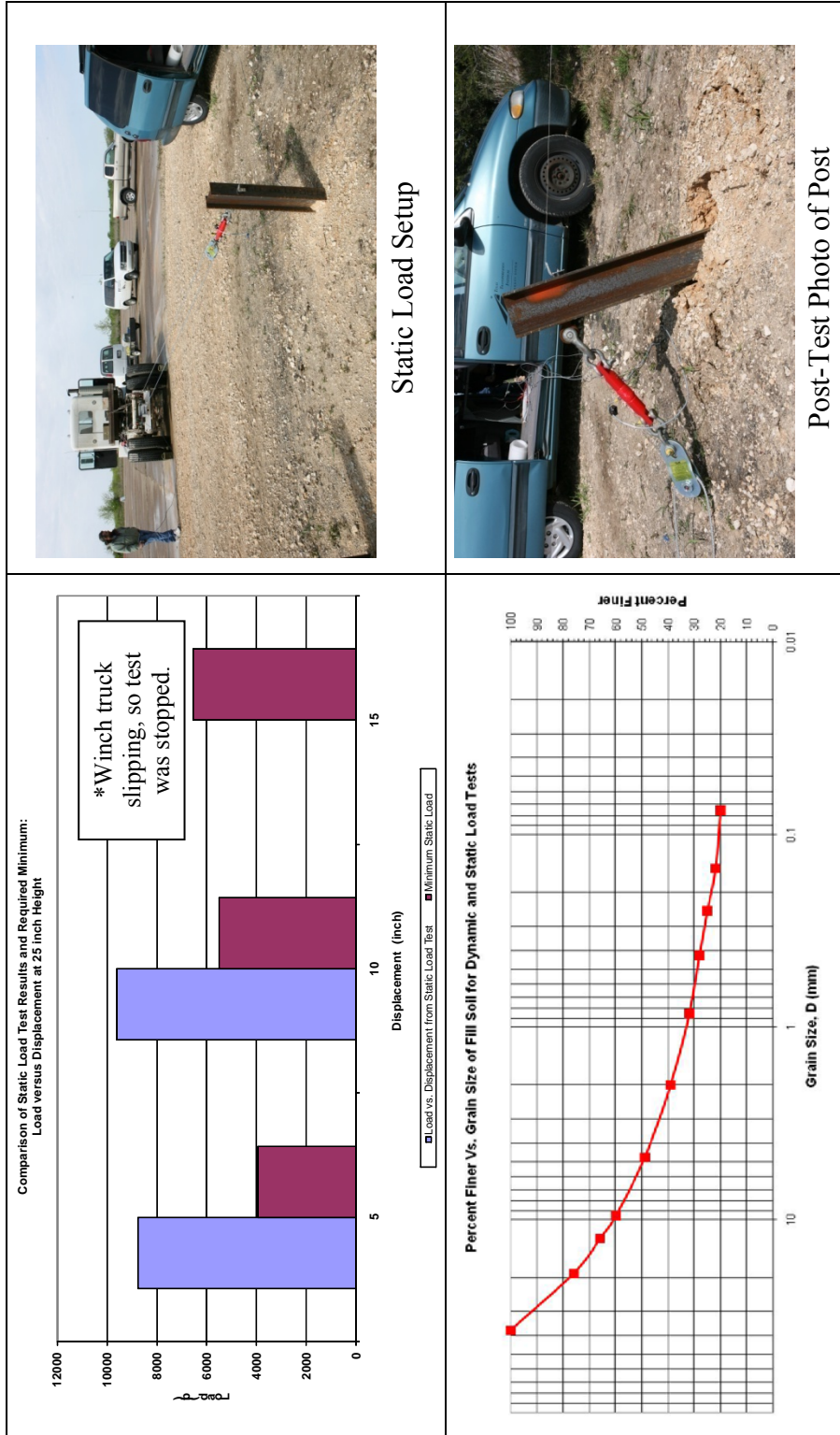


ET PLUS
DETAIL N

The Texas A&M University System					
TEXAS TRANSPORTATION INSTITUTE					
COLLEGE STATION, TEXAS 77843					
Project No.		Date		Drawn By / Scale	
460719-3		2009/07/29		NDE	
MODIFIED WOOD POST				Sheet No.	
THREE-BEAM GUARDRAIL				8 of 9	

Aug 31, 2009 - 10:11am

APPENDIX G. SOIL STRENGTH DOCUMENTATION



Date 2009-08-21

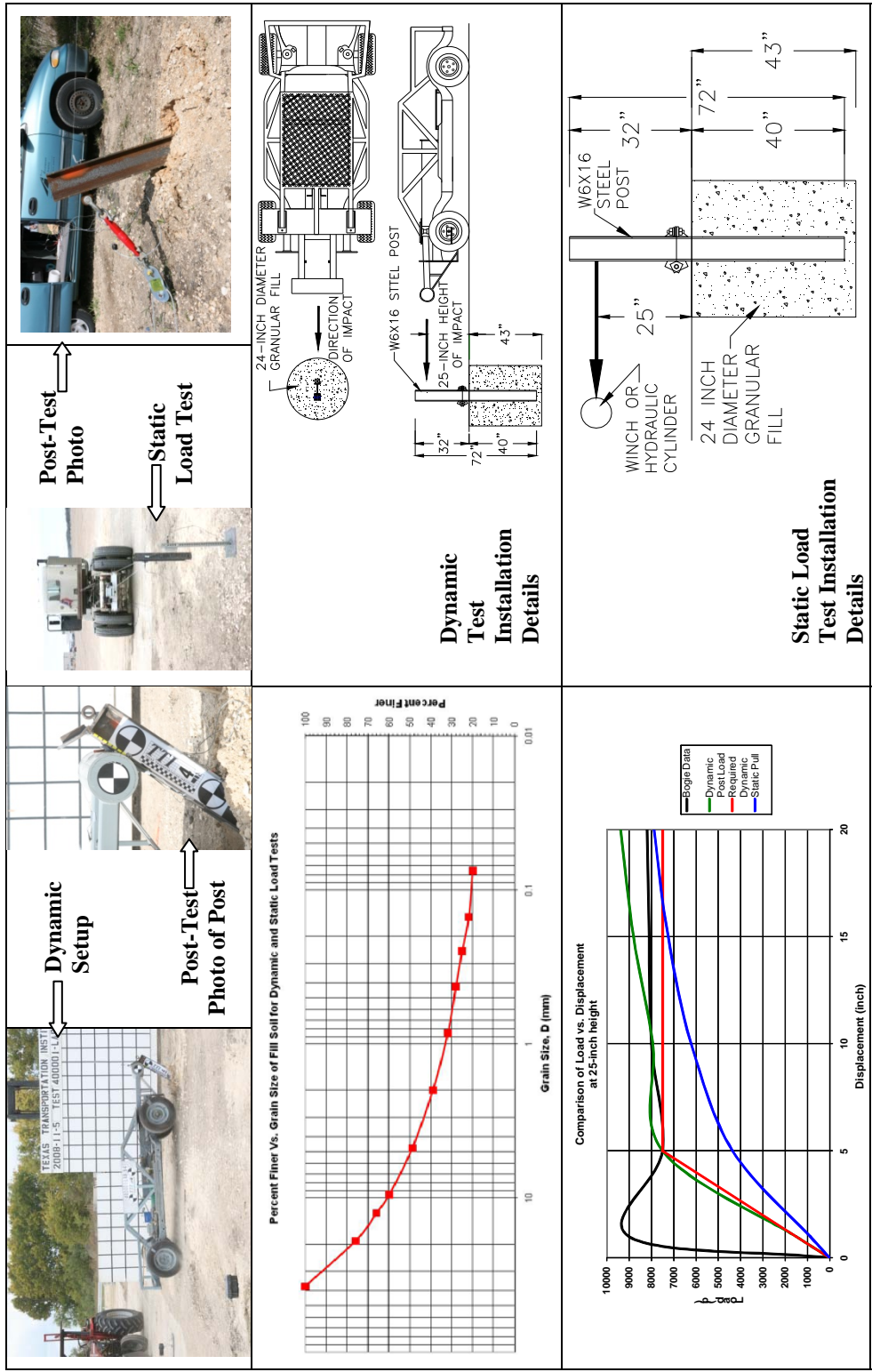
Test Facility and Site Location TTI Proving Ground – 3100 SH 47, Bryan, Tx

In Situ Soil Description (ASTM D2487) Sandy gravel with silty fines

Fill Material Description (ASTM D2487) and sieve analysis AASHTO Grade B Soil-Aggregate (see sieve analysis)

Description of Fill Placement Procedure 6-inch lifts tamped with a pneumatic compactor

Figure G1. Test Day Static Soil Strength Documentation.



Date.....	2008-11-05
Test Facility and Site Location.....	TTI Proving Ground, 3100 SH 47, Bryan, TX, 77807
In Situ Soil Description (ASTM D2487).....	Sandy gravel with silty fines
Fill Material Description (ASTM D2487) and sieve analysis.....	AASHTO Grade B Soil-Aggregate (see sieve analysis above)
Description of Fill Placement Procedure.....	6-inch lifts tamped with a pneumatic compactor
Bogie Weight.....	5009 lb
Impact Velocity.....	20.5 mi/h

Figure G2. Summary of Strong Soil Test Results for Establishing Installation Procedure.